PHOSPHORYLATION AND CELL ADHESION PROPERTIES OF MYELIN-ASSOCIATED GLYCOPROTEIN ISOFORMS

Daniel E.H. Afar

Thesis submitted to
the School of Graduate Studies and Research
in partial fulfillment of the requirements for the degree of
Doctor of Philosophy

Department of Biochemistry,
University of Ottawa,
Ottawa, Ontario
CANADA

ISBN 0-315-85778-1

UNIVERSITÉ D'OTTAWA
UNIVERSITY OF OTTAWA

ABSTRACT

The phosphorylation and cell adhesion properties of myelin-associated glycoprotein (MAG) isoforms were investigated. MAG is a member of the immunoglobulin supergene family and is thought to mediate interactions between myelinating glial cells and neurons in the central and peripheral nervous systems. Two isoforms of MAG exist, L-MAG and S-MAG, which exhibit differential expression patterns. Using retroviral infection and transfection of the cDNAs encoding L-MAG and S-MAG, L cell fibroblasts and NIH3T3 cell lines that express either isoform were generated. The expression of both isoforms on the cell surface of L cells induced the cells to aggregate in a MAG-dependent fashion. The adhesion phenomena was determined to be calcium and temperature independent. A critical level of cell surface MAG expression was required for cell aggregation to occur. The adhesion was found to be heterotypic in nature, signifying the presence of a MAG receptor on the cell surface of L cells.

The MAG isoforms are identical in their extracellular and transmembrane domains. They share a common region in their cytoplasmic domain, but are distinct at their carboxyl termini. The unique carboxyl tails are comprised of 54 amino acids in L-MAG and 10 residues in S-MAG. Both isoforms were determined to be phosphorylated in fibroblasts. L-MAG exhibited phosphorylation on serine, threonine and tyrosine residues. The phosphorylation on tyrosine was augmented by treatment of cells with ammonium vanadate. S-MAG phosphorylation occurred mainly on serine residues, but some phosphotyrosine was also detected. The phosphorylation of S-MAG, however, was relatively insensitive to vanadate treatment. Tryptic digest analysis showed that two serine and the major tyrosine phosphorylation site in MAG were identical in L-MAG and S-MAG. The major tyrosine phosphorylation site in MAG was, thus, identified as tyrosine 558. This tyrosine residue is homologous to the major tyrosine phosphorylation site in the fibronectin receptor, integrin. A similar phosphorylation pattern of L-MAG was observed in primary rat oligodendrocytes.

Determination of the stoichiometry of phosphorylation revealed that phosphorylation of L-MAG was at least one order of magnitude greater than S-MAG, especially with respect to tyrosine phosphorylation. This result indicates the presence of a carboxyl terminal sequence unique to L-MAG that activates the phosphorylation of tyrosine 558. This region may represent docking sites for protein tyrosine kinase binding, making L-MAG-kinase interactions more efficient.

Two populations of L-MAG molecules were discovered: those that are phosphorylated on tyrosine residues, and those that exhibit serine/threonine phosphorylation. In effect, tyrosine phosphorylation precludes serine/threonine phosphorylation, suggesting that the alternatively phosphorylated L-MAG molecules perform different functions. Increasing the tyrosine phosphorylation of MAG had no detectable effect on the cell adhesion behaviour of the cells. Tyrosine phosphorylation of L-MAG, however, induced its capacity to bind the SH2 domain of phospholipase C-gamma.

Therefore, L-MAG has the potential to interact with a variety of signalling molecules via its cytoplasmic domain. While L-MAG may participate in signal transduction pathways, S-MAG may function in a more restricted manner and perform only as a cell adhesion molecule. Thus, the differential regulation of MAG isoform expression may serve to increase the repertoire of MAG functions at specific times during development.

DEDICATION

In memory of Joseph E. Afar (Baku 1926- Montreal 1991).

ACKNOWLEDGEMENTS

I would like to express my sincere gratitude to the many people who have contributed to my education as a scientist and to those who have made life pleasurable at McGill and at the University of Ottawa:

In particular, I would like to thank my supervisor Dr. John Bell, who was brave enough to take me into his lab. Our interactions were filled with his relentless patience and humour. I thank him for his inspiring ideas and teaching me science.

I am grateful to Dr. Douglas Gray for his sharp wit and Dr. Michael McBurney for keeping me on my toes during numerous WIP sessions (and in my ski boots, during an infamous ski-outing).

I would like to thank the secretarial staff: Beth Mason and Sylvie Carriere for helping me throughout my graduate student years as well as in the final wrap up of my thesis.

My appreciation and thanks also go out to:

Brian Howell, Ninan Abraham and Mireille Cartier for their friendships, camaraderie, Thompson House, and many good times.

Ricardo Marius, for introducing me to mountain biking and Rap.

Peterus Duncan, for many humorous alpine skiing moments (especially in Banff).

Elizabeth (Doo) Douville, for teaching me new English words and putting up with me as a roommate.

Maria Jaramillo for actually reading my thesis and making an excellent lab bench teammate.

Marco Difruscio, for his photographic talent and his uncanny Halloween costume.

Drs. Dante Morassuti and Guillermina Almazan for many interesting scientific discussions.

Nicole Laferriere, for being an extraordinary person and friend.

Kalpana Gupta, Josee Coulombe, Gael Vidricaire and Jim Gordon, for contributing to an enjoyable working environment.

My brother Michael, for his unique sense of humour; my sister Ronith, for bailing me out of trouble on numerous occasions; my mother Arlette, for her strong character; and my father Joseph, for his constant encouragement of my education.

I would like to extend special thanks to my best friend, Elaine Petrof (otherwise known as the Brat or the Worm). Despite her devious practical joke oriented mind, her companionship has given me many wonderful and interesting moments to remember. I am eternally grateful to her.

Finally, I would like to thank the Fonds de la Recherche en Sante du Quebec and the University of Ottawa for providing me with scholarships.

PREFACE

The work presented in this thesis has been or will submitted for publication as described below:

CHAPTER 3 (in part):

Afar, D.E.H., R.M. Marius, J.L. Salzer, C.P. Stanners, P.E. Braun and J.C. Bell. 1991. Cell adhesion properties of myelin-associated glycoprotein in L cell fibroblasts. J.Neurosci.Res. 29:429-436.

CHAPTER 4:

Afar, D.E.H., J.L. Salzer, J. Roder, P.E. Braun and J.C. Bell. 1990. Differential phosphorylation of myelin-associated glycoprotein isoforms in cell culture. J.Neurochem. 55:1418-1426.

Afar, D.E.H., M. Jaramillo, G. Almazan and J.C. Bell. Manuscript in preparation.

APPENDIX 1:

Afar, D.E.H., C.P. Stanners and J.C. Bell. 1992. Tyrosine phosphorylation of biliary glycoprotein, a cell adhesion molecule related to carcinoembryonic antigen. Biochim.Biophys.Acta 1134:46-52.

The experimental work in this thesis is entirely my own. Cell lines PA317-L-MAG and Psi_2-L-MAG were provided by Dr. J.L. Salzer, Department of Cell Biology, New York University. S-MAG expressing 3T3 cells ($3TV_2$-9) were obtained from Dr. J. Roder, Deptartment of Medical Genetics, University of Toronto. LR73 cell lines expressing BGPs were supplied by Dr. C.P. Stanners, McGill University Cancer Centre. Primary rat oligodendrocyte cultures were prepared by Dr. G. Almazan, Department of Pharmacology, McGill University. Ricardo Marius provided excellent technical assistance in selecting and screening L-MAG expressing L cell clones.

TABLE OF CONTENTS

LIST OF FIGURES AND TABLES

LIST OF ABBREVIATIONS

ALL	acute lymphoblastic leukemia
ATP	adenosine triphosphate
BGP	biliary glycoprotein
C5	L cell clone expressing L-MAG
Ca2+	cytosolic free calcium
CAM	cell adhesion molecule
CEA	carcinoembryonic antigen
CML	chronic myelogenous leukemia
CNS	central nervous system
dbcAMP	dibutyryl-cyclic adenosine 3',5'-monophosphate
DMEM	Dulbecco's modification of Eagle's medium
DNA	deoxyribonucleic acid
EDTA	ethylenediaminetetraacetic acid
EGF	epidermal growth factor
ES	embryonic stem cells
FCS	fetal calf serum
FGF	fibroblast growth factor
FITC	fluoresceine iso-thiocyanate
GalC	galactocerebrocide
GAP	GTPase activating protein
GFR	growth factor receptor type protein tyrosine kinase
GTP	guanosine triphosphate
HEPES	N-2-hydroxyethylpiperazine-N'-2-ethanesulphonic acid
ICAM	intercellular adhesion molecule
Ig	immunoglobulin
IGF-1	insulin-like growth factor
kd	kilodaltons
L-MAG	long isoform of myelin-associated glycoprotein (p72)
L1	mouse neural-glia cell adhesion molecule

LAR	leukocyte common antigen related protein
LFA-1	leukocyte function associated antigen-1
LM	PA317 cells (NIH3T3 cells) expressing L-MAG
MAG	myelin-associated glycoprotein
MBP	myelin basic protein
MEM	minimum essential medium
mRNA	messenger ribonucleic acid
NCAM	neural cell adhesion molecule
NGF	nerve growth factor
PAGE	polyacrylamide gel electrophoresis
PBS	phosphate buffered saline
PC12	pheochromocytoma cells
PDGF	platelet-derived growth factor
PECAM-1	platelet-endothelial cell adhesion molecule-1
PI	phosphatidyl inositol
PKA	cAMP-dependent protein kinase
PKC	protein kinase C
PKG	cGMP-dependent protein kinase
PLC	phospholipase C-gamma
PMSF	phenylmethyl-sulfonylfluoride
PNS	peripheral nervous system
PSA	polysialic acid
PTK	protein tyrosine kinase
PVsrcLM	pool of src-transformed 3T3 cells expressing L-MAG
PVsrcSM12	clone of src-transformed 3T3 cells expressing S-MAG
S-MAG	short isoform of myelin-associated glycoprotein (p67)
SDS	sodium dodecyl sulfate
SFM	serum free medium
SH2	src-homology region 2
SH3	src-homology region 3

SM	NIH3T3 cell line expressing S-MAG ($3TV_2$-9)
SM1-48	L cell clones expressing S-MAG
TCA	trichloroacetic acid
TCR	T-cell receptor
TFMS	trifluoromethane sulfonic acid
TLC	thin-layer chromatography
TLE	thin-layer electrophoresis
TPA	12-O-tetradecanoylphorbol 13-acetate
TRIS	tris (hydroxymethyl) aminomethane

CHAPTER 1

GENERAL INTRODUCTION

An important property of cells during development is the ability to recognize cellular and extracellular targets. This property is a function of the **cell adhesion molecules (CAMs)** expressed on the cell surface. They confer to cells the ability to adhere selectively in space and time and are generally responsible for moulding and maintaining tissue architecture in a developing organism. The initial observation suggesting the existence of CAMs in embryonic cells was provided by Townes and Holtfreter (1955) in their classic experiments on amphibian development (176). They observed that dissociated embryonic cells from gastrulae aggregate and sort themselves into the distinct germ layers of normal intact embryos. Holtfreters' work set the stage for future studies on selective aggregation and adhesion, which were essential in defining the properties of CAMs.

Recently it has also become evident that cell adhesion is a dynamic process linked to **signal transduction** pathways. While CAMs themselves do not possess any enzymatic activity, CAM-ligand binding has been implicated in calcium fluxes across the cell membrane, changes in inositol phosphate turnover, and protein kinase activation (31,41,51,93,100,152). These findings demonstrate that the developmental processes underlying cell adhesion are not simply due to intercellular binding, but also due to the activation of intracellular signalling events.

The work in this thesis concerns itself with **myelin-associated glycoprotein (MAG)**, a myelin specific CAM. MAG is a member of the **immunoglobulin (Ig) supergene family** and is essential for myelination in the central and peripheral nervous systems (CNS and PNS). MAG has been shown to be phosphorylated <u>in vivo</u> in rodent brain

(32,36), suggesting a link between MAG mediated cell adhesion and signal transduction processes. The objective of this thesis was to characterize the functional significance of MAG phosphorylation.

A brief review of signal transduction involving **protein tyrosine phosphorylation** will be provided, followed by a review of the **major classes of CAMs** and a summary of recent findings implicating **CAMs in signal transduction.** The last part of the introduction will concern itself with the **role of MAG in myelination.**

1.1 Protein Tyrosine Phosphorylation

Phosphorylation is one of the most common post-translational modifications of proteins and is involved in a wealth of cellular regulatory pathways. The most common amino acid residues phosphorylated are the three hydroxy amino acids serine, threonine and tyrosine, although rare functional phosphorylations of other amino acids do occur (65). The enzymes that catalyze the phosphotransferase reaction are the protein kinases, which have been classified according to conserved homologies in their catalytic domains (61). Eukaryotic protein kinases are divided into 3 main groups: the serine/threonine kinases, the protein tyrosine kinases (PTKs) and the recently identified serine/threonine/tyrosine (STY) kinases (12,73), named for their ability to phosphorylate all three hydroxy-amino acids. Tyrosine phosphorylated proteins account for as little as 0.01% of cellular phosphoproteins, the rest comprising serine and threonine phosphorylated proteins (76). An increase in cellular phosphotyrosine levels correlates with transformation of normal cells into cancerous cells (155,156), illustrating the importance of regulating tyrosine

phosphorylation. Since the discovery of phosphotyrosine, it has become apparent that PTKs play key roles in regulating processes leading to cell growth and differentiation (43,56,58,85).

In general, PTKs can be classified into growth factor receptor (GFR) type PTKs exemplified by the epidermal growth factor (EGF), platelet-derived growth factor (PDGF) and insulin receptors (182), and the non-receptor PTKs typified by the c-src, c-fps and c-abl proto-oncogenes (61,74).

1.1.2 Growth Factor Receptor Tyrosine Kinases

The GFR kinases are typically transmembrane proteins with a growth factor binding site in the extracellular region and a catalytic domain residing in the cytoplasmic carboxyl terminus. Ligand binding causes GFR oligomerization and subsequent activation of PTK activity, which results in autophosphorylation on tyrosine residues of the GFR (182). Following receptor activation a number of cellular responses ensue, including activation of other PTK, hydrolysis of phosphatidyl inositol (PI) and calcium mobilization, leading ultimately to a mitogenic effect (182). Interestingly, the enzyme responsible for PI hydrolysis, phospholipase C-gamma (PLC), becomes tyrosine phosphorylated soon after GFR activation (187). This causes the activation of PLC activity itself (114), leading to a cascade of signal transduction events. Apart from PLC, other signalling molecules such as the cytoplasmic PTKs Src, Fyn and Yes, the Raf-1 serine/threonine kinase, the PI3 kinase, and the GTPase activating protein (GAP) involved in controlling ras activity are known to become tyrosine phosphorylated and associate with activated GFRs

(28,86,95,110). Furthermore, these signalling molecules associate only with autophosphorylated GFR. Site-directed mutagenesis studies demonstrate that the GFR binding sites correspond to specific tyrosine residues that become autophosphorylated during GFR activation (87). The GFR, therefore, serves as a docking site for multiple molecules, activating a number of signalling pathways during receptor stimulation.

1.1.3 Src Related Tyrosine Kinases

The gene encoding the v-Src PTK was first identified as the causative factor in chicken sarcomas infected with Rous sarcoma virus. It was then realized that the viral gene was derived from the normal cellular homologue c-src (166). To date, the c-Src related PTKs encompass eight well characterized members encoded by the src, lyn, fyn, yes, lck, hck, fgr, and blk proto-oncogenes (35,61). They encode cytoplasmic plasma membrane associated PTKs of molecular weights ranging from 56-62 kilodaltons (kd). A number of conserved features are present in all members, including an amino-terminal myristic acid group, which is in part responsible for plasma membrane anchoring, a catalytic domain, and two non-catalytic functional domains designated the src-homology regions -2 and -3 (SH2 and SH3 respectively) (74,91,148).

There are two major tyrosine phosphorylation sites in c-Src, which regulate its kinase activity. Phosphorylation of tyrosine residue 527 down-regulates c-Src activity, while phosphorylation of tyrosine 416 activates kinase activity (74). In cells in culture c-Src is constitutively inactive and phosphorylated on tyrosine 527. Mutation of tyrosine 527 to a phenylalanine, or deletion of tyrosine 527 (as in v-Src) results in the constitutive

phosphorylation of tyrosine 416 and activation of Src kinase activity (74). While the activities of GFRs are regulated by growth factor binding, the normal cellular mechanisms for regulating c-Src activity are unknown. PDGF stimulation results in an increase in PDGF receptor associated c-Src activity. The mechanism of this activation, however, is unclear, since no change in tyrosine phosphorylations of residues 416 and 527 were detected (55). Interestingly, other members of the src family exhibit a non-covalent association with cell surface receptors or adhesion molecules. Activation of these kinases ensues after receptor cross-linking or ligand binding (1,62,150,185,194) (also see section 1.2.14).

In mice, c-src is expressed ubiquitously in all tissues, with particularly high expression occurring in brain and platelets (19,53). Other members of this family exhibit a more restricted tissue expression pattern (1). The multitude of kinases in the Src-related PTKs possibly indicates a functional redundancy, which is reflected by recent experiments where a c-src null mutation was introduced into embryonic stem (ES) cells using homologous recombination. Mouse chimeras produced from these ES cells were used to transmit the mutated gene to their offspring. Mice homozygous for the mutation unexpectedly displayed a severe deficiency in bone remodelling and died within the first two weeks of life (161). However, general cell viability was not affected and no detectable defects in brain and platelet function were observed (161). These findings imply that the c-Src kinase is not essential for cell viability and its loss in activity can be compensated for by the presence of other PTKs (161).

1.1.4 The SH2 and SH3 Domains

Non-receptor type PTKs exhibit conserved non-catalytic regions at their amino-termini, which appear to function as regulatory domains. These regions have been named SH2 and SH3 domains, which play a role in regulating protein-protein interactions. While SH3 domains may be involved in mediating cytoskeletal association, SH2 domains bind specifically to phosphotyrosine residues in cellular proteins (6,91,107). A fascinating finding is that these domains also exist in other signal transducers such as PLC, GAP, PI3 kinase, and the crk oncogene encoded protein (6,91,106). In fact, in vitro studies show that the SH2 domains in PLC and GAP are responsible for the association of these proteins with activated GFRs (6). This suggests that protein-protein interactions via SH2 and SH3 domains may be essential in the transmission of signals leading to cellular proliferation or differentiation.

An interesting example of the importance of these non-catalytic regions in regulating PTK activity is illustrated with the abl encoded PTK. The oncogenic counterpart of c-Abl, v-Abl was first identified as a gag-Abl fusion protein of Ableson murine leukemia virus (191). Subsequent to this finding several other transforming mutants of the abl gene were identified in, among others, the bcr-abl fusion genes of human chronic myelogenous leukemia (CML) (92) and human acute lymphoblastic leukemia (ALL) (26). Oncogenic activation of v-abl has been shown to be due to certain N-terminal deletions (which include the SH3 domain) and replacement by viral gag sequences. Similarly, mutations in the SH3 domain of c-abl also result in its oncogenic activation (44,79), suggesting that the SH3 domain may be important in regulating Abl activity. In addition, an intact SH2

domain in v-abl also seems to be essential for its activity, since truncation of this domain results in loss of its transformation potential (136). In CML and ALL, however, the bcr-abl genes are a result of the fusion of c-abl sequences upstream of the SH3 domain to the first exon of the bcr gene, leaving the SH2 and SH3 domains intact. Recently, Pendergast et al. (130) demonstrated that Bcr interacts with high affinity with the SH2 domain in Abl. Unlike the previously identified dependence on tyrosine phosphorylation of SH2 binding proteins, the interaction of Bcr with the Abl-SH2 domain was dependent on the phosphorylation of Bcr on serine/threonine residues (130). Therefore, these results suggest that the SH2 and SH3 domains are essential for controlling Abl kinase activity. Furthermore, since serine/threonine phosphorylated proteins can also bind SH2 domains, the repertoire of possible protein-protein interactions is dramatically increased.

1.2 Cell Adhesion Molecules

It has become apparent that a multitude of different CAMs exist, often with cell-type specific expression patterns (78,82,99,163,170,189). Protein sequence analysis of these CAMs shows that extensive homologies exist between individual CAMs which have subsequently been classified into distinct categories. Three of these major groups of CAMs, the **cadherins** (169,170), the **integrins** (78), and the members of the **Ig supergene family** (189) will be reviewed here, as they are pertinent to the content of this thesis.

1.2.1 The Cadherins

A number of different cadherin molecules have been identified, such as E-cadherin (also frequently referred to as uvomorulin), N-cadherin- a neuron specific sub-type, and P-cadherin- an isoform found in placenta (170). E-cadherin is expressed early on during mouse embryogenesis and is essential for compaction of the blastomere at the 8-to -16 cell stage (77,169). All cells in the embryo express E-cadherin at the implantation stage. As the embryo differentiates into the three germ layers, E-cadherin expression is lost in the mesoderm (169,173). Likewise, during neurulation (the invagination of the neural plate to form the neural tube) E-cadherin disappears from the neuroectoderm and is replaced by N-cadherin upon closure of the neural tube (99,169). Furthermore, N-cadherin expression in neural crest cells is lost prior to their peripheral migration from the neural tube, and reappears as these cells form the sensory ganglia (99,169). These changes in temporal and spatial expression of cadherins reflect the importance of regulating CAM expression during development. Together with other CAMs, the cadherins are molecules indispensable for controlling animal morphogenesis.

In order to study how these molecules cause the selective adhesion and sorting of cells during embryogenesis, cadherin molecules have been expressed in non-adherent L cell fibroblasts (109,116). Using cell aggregation experiments, in principle similar to the ones devised by Holtfreter, it was determined that cadherin expression causes L cells to adhere to each-other (109,116). This aggregation phenomena could be specifically blocked using anti- cadherin antibodies (109,116). The binding properties of cadherins show an absolute requirement for calcium (Ca^{2+}) and are found to be homophyllic in nature

(109,116,169,170). This means that a cadherin molecule will selectively recognize and bind with high affinity to another cadherin molecule of the same class. Recently, it was determined that the amino-terminal 113 amino acids in cadherins determine their selective binding specificities (117). Site-directed mutations at only two amino acids in this region can change the binding specificity of one cadherin sub-type to bind to a different sub-type (117). Although these residues are essential for directing specificity of cell adhesion, binding activity occurs only in the context of the surrounding amino acids (117).

1.2.2 The Role of Cytoplasmic Domains

Amino acid sequence comparisons of each cadherin isoform demonstrate that these molecules are most conserved in their cytoplasmic domains (111). This finding suggested an essential role for the cytoplasmic domain in cadherin function. Indeed, cytoplasmic deletion mutants of E-cadherin lose the ability to confer cell adhesion properties to L cells (111). This loss of cell adhesion function correlates with the inability of the mutant cadherins to co-localize with cortical actin bundles at the zonula adherens junctions (111). Functional cadherins interact with three cytoplasmic proteins known as the catenins (125,126). The loss of cell adhesion function and cytoskeletal association of the mutant cadherins is associated with their inability to bind the catenins (125,126). Therefore, the catenins function as molecular bridges, linking the cadherin molecules to the cytoskeleton (170). Cytoskeletal anchoring probably serves to aggregate cadherins laterally at intercellular contact sites to generate sufficient cell adhesive forces (170). Deletion of the cytoplasmic domain prevents cytoskeletal association and results in a lack of cell adhesion

due to a diffuse expression of cadherins on the cell surface.

1.2.3 Cadherins in Signal Transduction

The ability of cadherins to function as morphoregulatory molecules was recently attributed not only to their cell adhesive properties, but also to signals transmitted across the plasma membrane via the CAM (31). Pheochromocytoma (PC12) cells have an adrenal chromaffin cell morphology and can be induced to differentiate into sympathetic-like neurons when treated with nerve growth factor (NGF) or fibroblast growth factor (FGF) (57,175). Doherty et al. (31) recently show that undifferentiated PC12 cells express N-cadherin. Co-cultivation of PC12 cells with 3T3 cell fibroblasts transfected with recombinant N-cadherin, will also cause PC12 cells to differentiate into neurons in the absence of NGF or FGF (31). This morphologic response is prevented by anti-N-cadherin specific antibodies, suggesting that it is due to N-cadherin specific homotypic interactions between PC12 cells and 3T3 cells (31). Moreover, Ca^{2+} channel blockers, pertussis toxin and the general kinase inhibitor K-252b also block this phenomena (31). The mechanism may, therefore, involve a CAM-dependent change in the cytoskeleton, causing the opening of G-protein coupled Ca^{2+} channels. The influx of extracellular Ca^{2+} may set signals in motion resulting in differentiation into a neuronal phenotype. The role of kinases is less clear and it is unknown whether protein phosphorylation occurs upstream or downstream of Ca^{2+} channel activation (31). Induction of PC12 cell differentiation by NGF is accompanied by an increase in cellular phosphotyrosine levels (101). Since studies on isolated zonula adherens junctions have localized members of the

src PTK family to these structures, it is possible that the intracellular domain of cadherins may also influence tyrosine phosphorylation in the cells (170). The exact mechanisms of cadherin mediated intracellular signalling remain to be resolved.

1.2.4 The Integrins

The integrins are heterodimeric molecules composed of non-covalently linked α- and ß- subunits (78). They bind components of the extracellular matrix as well as other CAMs expressed on the surface of adjacent cells. To date, twelve α-subunits and three main ß subunits have been identified that can combine in various ways to confer different ligand specificities. Due to their diversity, integrins make up a versatile recognition system providing cells with anchorage, traction for migration, and signals important for development and growth. Most integrins of the $ß_1$ subfamily function as receptors for extracellular matrix proteins, such as fibronectin, collagens, tenascin, vitronectin, osteopontin, thrombospondin and laminin (78,143,163). Integrins function by binding the tripeptide RGD in fibronectin and other extracellular matrix proteins in a Ca^{2+} dependent manner (143,163). The importance of integrin function during development is demonstrated by the disruption of amphibian gastrulation and avian neural crest cell migration, with RGD containing peptides (16). These are processes that involve major cell migratory events and are dependent on fibronectin (64). It is interesting to note that in migratory embryonic cells, which exhibit labile adhesion, integrins are distributed diffusely on the cell surface (16). In stationery adherent cells, however, integrins are concentrated at focal contacts where the cells are anchored to the substratum (16). There

they function as a transmembrane linkage between cytoskeletal elements and the extracellular matrix (21,171). The cytoplasmic domains of integrins interact with the cytoskeletal proteins talin, vinculin, α-actinin and actin (21).

1.2.5 Integrin Cytoplasmic Domains

Several lines of evidence have suggested that integrins can function as bi-directional signal transducers. Examples of "inside- out" signalling via the cytoplasmic domains of certain integrins and the possible role phosphorylation plays in regulating integrin binding activity will be discussed first.

Mutant integrins exhibiting cytoplasmic domain deletions in the $ß_1$ subunit are unable to bind components of the extracellular matrix and do not localize to focal adhesion contacts (53). This suggests that, similar to cadherins, the cytoplasmic domains of the integrin subunits are directly involved in regulating cell adhesion properties of the molecule. In v-src transformed cells the fibronectin receptor ß subunit is shown to be phosphorylated on tyrosine residues (70). Tyrosine phosphorylation results in a more diffuse expression of integrin on the cell surface and correlates with the transformation phenotype (72). Furthermore, tyrosine phosphorylated integrins have a decreased ability to bind fibronectin and talin compared to non-phosphorylated receptor (172). These results suggest that tyrosine phosphorylation may serve as a reversible regulatory mechanism of controlling cell adhesion function and that cell adhesion function may at least in part be involved in controlling cell phenotype.

In the case of $\alpha_{IIb}ß_3$ (also known as gpIIb-IIIa, a platelet specific integrin) truncations

of the α subunit cytoplasmic tail increase the affinity for the ligand fibrinogen (118). Fibrinogen binds to $\alpha_{IIb}ß_3$ after agonist mediated activation of the integrin (14). This is presumably due to the induction of a conformational change that exposes a fibrinogen binding site (157). Heterologous cells expressing the mutant integrins will bind fibrinogen in the absence of agonist stimulation, while cells expressing the wild-type molecules are still dependent on activation for fibrinogen binding (118). Therefore, cytoplasmic tail deletions of the α subunit mimic agonist stimulation, probably by inducing a structural change in the extracellular domain, thereby exposing the ligand binding site.

1.2.6 LFA-1

Integrins of the $ß_2$ subfamily are also known as the leukocyte integrins, since their function is limited to white blood cell adhesion (163). This group includes LFA-1 (leukocyte function related antigen-1) which mediates cell-cell adhesion by binding to the intercellular adhesion molecules (ICAMs) ICAM-1 (104) and ICAM-2 (165), which are members of the Ig supergene family. During T cell activation, LFA-1 binds the antigen presenting cell via ICAM-1 (34,163). Cross-linking of the T cell receptor complex (TCR) with monoclonal antibodies transiently increases the avidity of LFA-1 for ICAM (34). The increase in adhesion is not due to quantitative changes in cell- surface expression of the CAMs, but rather due to the conversion of LFA-1 from a low avidity state to a high avidity state (34). By contrast, ICAM-1 is constitutively avid (34,163). Thus, in the absence of antigen the T cells are free to roam for efficient immune surveillance. During infection, this mechanism of adhesion regulation may then serve to localize activated T

cells to sites of antigen accumulation. This effect can be mimicked by phorbol ester treatment of the T cells (34) which activates protein kinase C (PKC) (115). Furthermore, TCR activation results in a PKC- dependent cytoskeletal rearrangement, causing LFA-1 to become physically associated with F-actin via vinculin and α-actinin (127). PKC mediated phosphorylation of several integrin ß and α chains are known to occur (25,45,158) and may temporarily increase the interaction of integrins with the cytoskeleton, resulting in enhanced adhesion (163). Recently, Hibbs et al. (66) showed that cytoplasmic deletions in the ß chain, but not in the α chain, of LFA-1 eliminates its ability to bind to ICAM-1 even during phorbol ester treatment. This data demonstrates that the ß subunit cytoplasmic domain is the site of adhesion regulation in LFA-1.

1.2.7 Integrins in Signal Transduction

These examples of "inside-out" signalling in integrins demonstrate the importance of the cytoplasmic domain in the regulation of adhesion. Recently it has become apparent that integrins are also involved in "outside-in" signal transduction events, lending another dimension to the importance of integrins in cell regulation. For instance, LFA-1-mediated adhesion of neutrophils triggers a rise in cytosolic-free calcium levels (80). Presumably, the change in intracellular calcium may control secretion events, thus providing a link between adhesion and activation of leukocytes.

An intriguing signal transduction event involves the platelet integrin $\alpha_{IIb}ß_3$ during thrombin induced platelet aggregation. Thrombin treatment of platelets rapidly induces an increase in tyrosine phosphorylation of platelet proteins (41,51,52). This effect is not

seen when fibrinogen is prevented from binding to $\alpha_{IIb}ß_3$ using specific peptides (41), or when $\alpha_{IIb}ß_3$ mediated platelet aggregation is inhibited (52). Furthermore, platelets deficient in $\alpha_{IIb}ß_3$ (isolated from patients with Glanzmann thrombastenia) do not respond to thrombin with an increase in tyrosine phosphorylation, which directly implicates the integrin in the activation of PTKs (41). Aggregation of platelets involves many changes in cytoskeletal architecture. Since many cytoskeletal proteins are known to be phosphorylated on tyrosine, tyrosine phosphorylation may be required for events leading to or subsequent to platelet aggregation (52).

In a similar set of experiments, cross- linking of $ß_1$ integrins on the surface of human epidermal carcinoma cells with monoclonal antibodies induces the tyrosine phosphorylation of several cellular proteins (93). The time course of tyrosine phosphorylation parallels the formation of integrin clusters on the cell surface (93). Since integrin clusters occur at focal contacts (21), the induction of tyrosine phosphorylation may reflect a normal cellular response to environmental stimuli transmitted via integrin. Therefore, it is likely that the cytoplasmic domain in integrin may function as a binding site not only for cytoskeletal proteins, but also for signal transduction molecules. The integrin molecule then functions by sending bi-directional messages across the cell membrane, thereby modulating cell behaviour.

1.2.8 The Immunoglobulin Related CAMs

A large number of CAMs are included in this group due to their sequence and structural similarities to the immunoglobulins (189). There are essentially two Ig domains

with similar, yet distinct, structural features represented in this family of proteins. These are the V- and the C- domain folding patterns, which are essentially comprised of two ß strands stabilized by a disulphide linkage, thereby forming the characteristic Ig fold (189). Of particular interest are the proteins that exhibit C2-domains which include, among others, neural-cell adhesion molecule (NCAM), neural-glia cell adhesion molecule (NgCAM, NILE or L1), the inter-cellular adhesion molecules (ICAMs), members of the carcino-embryonic antigens (CEAs), CD4, the Drosophila CAMs fasciclin II and neuroglian, and the myelin-associated glycoproteins (MAGs) (189). Other non-CAM members of the Ig supergene family include proteins related to the platelet derived growth factor (PDGF) receptor, which are a group of transmembrane receptor PTK (reviewed in section 1.1.2). They do not function as CAMs, but have important roles in signalling events related to cell growth, proliferation and differentiation.

1.2.9 NCAM and L1

NCAM plays an essential role in embryogenesis and development of the nervous system. Similar to N-cadherin, NCAM appears soon after neural induction in the neuroectoderm (82,174) and is expressed uniformly throughout the neural tube and the neural crest cells. NCAM expression is lost during the peripheral migration of the neural crest cells, but reappears during the subsequent formation of the sensory and sympathetic ganglia (82,174). In the adult brain, NCAM occurs uniformly in neurons and to some extent also in astroglia and oligodendrocytes (82,99). NCAM exists as three isoforms, NCAM-180, NCAM-140 and NCAM-120 that are generated by alternative splicing of

the same primary transcript (82). All three isoforms exhibit identical extracellular domains and are heavily glycosylated with the major carbohydrate moieties consisting of polysialic acid (PSA) residues (82). The NCAMs, however, differ in their cytoplasmic carboxyl termini, where NCAM-120 is anchored to the plasma membrane via a PLC sensitive phosphatidyl-inositol linkage and does not contain a cytoplasmic domain. NCAM-120 and NCAM-140 are expressed early on in development during neurulation, while NCAM-180 appears only in post-mitotic neurons after termination of neuron migration (82). Furthermore, only NCAM-180 associates with the cytoskeletal proteins spectrin and actin, which results in a reduced lateral mobility of this isoform (132). Together, these findings suggest that NCAM-180 functions in stabilizing neuronal contacts.

NCAM is a calcium independent homophyllic CAM (71,146). The cell adhesion properties of NCAM increase during development from the embryonic forms to the adult forms (71,146). The increase is attributed to a decrease in the PSA content of the adult NCAM (71,146,164). NCAM adhesion in vitro can also be markedly affected by small changes in concentration. A two-fold increase of NCAM in liposomes increases adhesion thirty fold (71). NCAM is also shown to promote neurite outgrowth in cell culture. In a manner similar to the liposome studies, the ability of NCAM transfected 3T3 cells to promote neurite extension increases dramatically with small increments of NCAM expression (32). These results suggest that a critical threshold value for NCAM expression is required for promoting neuronal process outgrowth (32). Thus, small changes in NCAM expression may drastically affect neuronal architecture.

Another neural CAM with high homology to NCAM is L1, a glycoprotein that during development makes its first appearance in fully differentiated neurons (99). L1 and NCAM are both responsible for the granule cell migration during the formation of the cerebellar layers (99). This process involves neurite extension and migration of the granule cells along the Bergman glia (99). As is the case with NCAM, L1 functions as a calcium independent homophyllic CAM (147). But unlike NCAM, L1 can also participate in heterophyllic binding. This binding mechanism is unique in that it involves an interaction of L1 with NCAM (in cis) on the same cell to provide a potent receptor for L1 (in trans) on an adjacent cell (147). NCAM does not bind the L1-NCAM heterodimer. Both L1 and NCAM are phosphorylated in brain (147,162). Although the significance of phosphorylation is currently unknown, protein kinases can be co-purified with L1 from brain extracts, suggesting a function for L1 in kinase mediated signalling (147).

1.2.10 The ICAMs

The ICAMs, as described earlier, function as receptors for the leukocyte integrin LFA-1. ICAM-1 is a transmembrane glycoprotein that exhibits five Ig-like domains (104). In the absence of an immune response its expression is limited to only a few cell types (163). Unlike LFA-1, its adhesion properties are a function of its cell surface expression. Inflammatory mediators, such as interleukin-1 and tumor necrosis factor can dramatically induce the expression of ICAM-1 in a variety of tissues (163). This mechanism ensures the rapid and avid binding of LFA-1 expressing leukocytes and can lead to T-cell

mediated killing. ICAM-2 is highly homologous to ICAM-1, but exhibits only 2 Ig-like domains (165). ICAM-2 expression is constitutive in endothelial cells and remains unchanged during an inflammatory response (163).

ICAM-1 also serves as a receptor for Mac-1, another leukocyte integrin. While the binding site of LFA-1 is restricted to the first Ig-like domain in ICAM-1, Mac-1 binds to the third Ig-like domain (30). These results suggest that the tandem duplication of the Ig-like domains in ICAM-1 provides a means to increase the repertoire of adhesive interactions. This finding may have significant implications for other members of the Ig supergene family.

1.2.11 CEA and BGP

CEA was initially identified as a tumor specific antigen in colorectal cancer (50). The in vivo function of CEA and its importance in development is still unclear. However, it's overproduction in certain human tumors led to the development of valuable clinical assays (13). CEA is a 180 kd glycoprotein, linked to the cell surface via a phosphatidyl-inositol linkage, that can function as a homophyllic calcium independent CAM in cell culture (13). Many members of the CEA family have since been identified. They encompass a variety of cell surface and secreted glycoproteins (8,10,68,89,112,159,188) and some appear to also function as CAMs (13,142,196). An interesting addition to the CEA family was identified with the cloning of biliary glycoprotein (BGP) and its alternatively spliced isoforms (8,68). BGPs are expressed in human liver and several human tumor cell lines (8). Unlike other members of this group of proteins, the BGPs

exhibit transmembrane and cytoplasmic domains. BGPa and BGPc are identical in their extracellular and transmembrane domains, but differ in their cytoplasmic tails (8). BGPb and BGPd have their extracellular domains in common, but share cytoplasmic domains with BGPa and BGPc respectively (8). The longer cytoplasmic coding region for BGPa and BGPb reveal several potential phosphorylation sites, which are absent in BGPc and BGPd (8). The significance of splicing the intra- and extracellular domains in such a fashion remains to be investigated.

1.2.12 MAG

MAG is a myelin specific glycoprotein of 100 kd molecular weight that exhibits five Ig-like domains in the extracellular region (7,96,149). It is a type 1 integral membrane protein, with an amino-terminal ectodomain, a single transmembrane domain, and a cytoplasmic carboxyl-terminus (129). Expression of MAG is limited to oligodendrocytes in the CNS and Schwann cells in the PNS (167). Using in situ hybridization, MAG mRNA has also been localized to CNS neurons (67). However, in the absence of conclusive reports on MAG protein expression in neurons, the significance of this finding remains unclear. Earlier reports of MAG protein detection in neurons (119,131) using antibodies have been dismissed as cross reactivities to other neuronal antigens (9).

MAG is encoded by a single gene located on chromosome 7 in the mouse (29). The MAG gene contains 13 exons, 10 of which are coding (7,96,149). MAG exists as two developmentally regulated isoforms that are generated by alternative splicing of the same primary mRNA transcript. They are designated L-MAG (for long-MAG, also p72) and

S-MAG (for short-MAG, also p67) which exhibit molecular weights of 72 kd and 67 kd, respectively, in the unglycosylated forms. L-MAG and S-MAG are identical in their extracellular and transmembrane domains. They also share a common region in their cytoplasmic tails, but differ in their carboxyl-termini. The structural features and differences between L-MAG and S-MAG are summarized in a schematic diagram (Figure 1.1). S-MAG exhibits a unique 10 amino acid carboxyl-end due to the inclusion of exon 12, which introduces a 45 base pair sequence at the 3'end of the MAG transcript (7,96,149). L-MAG contains an extra 54 amino acid residues, which are encoded by exon 13 (7,96,149). Exon 13 is not translated in S-MAG, due to an in frame stop codon at the 3'end of exon 12.

Analysis of the protein sequence data reveals that L-MAG and S-MAG exhibit an amino acid sequence in their cytoplasmic domains that bears striking homology to the carboxyl 21 amino acids in the β_1 subunit of integrin (149,171). This region in integrin is responsible for binding the cytoskeleton (172). It is, therefore, possible that the MAGs also interact with cytoskeletal components. In this context, it is interesting that F-actin and spectrin have been localized to similar periaxonal regions as MAG in Schwann cells (179). Both isoforms also exhibit several potential phosphorylation sites, including a putative PKC site and a tyrosine homologous to the integrin β_1 tyrosine phosphorylation site identified in src-transformed fibroblasts (7,149). An additional potential PKC phosphorylation site as well as a region closely resembling the tyrosine-autophosphorylation site of the EGF receptor are identified in sequences unique to L-MAG (7,149).

Figure 1.1: Schematic representation of L-MAG and S-MAG. The extracellular domains of L-MAG and S-MAG are characterized by Ig-like C2 domains. The cytoplasmic domains contain multiple potential phosphorylation sites which are indicated as S (serine), T (threonine) and Y (tyrosine). Sequences homologous to phosphorylation sites for protein kinase C (PKC), protein kinase A (PKA) and protein kinase G (PKG) are shown as shaded boxes. Furthermore a stretch of amino acids resembling the EGF-receptor tyrosine autophosphorylation site (EGF-R) as well as sequence homologous to the integrin ß-chain cytoplasmic domain (INTEGRIN) are displayed.

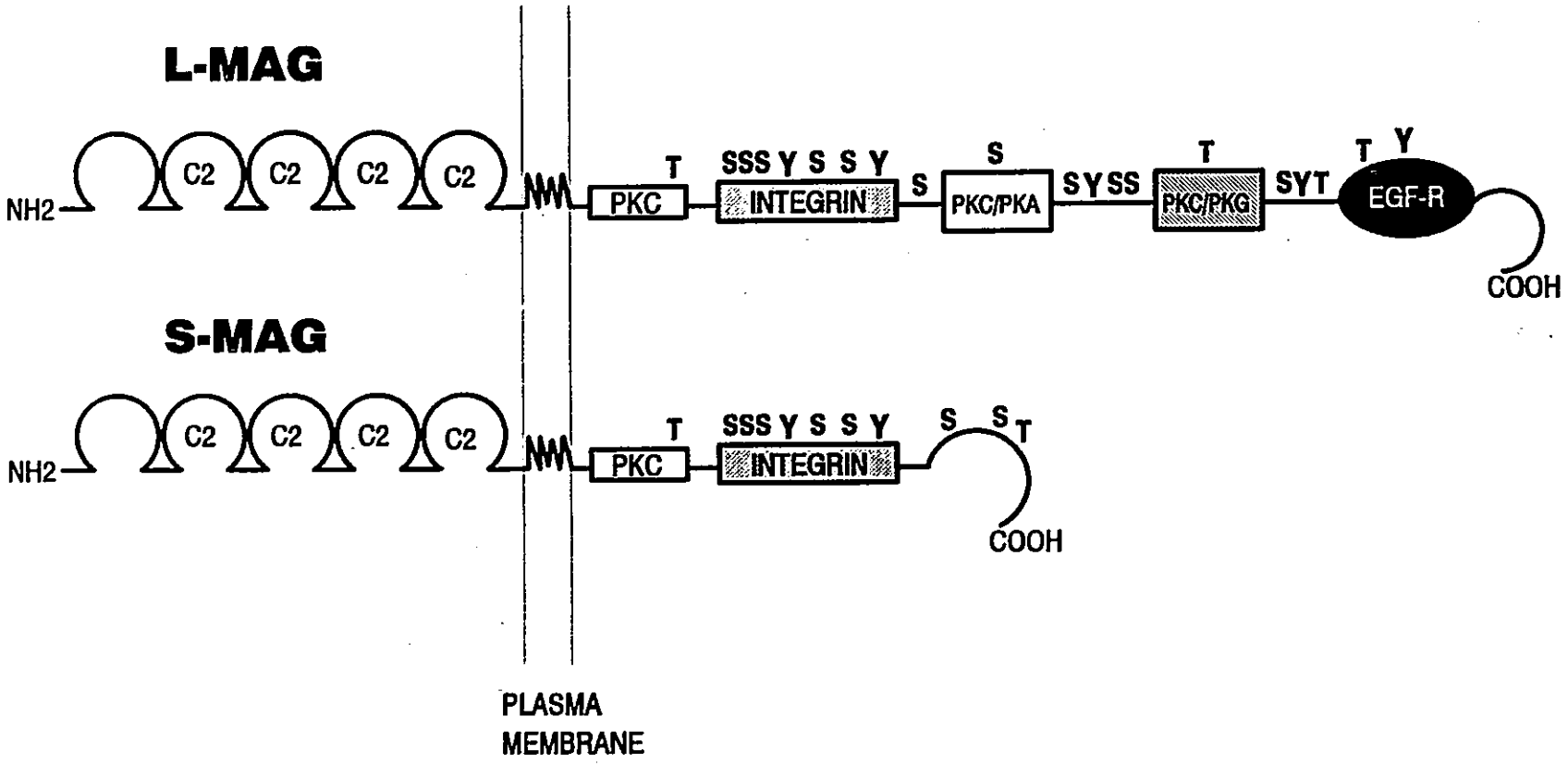
L-MAG
NH2
C2
C2
C2
C2
T
PKC
SSS Y S S Y
INTEGRIN
S
S
PKC/PKA
SYSS
T
PKC/PKG
SYT
T Y
EGF-R
COOH
S-MAG
NH2
C2
C2
C2
C2
T
PKC
SSS Y S S Y
INTEGRIN
S S T
COOH
PLASMA
MEMBRANE

In vivo and in vitro studies on rodent brains show that MAG is phosphorylated mainly on serine, but to some extent also on threonine and tyrosine residues (36,37). This phosphorylation seems to be restricted to L-MAG and occurs during the period of rapid myelination (36,37). These findings suggest a potential role for serine/threonine kinases and PTKs in the regulation of MAG function.

1.2.13 MAG as a CAM

The sequence homology of MAG to other members of the Ig supergene family led to the notion that MAG functions as a CAM. Ultrastructural data reveals that membranes enriched in MAG appose other membranes by a characteristic 12-14nm gap (177). The maintenance of this space is in agreement with the size and polarity of the ectodomain of MAG (177). The first in vitro evidence to suggest that MAG may function as a CAM stems from studies using purified MAG incorporated into liposomes. These liposomes bind specifically to neurons, oligodendrocytes, astrocytes and fibroblast-like cells in culture (133,145). As MAG expression is restricted to oligodendrocytes, the binding was postulated to be heterophyllic in nature. The identity of the MAG receptor is unknown. However, the time period of rapid myelination of neurons in culture coincides with maximal liposome binding, suggesting that MAG receptor expression correlates with the state of myelination (145). Furthermore, MAG liposomes only bind spinal cord and dorsal root ganglia neurons, which are myelinated in intact tissue (145). Cerebellar granule cell neurons, which are not myelinated, show very little liposome binding (145). These findings suggest that the MAG receptor exhibits a definite cell specific and

temporal expression pattern. Since the liposomes also bind non-neuronal cells, MAG may mediate oligodendrocyte-oligodendrocyte and astrocyte-oligodendrocyte interactions.

MAG contains an RGD sequence in its ectodomain domain, raising the possibility that, similar to ICAM, MAG may bind an integrin-like molecule. However, RGD peptides do not block MAG liposomes from binding to cells in culture (145). Additionally, the RGD sequence is buried in an inaccessible site within the first Ig-like domain (129). This finding renders the RGD sequence an unlikely candidate as the receptor binding site.

Soluble MAG purified from brain homogenates binds several collagen types, but not other extracellular matrix proteins (40). The significance of this finding is uncertain, since soluble MAG does not interfere with the binding of MAG liposomes, even when used in a thousand-fold excess (145). This may mean that soluble MAG, which does not contain the transmembrane and cytoplasmic domains, exists in a different conformational form compared to membrane bound MAG. Moreover, the binding ability of MAG possibly depends on oligomerization in the membrane and may not proceed in the monomeric state. Alternatively, membrane anchoring of MAG may hide its collagen binding site.

Expression of recombinant S-MAG in 3T3 cells induces neurite outgrowth from dorsal root ganglia, demonstrating a further function for MAG binding activity (83). The physiological significance of this study, however, is not clear. Neurite outgrowth in vivo is complete by the time myelination commences (140). Secondly, oligodendrocytes in the CNS express proteins inhibitory to neurite extension (24,153) resulting in poor neuronal regeneration after injury (154). Therefore, MAG is unlikely to function as a promoter

of neurite outgrowth in the CNS in vivo. In the PNS, a similar situation occurs, in which MAG appears after neuronal outgrowth is complete (140). Neuronal regeneration in the PNS is solely dependent on basement membrane formation (23,151,154). Although soluble MAG has been found in the extracellular matrix (40), the cell adhesion properties of soluble MAG are clearly different from membrane bound MAG. Hence, MAG function in vivo is likely restricted to a role in myelination. Expression of MAGs in heterologous cells, however, may provide a system in which the function of each isoform can be investigated separately.

1.2.14 Ig Related CAMs in Signal Transduction

In a manner analogous to integrins and cadherins, Ig related CAMs are also known to function in signal transduction. PC12 cells, which express NCAM and L1 on the cell surface, show an increase in intracellular Ca^{2+} and a decrease in intracellular concentrations of D-myo-inositol 1,4-bisphosphate (IP2) and D-myo-inositol 1,4,5-trisphosphate (IP3), when triggered with anti-NCAM and L1 specific antibodies (152). This effect is reproduced when PC12 cells are allowed to adhere to one another. The significance of this finding is illustrated in a more recent study by Doherty et al. (31) showing that PC12 cells can differentiate into neuron-like cells in an NCAM and N-cadherin (see also section 1.2.3) homophyllic adhesion dependent fashion. In both studies, a similar mechanism has been proposed, involving G protein-linked signal transduction events and activation of N- and L-type Ca^{2+} channels. In the Doherty study, however, antibodies directed against NCAM and N-cadherin inhibit PC12 cell

differentiation, rather than mimicking the effect of CAM homophyllic adhesion (31). This result may reflect the action of different antibodies used in the two studies. Alternatively, the morphoregulatory effect of NCAM and N-caherin may be more complex in nature, requiring other intercellular signals, which are not transmitted by antibody binding.

In the immune system, T-cell activation is a function of several different CAMs binding to their ligands on the antigen presenting cells (163). T-cell activation is characterized by mobilization of second messengers and the activation of PTK activity resulting in the proliferation and differentiation of functional T-cells (48). The increase in tyrosine phosphorylation precedes the generation of second messengers and is attributed to a number of PTKs. Fyn, a member of the src family of PTKs, was recently shown to be associated with the TCR complex (150). Two other CAMs involved in T-cell activation, CD4 and CD8, function by binding MHC class II and MHC class I on the antigen presenting cell, respectively. CD4 and CD8 are tightly linked to another src-like cytoplasmic PTK- $p56^{lck}$ (185). Antibody mediated cross-linking of CD4 and CD8 on the cell surface activate the PTK activity of $p56^{lck}$, resulting in the phosphorylation of several protein substrates (186). In an analogous system, the B-cell surface antigen receptor (Ig) is linked to the cytoplasmic PTK Lyn (194).

The Drosophila CNS specific CAM fasciclin I (fas I, not an Ig supergene family member) has been shown to exhibit a functional interaction with the PTK encoded by the abl proto-oncogene. Drosophila embryos doubly mutant for fas I and abl show marked defects in CNS development, while embryos deficient in either gene alone exhibit a normal phenotype (39). This suggests that a functional redundancy exists in Drosophila

CNS development. A physical association of fas I protein with Abl has not been demonstrated (39), distinguishing this interaction from that of CD4 with Lck.

An interesting member of the Ig supergene family is the leukocyte common antigen related protein (LAR). The cDNA for LAR encodes a putative transmembrane phosphotyrosine-specific protein phosphatase with homologies to NCAM (168). While this protein may not function as a bona fide CAM, it may act as a signalling molecule in a manner comparable to the PDGF-R family of PTKs.

These examples illustrate the complexity of intercellular interactions and demonstrate that cell adhesion and signal transduction are often closely linked processes.

1.3 Myelin

Myelin is a membrane that envelops selected nerve fibres in the CNS and PNS (reviewed in (140)). It developed as an evolutionary adaptation to render nerve conduction more efficient as organisms increased in size and complexity. Myelin functions as an insulator for increasing nerve impulse velocity by inhibiting the flow of ions across the axonal membrane. Unmyelinated nodes are distributed along the entire axonal surface at regular intervals in order to prevent the loss of nerve conduction. These are named the nodes of Ranvier and they are rich in ionic channels. The action potential propagates by jumping from node to node. Hence, this process, described as saltatory conduction, is the basis for the rapid velocity of conduction.

Myelin is rich in lipids and expresses a distinct set of myelin specific proteins. There are certain fundamental differences between PNS and CNS myelin (reviewed in (97)).

The major proteins of PNS myelin are P_0, myelin basic protein (MBP) and MAG. While P_0 and MBP make up well over 50% of peripheral myelin proteins, MAG is a relatively minor constituent and accounts for only 0.1% of myelin proteins (97). Myelin in the PNS is produced by a specialized cell type: the Schwann cell. Any single axon has several Schwann cells associated with it, where each internodal region is myelinated by a single Schwann cell (140). Schwann cells associate with neurons prior to myelination. This neuronal association induces the expression of several myelin specific proteins and a myelin specific lipid, galactocerebroside (GalC), which are essential for the initiation and progression of myelin synthesis (122,123). Furthermore, a basal lamina, composed of several extracellular matrix proteins, is laid down just prior to myelination (20). In the PNS, myelin synthesis starts with the expansion of mesaxon membranes. The mesaxon is a Schwann cell process that grows spirally around the axon. After several spiral turns, the mesaxon membranes fuse to form the major dense line of compact myelin (140). The cytoplasm is extruded from this region, but is maintained in the periaxonal region, the paranodal loops and the Schmidt-Lantermann incisures, which are cytoplasmic channels that run through the myelin sheath (140).

The major CNS myelin constituents are proteolipid protein (PLP) and MBP which account for 60-80% of myelin proteins (97). MAG in the CNS constitutes approximately 1% of total myelin proteins (97). In the CNS myelin is produced by the oligodendrocyte, which in contrast to Schwann cells, myelinates dozens of axons at the same time (140). They initiate myelination by extending a process into the neuropil and selectively myelinate axons. This implies that a mechanism is in place to recognize the specific

axons that are to be myelinated. Unlike Schwann cells, oligodendrocytes express the proteins necessary for myelination prior to neuronal contact and do not need a basal lamina for this process. In CNS myelin, compaction occurs almost immediately and the cytoplasm is restricted to the inner periaxonal region, the external lip of the oligodendrocyte process and the lateral loops adjacent to the nodes of Ranvier (140).

1.3.1 The Role of MAG in PNS Myelination

At the start of peripheral myelination, Schwann cells select axons with a sufficient diameter ($> 1\mu m$) that are destined to be myelinated (123,124). Just prior to myelination, the axonal interaction with Schwann cells induces the expression of MAG and GalC (122,123). Cell culture studies show that prevention of basal lamina formation by excluding ascorbic acid and serum in the medium will prevent Schwann cell differentiation. In the presence of neurons, however, these undifferentiated Schwann cells are still induced to produce MAG and GalC (123). With the addition of serum and ascorbic acid, myelination proceeds to completion. Similarly, depletion of GalC from the Schwann cell surface with an anti-GalC antibody does not affect MAG expression. In this case myelination is initiated, but not continued (123). In an elegant study by Owens and Bunge (124) Schwann cells were infected with recombinant retroviruses expressing either sense or antisense MAG RNA. Schwann cells infected with the antisense virus expressed lower levels of MAG and failed to initiate myelination, despite having formed a basal lamina (124). Sense-virus infected cells formed normal myelin and expressed high levels of MAG (124). Thus, the function of MAG is to select the axons destined to be

myelinated, most likely by initiating one of the first recognition events.

These results are in contrast to Martini and Schachner (105), who show that Schwann cells express MAG only after the mesaxon has looped around the axon 1.5-2 times. Although these differences in MAG staining may be accounted for by alternate tissue and cell fixing procedures, it is now generally accepted that MAG expression precedes myelin synthesis. Their finding that the initial binding of Schwann cells to neurons is mediated by NCAM and L1 (105), is corroborated by recent work demonstrating that anti-L1 antibodies block Schwann cell myelination in culture and prevent the expression of MAG and GalC (193). Binding of L1 to its receptor may, consequently, transduce a signal to cause an increase in MAG and GalC expression. Presumably, MAG then binds its receptor on the axonal surface and myelination is initiated. After myelination is initiated, L1 expression is no longer detectable, while MAG expression is retained (105). This suggests that MAG is also involved in maintaining Schwann cell-neuron contact. Thus, the process leading to myelin synthesis in the PNS is a complex series of events consisting of binding phenomena that involve at least two CAMs, MAG and L1. These findings illustrate how MAG is essential for the initiation and maintenance of myelination in the PNS.

S-MAG is the predominantly expressed isoform in the PNS (43,181). Previously S-MAG was thought to be the only isoform expressed in the PNS. Recently, using isoform specific antibodies, low level L-MAG expression was detected at the start of myelination in rats, but was virtually absent in adult animals (128). An interesting finding is that overexpression of L-MAG in Schwann cells using a retroviral expression vector does not

affect myelination (121). Initially, infected Schwann cells overexpressed L-MAG and induced the ensheathment of about ten times as many sensory neurons as compared to control cultures (121). This illustrates how MAG expression can be a determining factor for axonal myelination. After long-term co-cultivation of recombinant Schwann cells with the neurons MAG expression was decreased to levels comparable to uninfected cells involved in myelination (121). Furthermore, while normal Schwann cells lose MAG expression when not in contact with axons, infected cells retained strong MAG immunoreactivity. The transcription of recombinant MAG cDNA is driven by a viral long terminal repeat, which is removed from cellular control. Accordingly, this implies a post-transcriptional level of MAG down-regulation, which is induced by axonal contact (121).

In mature PNS myelin, MAG immunoreactivity occurs on the periaxonal surface, at the paranodal loops and at the Schmidt-Lanterman incisures (177,180). MAG is completely absent from compact myelin (177). Compaction seems to be a function of MBP and P_0 expression (120,134,135,141,177). MBP deficient mice do not exhibit properly compacted myelin (134,135,141). The mode of action of MBP in compaction is, however, unclear. P_0 has recently been shown to exhibit homophyllic binding properties (42). Hence, it may serve as a CAM between apposing myelin membranes in the major dense line. Ultrastructural data demonstrates that apposing membranes in compact myelin are separated by a 2nm gap, which is in agreement with the smaller extracellular domain of P_0 (177). Expression of antisense P_0 RNA in Schwann cells seriously limits the development of the myelin sheath (120). P_0 expression is markedly

reduced, yet MAG expression occurs and initiation of myelin synthesis is unaffected (120). It is interesting to note that in normal Schwann cells, MAG expression is restricted to mesaxons containing Schwann cell cytoplasm (120,177). A function of MAG may, thus, be to maintain Schwann cell cytoplasmic channels. Therefore, a consequence of limiting P_0 expression is to allow MAG expression to persist and prevent compaction.

A comparable situation occurs in the Quaking mouse mutant. Quaking mice display a slow progressive demyelination and remyelination and are characterized by a dilation of the periaxonal space with a resulting loss of Schwann cell periaxonal cytoplasm (177). MAG expression is limited to periaxonal membranes that exhibit the normal spacing of 12-14nm from axonal membranes (177). These areas appear to show normal periaxonal Schwann cell cytoplasm (177). However, in regions where dilation of the periaxonal space has developed, MAG is absent and the Schwann cell membranes resemble compact myelin of the major dense line. Thus, MAG expression correlates with the maintenance of the periaxonal space and the Schwann cell periaxonal cytoplasmic collar. Since the Quaking locus does not map to the MAG gene (98), the change in MAG distribution is secondary to the main defect. This leads to the possible interpretation that MAG functions by interacting with cytoplasmic components, such as cytoskeletal proteins, or signal transduction molecules. A possible reflection of this interaction is the maintenance of Schwann cell cytoplasm by MAG.

1.3.2 The Role of MAG in CNS Myelination

Analysis of CNS myelination has so far been restricted to in vivo studies, since in vitro work on oligodendrocytes show that these cells only poorly myelinate neurons (192). Using the developing mouse optic nerve as a model system, Bartsch et al. (105) describe the initial events in CNS myelination. MAG immunoreactivity is detected early on, prior to axonal ensheathment by the oligodendrocyte. After the initiation of myelination, MAG disappears from compacted myelin but stays strongly expressed in the periaxonal region (9). MAG was also weakly expressed in other non-compacted myelin structures, such as the inner mesaxon and paranodal loops (9). Compaction in the CNS seems to be a result of MBP expression (134,141). Consequently, a suggested function for MAG is mediating the initiation of neuron-oligodendrocyte contact, possibly by inducing the first binding event. Based on the later expression of MAG in the inner mesaxon, a subsequent role in stabilizing neuron-oligodendrocyte and oligodendrocyte-oligodendrocyte interaction is also proposed (9).

The function of other CAMs, such as L1 and NCAM, seem less important in CNS myelination. In contrast to the PNS, L1 does not appear to be involved in CNS myelination and its expression disappears in myelinated axons (9). Additionally, NCAM appears to serve as a general CAM involved in preserving the tissue integrity, rather than playing a specific role in myelination (9).

During the early stages of CNS myelination, the predominant MAG isoform is L-MAG (43,181). L-MAG expression appears just prior to formation of the myelin sheath and persists at a high level during the period of rapid myelination. As myelination is

completed in the adult brain, L-MAG expression declines to lower levels and S-MAG expression predominates (43,181).

The purpose of regulating the expression of the different MAG isoforms in the CNS is unknown. Nonetheless, it is interesting to speculate that these isoforms have different functions during the initiation and maintenance of the myelin sheath. In Quaking mice there is an apparent lack of L-MAG expression during the period of rapid myelination in brain (46,47). This is evidently due to a deficiency in the splicing mechanism for MAG (47). S-MAG expression dominates during all stages of myelination. Therefore, the lack of L-MAG expression may contribute to the Quaking phenotype. It was proposed that the Quaking mutation resides in a gene responsible for the correct splicing of MAG isoforms during development (46). This data suggests that L-MAG performs a specific role in CNS myelination, which cannot be performed by S-MAG.

Immunohistochemical staining of CNS myelin using L-MAG specific antibodies reveals a difference in the staining pattern between 7 day old myelin (which predominantly expresses L-MAG) and adult myelin (which contains mostly S-MAG). While the staining of periaxonal MAG is the same in young and in adult myelin, 7 day old MAG is also enriched in cytoplasmic endosomes (178). Endosomal staining of MAG is not seen in adult myelin or in PNS myelin, implying that endosomal MAG is analogous to L-MAG only (178). Furthermore, early MAG has also been co-localized to clathrin coated pits (178). Clathrin coated pits are associated with ligand induced internalization of membrane bound receptors during signal transduction events (18,182). Internalized receptors are then found in endosomes from which they are channelled to a lysosomal compartment

for degradation, or alternatively, recycled back to the cell surface (18). Therefore, the localization of MAG to an endosomal compartment raises the possibility that MAG internalization is caused by the binding of a ligand. Similar to other CAMs, MAG may be implicated in signal transduction. L-MAG is known to be phosphorylated in oligodendrocytes in vivo (36), demonstrating an interaction of MAG with signalling molecules. The generation of alternative MAG isoforms, therefore, might serve to increase the biological repertoire of MAG action. While L-MAG may act both as a CAM and a signal transducing molecule during the period of rapid myelination, the function of S-MAG may be more restricted.

1.4 Thesis Project

The objective of this thesis was to examine the functional significance of MAG phosphorylation. Previously, MAG was shown to function as a putative CAM when expressed in liposomes (133,145). In chapter 3 a more physiological approach is undertaken and the cell adhesion properties of MAG expressed in non-adherent L cell fibroblasts are described. L cell fibroblasts have been chosen for this experiment, since they do not adhere to each other when grown in suspension. The results show that MAG functions as a heterophyllic, calcium and temperature independent CAM.

Prior to this investigation, MAG was shown to be phosphorylated in mouse brain during the active period of myelination (36,37). In chapter 4 the phosphorylation of L-MAG and S-MAG is characterized. Similar to the in vivo studies, L-MAG is found to be phosphorylated on serine, threonine and tyrosine residues. While L-MAG and S-MAG

share the major phosphorylation sites, the stoichiometry of L-MAG phosphorylation is an order of magnitude higher than that of S-MAG. The significance of this finding with respect to signal transduction is discussed.

In chapter 5 an attempt is made to link the phosphorylation of MAG with its function as a cell adhesion molecule and its possible role in signal transduction.

Appendix I deals with a side project that emanated from the interest in CAMs as PTK substrates. The biliary glycoproteins, BGPa and BGPb, are identified as substrates for protein kinases. Similar to MAG, the phosphorylation occurs on all three hydroxy-amino acids. The significance of this finding with respect to MAG and other CAMs is discussed.

CHAPTER 2

MATERIALS AND METHODS

2.1 Cell Lines

NIH 3T3 cell lines (PA317 and Psi_2) expressing L-MAG were obtained from the laboratory of Dr. J.L. Salzer. Stable L-MAG expressing cells were maintained in αMEM, 10% fetal calf serum, supplemented with G418 resistance (600μg/ml) and are referred to as LM cells in the text. Stable S-MAG expressing 3T3 cells were obtained from Dr. J. Roder's laboratory (Johnson et al., 1989). The S-MAG expressing clone used in our study ($3TV_2$-9) is referred to as SM cells in the text. The v-src transformed NIH 3T3 cell line, PVsrc, was infected by co-cultivation with virus from the Psi_2 cells expressing L-MAG. Psi_2-L-MAG cells were treated with mitomycin C (200 μg/ml) for 2 hours and then co-cultured with PVsrc cells in a ratio of 1:2 for 24 hours. After 24 hours, stable infectants were selected by G418 resistance (600 μg/ml in αMEM, 10% FCS) and are referred to as PVsrcLM cells.

L-MAG expressing L cell fibroblasts were generated by co-cultivation with virus from Psi_2 cells expressing L-MAG as described above. Stable infectants were selected by G418 resistance and colonies were screened for MAG expression using immunofluorescent cytochemistry on live cells and immunoblot analysis of whole cell extracts. Five independent clones were selected based upon their graded immunofluorescence staining and analysis by immunoblotting and were used in all subsequent experiments. These clones are referred to in the text as C3, A2, D2, A1 and C5 in increasing order of MAG expression.

Stable S-MAG expressing PVsrc and L cell lines were generated by transfection of cells with the pecep67AX1 vector (a kind gift from M. Tropak and Dr. J. Roder) using

electroporation. After 24 hours, stable transfectants were selected by G418 resistance (600 μg/ml in αMEM, 10% FCS). The cell lines generated were screened by immunoblot analysis and are referred to as PVsrcSM12 for the src-transformed cells, and SM1, SM3, SM9, SM23, SM31, SM32, SM33, SM36, SM38, and SM48 for the L cells.

Primary oligodendrocyte cultures were the generous gift of Dr. G. Almazan. The oligodendrocyte precursors were generated from newborn rat cerebral hemispheres and were expanded in serum-free medium (SFM= DMEM:F12, 1:1) in the presence of 2.5 ng/ml PDGF and 2.5 ng/ml basic fibroblast growth factor (bFGF). After 5 days the precursors were allowed to differentiate in SFM for 12-14 days prior to the experimental treatments.

2.2 Immunofluorescence Cytochemistry

Cells were plated onto coverslips and incubated with anti-MAG monoclonal antibody 513 (generously provided by Dr. M. Schachner) (1:1000 in PBS 2% calf serum) for one hour at 4°C. The cover slips were then washed three times in PBS 2% calf serum and subsequently incubated with a fluorescein conjugated goat anti-mouse second antibody (Bio Can) for one hour at 4°C. After three washes in PBS 2% calf serum, the cells were fixed in 4% formaldehyde for 20 minutes and then mounted onto slides. Visualization of the immunofluorescence was achieved using epifluorescent microscopy.

2.3 Cell Membrane Isolation

Cell membranes were prepared by harvesting cells in 10 ml of ice cold hypotonic Hepes buffer (20 mM Hepes pH 7.2, 3 mM KCl, 1mM EDTA, 500 μM NH_4 VO_4, 2 mM Na F, 2μg/ml aprotinin, 5 μg/ml leupeptin, 0.4μg/ml pepstatin, 200 μgm/ml PMSF). The cells were lysed in a tight fitting glass homogenizer using 15 strokes on ice. DNA and cellular debris were removed by a 1000 x g centrifugation for 10 minutes. A membrane enriched fraction was obtained by subjecting the supernatant to centirfugation for 30 minutes at 100,000 x g. The membrane pellet was resuspended in the hypotonic Hepes buffer with 40% glycerol. Protein content was determined using the Bio Rad reagent.

2.4 Immunoblot Analysis

Whole cell extracts or membrane extracts dissolved in sodium dodecyl sulfate (SDS) sample buffer (5% SDS, 20% glycerol, 50 mM Tris pH 6.8, 5% ß-mercaptoethanol, 0.01% bromophenol blue) were resolved on SDS-polyacrylamide gel electrophoresis (SDS-PAGE) (7.5% or 10% polyacrylamide), transferred to nitrocellulose paper (Schleicher and Schuell Inc.) and probed with a polyclonal antibody directed against MAG, or anti-MAG monoclonal antibodies Gen 3 S1 and Gen 3 S3 (1:1000) (generously provided by Dr. N. Latov) or an antiphosphotyrosine monoclonal antibody (1:1000) (PY20 from ICN). Visualization of the blots were carried out using either an alkaline phosphatase-coupled goat anti-rabbit second antibody (for the polyclonal anti-MAG) or a ^{125}I labeled sheep anti-mouse second antibody (for all the monoclonal antibodies).

2.5 MAG Aggregation Assay

MAG expressing cells were trypsinized in 0.125% Trypsin (Gibco), 1mM EDTA for 2 minutes. The cells were resuspended in αMEM containing 0.8% fetal calf serum, 20 mM Hepes (Flow), at $0.5x10^6$ cells/ml. To obtain a single cell suspension, the cells were passaged 2 times through a 25 gauge syringe. In order to assay the cells for aggregation, 3 ml of cells were agitated at 37°C for different time periods on an orbital shaker at 80 rpm. At every time point an aliquot was removed and the total number of cells versus the number of single cells were counted using a haemocytometer. The degree of aggregation was calculated as the %single cells at time t (S_t) subtracted from the %single cells at time 0 (S_0) divided by S_0.

2.6 Cell Sorting

Cell sorting experiments were performed essentially as described by Benchimol et al.(13). Cells were harvested by trypsinization as described above (section 2.12) and resuspended in 100 μl of Puck's saline (5 mM KCl, 140 mM NaCl, 5 mM D-glucose, 4 mM $NaHCO_3$, 25 mM Hepes pH 7.4). The cells were then fluorescently labeled by the addition of 20 μl of fluorescein iso-thiocyanate (FITC, 500 μg/ml) for 15 minutes. The cells were then layered over 10 ml of FCS and pelleted to remove the excess FITC. They were then resuspended in αMEM, 0.8% FCS, and mixed in a 1:1 ratio with unlabeled cells.

2.7 Quantification of L-MAG in L cells by ^{35}S-Methionine Labeling

In order to determine the relative amounts of L-MAG in L cells, L-MAG expressing L cells were labelled for 18 hours at 37°C with ^{35}S-methionine (Amersham) (50μCi/ml) in methionine free MEM, supplemented with 10% fetal calf serum and 5% αMEM. The cells were washed two times with PBS and were harvested in 2% SDS. L-MAG was immunoprecipitated as described below using anti-MAG monoclonal antibodies Gen 3 S1 and Gen 3 S3. The samples were resolved on SDS-PAGE and subjected to autoradiography. The relative levels of MAG in each sample were quantified using an LKB Ultroscan XL enhanced laser densitometer.

2.8 Quantification of S-MAG in L Cells by Flow Cytometry

MAG expressing L cells (2 x 10^6) were harvested by trypsinization as described in section 2.12 and resuspended in 100 μl of ice cold PBS, 2% FCS containg 513 anti-MAG antibody (1:500). After 30 minutes on ice, the cells were pelleted, washed 2 times in PBS and were subsequently incubated for an additional 30 minutes on ice with 100 μl of goat anti-mouse FITC conjugated antibodies in PBS, 2% FCS. The cells were pelleted and washed 3 times in PBS, resuspended in αMEM and analyzed for cell surface fluorescence using a Coulter Epics Profile II flow cytometer. Cell autofluorescence was determined using non-expressing L cells and MAG positive cells incubated with secondary antibodies only.

2.9 ^{32}P-Orthophosphate Labeling of Cells

Cells were labeled with 1 mCi ^{32}P-orthophosphate/ml of phosphate free D-MEM, 10% fetal calf serum for 4 hours in the presence or absence of ammonium vanadate (50-500 μM). The cells were harvested by lysis in 250 μl of hot (100°C) 2% SDS. The cell lysate was passaged several times through a 25 gauge syringe needle and diluted to 1 ml with immunoprecipitation buffer (10 mM Tris HCl pH 7.4, 150 mM NaCl, 1% Triton, 500 μM NH_4 VO_4, 2 mM NaF, 2 mM Na pyrophosphate, 2 μg/ml aprotinin,5 μg/ml leupeptin, 0.4 μg/ml pepstatin, 200 μg/ml PMSF).

2.10 Immunoprecipitation of MAG

Immunoprecipitation of MAG was performed on ice with a one hour incubation of the cell lysate with a mixture of anti-MAG monoclonal antibodies Gen 3 S1 and Gen 3 S3. Subsequently rabbit anti-mouse antibodies (Jackson Immunoresearch Lab) were added for one hour prior to addition of protein A coupled Sepharose beads (Pharmacia). After an additional hour incubation the beads were washed five times with ice cold immunoprecipitation buffer and MAG was eluted using SDS sample buffer. The immunoprecipated samples were resolved by SDS-PAGE (7.5% or 10% polyacrylamide) and detected by autoradiography.

2.11 Deglycosylation of Proteins Using TFMS

Samples containing immunoprecipitated ^{32}P-labeled protein or 150 μg of membrane protein were precipitated with 12% TCA. The precipitates were washed twice with 1 ml

-20°C acetone and then lyophilized. Chemical deglycosylation was performed using trifluoromethane sulfonic acid (TFMS) (Aldrich) as described by Horvath et al.(72). Essentially, the samples were incubated with 5 μl anisole and 45 μl TFMS for 2 hours on ice under nitrogen (extra dry). The reaction was stopped with the addition of 900 μl of anhydrous ether and 100 μl of pyridine on dry ice. A precipitate was allowed to form over 1.5 hours and the insoluble material containing proteins was pelleted. The supernatant was discarded and the pellet was lyophillized for 0.5 hours. The material was resuspended in 15% TCA in immunoprecipitation buffer and allowed to precipitate. The pellet was washed twice in acetone, lyophillized and dissolved in SDS sample buffer for analysis on SDS-PAGE.

2.12 Stoichiometry of L-MAG Phosphorylation

In order to determine the half-life of L-MAG in LM cells, LM cells were labeled for 18 hours at 37°C with ^{35}S-methionine (Amersham) (50μCi/ml) in methionine free MEM, supplemented with 10% fetal calf serum and 5% αMEM. Then the cells were washed two times with PBS and were either harvested in 2% SDS or were incubated for an additional 4 hours and 9 hours in αMEM. L-MAG was immunoprecipitated as described above and resolved on SDS-PAGE. The half-life was calculated by extracting radioactive L-MAG out of excised gel slices and determining the amount of radioactivity in the extracts using liquid scintillation counting.

To assess the extent of L-MAG phosphorylation, LM cells were labeled for 18 hours at 37°C with either ^{32}P-orthophosphate (200 μCi/ml) or ^{35}S-methionine (Amersham)

(50μCi/ml) in αMEM containing 10% fetal calf serum. L-MAG was immunoprecipitated and resolved on SDS-PAGE. The number of moles of phosphate in L-MAG was determined by scintillation counting of the excised L-MAG bands. The number of moles of immunoprecipitated L-MAG was estimated from the level of ^{35}S-methionine incorporated, assuming that L-MAG contains 9 methionine residues (149). The specific activity of label in the media was determined by scintillation counting of an aliquot of the medium and from the known concentrations of phosphate (10 mM in αMEM and 1.5 mM in FCS) and methionine (0.2μM in αMEM and 0.03 mM in FCS).

2.13 Treatment of Cells With Growth Factors, Dibutyryl- cAMP and Phorbol Esters

To assess the effects of growth factor treatment on L-MAG phosphorylation, LM cells were fed αMEM without serum for 24 hours. The next day the cells were ^{32}P labeled in phosphate free medium without serum for 4 hours. Epidermal growth factor (EGF) (150ng/ml) (Boehringer Mannheim), insulin-like growth factor 1 (IGF-1) (Boehringer Mannheim) or insulin (0.5μM) (generously provided by Dr. M. Bernier) were added to the cells at the end of the labeling period for 10 minutes at 37°C. The effects of cAMP mediated phosphorylation of L-MAG and S-MAG was assessed by incubating LM and SM cells with either 5mM dibutyryl-cyclic AMP (dbcAMP) (Sigma) or sodium butyrate (5mM) during the labeling procedure. Sodium butyrate was used to control for non-cAMP related effects of dbcAMP. To determine the effects of phorbol esters on MAG phosphorylation ^{32}P-labeled cells were treated with 100 nM 4α Phorbol or 100 nM 12-O-Tetradecanoylphorbol 13-acetate (TPA) for 10 minutes at 37°C at the end of the labeling

period. The cells were harvested in hot 2% SDS and processed as described before.

2.14 Phosphoamino Acid Analysis

Phosphorylated proteins were immunoprecipitated, resolved on SDS-PAGE, and transferred to Immobilon-P membranes (Millipore). Radioactive bands corresponding to the immunoprecipitated proteins were excised from the membranes and hydrolyzed directly in 6N double-distilled HCl for 75 minutes at 110°C as described previously (84). The hydrolysate was lyophilized, mixed with authentic phospho-amino acids, spotted onto Cell type-100 thin-layer cellulose plates (Sigma) and resolved by two dimensional thin-layer electrophoresis as described by Cooper et al. (27). In the first dimension the samples are migrated at pH 3.5 (pyridine 10 ml, acetic acid 100 ml, double distilled H_2O 1890 ml) for 15 minutes at 1500 volts. The thin-layer is dried, rotated 90° and resolved at pH 1.9 (88% formic acid 50 ml, acetic acid 156 ml, double distilled H_2O 1794 ml) for 30 minutes at 1500 volts. Phospho-amino acid standards were detected by ninhydrin staining of the thin-layer plates. Radioactive phospho-amino acids were detected by autoradiography.

2.15 Tryptic Digest Analysis

Two dimensional tryptic peptide mapping was essentially performed as described by Luo et al. (100). Immobilon-P or nitrocellulose membrane slices containing ^{32}P-labeled proteins were soaked in 0.5% polyvinylpyrrolidone in 100 mM acetic acid for 30 minutes. After briefly washing in water, the membranes were incubated with 25 μg of

trypsin in 50 mM ammonium bicarbonate (pH 8.5) at 37°C for two hours. After two hours an additional 25 μg of trypsin were added for an overnight incubation. The samples were then centrifuged and the liquid was lyophilized. After one wash with 100 μl of water and lyophilization, the samples were oxidized in 100 μl of performic acid for one hour at 0°C. One ml of water was then added and the samples were lyophilized. The dried phosphopeptides were resuspended in 10 μl of chromatography buffer (17), spotted onto CELL Type-100 thin-layer plates and were separated by ascending chromatography for 5 hours (n-butanol 204 ml, acetic acid 50 ml, pyridine 143 ml, double distilled water 143 ml). The chromatogram was dried, rotated 90°, and thin-layer electrophoresis was performed at pH 1.9 for 40 minutes at 1000 V. Phospho-tryptic peptides were then visualized by autoradiography.

2.16 Analysis of Tryptic Phosphopeptides by V8 Protease and Thermolysin Digestion

^{32}P-labeled tryptic phosphopeptides were recovered by scraping the cellulose off the thin-layer plates and eluting the peptides with 300 μl of pH 1.9 buffer. The samples were lyophilized and resuspended in 20 μl of ammonium bicarbonate (pH 7.6) containing either 5 μg of V8 protease, or 5 μg of thermolysin with 1 mM $CaCl_2$. Then digest was performed overnight at 37°C (V8) or at 55°C (thermolysin). The digests were then lyophilized, resuspended in pH 1.9 buffer and resolved by ascending chromatography. Analysis was performed by autoradiography.

2.17 CD4 Cross-Linking in HUT78 Cells

HUT78 cells were generously provided by Dr. L. Fillion. HUT78 cells (10^6 cells) in suspension were incubated with polyclonal (rabbit) anti-CD4 antibodies (kindly provided by Dr. L. Fillion) at 1:350 in ice cold αMEM. After 30 minutes on ice the samples were washed once with ice cold PBS. Cross-linking of CD4 was accomplished using Goat anti-rabbit IgG specific antibodies (Jackson Immunologicals) (1:350) in 500 μl of αMEM at 37°C. After two minutes at 37°C the cells were lysed by the addition of 500 μl of ice cold 2 x TNV (20 mM Tris, pH7.5, 2% NP-40, 1 mM ammonium vanadate, 4 mM NaF, 4 mM Na pyrophosphate, 10 μg/ml leupeptin, 4 μg/ml aprotinin, 400 μg/ml PMSF). CD4 was immunoprecipitated with 3 μl/ml of anti-CD4 antibodies for one hour at 4°C. Protein A coupled Sepharose beads were then added for an additional hour at 4°C. The immunoprecipitates were washed 4 times in 1 x TNV and once in kinase buffer (20 mM Hepes, pH7.1, 2 mM $MnCl_2$, 10 mM $MgCl_2$, 200 μM vanadate), prior to an immune complex kinase assay.

In vitro kinase activity was initiated by the addition of 5 μCi gamma-^{32}P-ATP to 50 μl of pelleted sepharose beads. After 15 minutes at room temperature, the kinase reaction was terminated by washing the immune complexes 2 times with 1 x TNV. Autophosphorylated kinases were eluted with sample buffer and resolved on SDS-PAGE. Polyacrylamide gels were fixed using 10% acetic acid, 20% methanol, for 20 minutes and treated with 1 M KOH for two hours at 55°C. The gels were rinsed in 10% acetic acid, 10% isopropanol for 2 hours, dried and subjected to autoradiography.

2.18 Cross-Linking of MAG on the Cell Surface

Primary rat oligodendrocytes or L-MAG expressing L cells were labeled with ^{32}P-orthophosphate, in serum and phosphate free DMEM, for 3 hours as described above (section 2.9). The cells were then incubated with ice cold SFM in the presence of 513 anti-MAG antibody (1:500). After 30 minutes on ice the samples were washed once with ice cold PBS. Cross-linking of MAG was accomplished using affinity purified rabbit anti-mouse antibodies (Hyclone) (1:350) in ^{32}P-orthophosphate containing DMEM at 37°C for 15 minutes. The samples were harvested in 100°C 2% SDS for immunoprecipitation and processed as described above. Phosphorylated MAG was analyzed by tryptic digest mapping.

2.19 Induction of TrpE Fusion Proteins

The TrpEGAP-SH2[N+SH3+C], TrpEPLC-SH2[N+C], TrpESrc-SH3SH2, and the TrpECrk-SH2(+) fusion proteins were generously provided by Dr. T. Pawson. To induce the TrpE-SH2 domain fusion proteins 5 ml of M9 media (102) (supplemented with ampicillin, vitamin B1 and tryptophan) were inoculated with frozen glycerol stock of transformed bacteria and were grown overnight at 37°C with rapid shaking. The following day 1 ml is added to 50 ml of M9 medium (supplemented with ampicllin and vitamin B1 only) and cultured for 2.5 hours at 37°C with rapid shaking. At this point 25 μl of indole acrylic acid (10 mg/ml in ethanol) is added to induce the trp operon. The bacteria are cultured for an additional 3 hours and are then pelleted by centrifugation for 15 minutes at 2000 x g at 4°C. The cell pellets were lysed in 0.5 ml of

immunoprecipitation buffer (section 2.6) and sonicated for 3 x 30 seconds on ice. The insoluble debris was removed by centrifugation (14000 x g in a microfuge) and the supernatant was diluted in 4.5 ml of 10 mM Tris pH 7.5, 5% skim milk powder, 500 μM ammonium vanadate, 140 mM NaCl, 10 mM NaF, 10 mM Na pyrophosphate, 2 μg/ml aprotinin, 5 μg/ml leupeptin, 0.4 μg/ml pepstatin, 200 μg/ml PMSF.

2.20 Probing of MAG Cell Lysates With TrpE-SH2 Domain Fusion Proteins

L-MAG and S-MAG expressing cells were lysed as in section 2.6 and immunoprecipitation of MAG was carried out as in section 2.7. The immunoprecipitates were resolved on SDS-PAGE and transferred to nitocellulose membranes as described in section 2.5. The filters were then incubated with the bacterial cell lysates containing TrpE-SH2 domain fusion proteins for 1.5 hours at 4°C. The blots were subsequently probed with an anti-TrpE monoclonal antibody (1:500) (Oncogene Science, Inc.), and visualization of the blots was carried out using a ^{125}I labeled sheep anti-mouse second antibody.

The data presented in this thesis represents experiments that were repeated at least 3-4 times and are, thus, entirely reproducable.

CHAPTER 3

CELL ADHESION PROPERTIES OF MYELIN-ASSOCIATED GLYCOPROTEIN IN L CELL FIBROBLASTS

SUMMARY

Myelin-associated glycoprotein (MAG) is a cell surface molecule expressed by oligodendrocytes and Schwann cells. In order to determine whether MAG expression can confer adhesive properties to cells which normally do not aggregate in suspension, the cDNA encoding the long form of MAG (L-MAG) and the short MAG isoform (S-MAG) were introduced into L cell fibroblasts by retroviral infection and electroporation, respectively. Clonal L cell lines expressing MAG were then subjected to a cell aggregation assay. Our results indicate that L-MAG and S-MAG can both function as intercellular adhesion molecules in a heterologous cell system. A critical threshold value of MAG expression is required for cell aggregation to occur. The adhesive properties of these cells were specific to MAG, since monoclonal antibodies directed against its extracellular domain inhibited aggregation. Furthermore, the adhesion was found to be calcium and temperature independent. Cell sorting experiments demonstrated that MAG expressing cells bind in a heterotypic fashion to parental L cell fibroblasts. These results suggest that L-MAG and S-MAG can both function as heterotypic cell adhesion molecules recognizing a cell surface molecule(s) expressed by L cells.

3.1 Introduction

The organization of tissues in higher organisms requires sophisticated mechanisms of cell sorting and selective adhesion. It is believed that certain types of cell surface glycoproteins play fundamental roles in this process by virtue of their ability to adhere selectively in either a heterotypic or homotypic fashion to adjacent cells or extracellular matrix molecules. For instance a family of related molecules referred to as the cadherins have been shown to facilitate cell sorting through specific homotypic adhesion mechanisms (117). Integrins on the other hand comprise a family of heteromeric molecules which mediate cell attachment through specific ligand binding (171). A third class of molecules involved in cell adhesion processes share sequence and structural homologies which place them in the immunoglobulin supergene family (82,99,189). One member of this family is myelin-associated glycoprotein or MAG, a transmembrane glycoprotein whose molecular weight is approximately 100 kD. The expression of MAG is restricted to oligodendrocytes in the central nervous system (CNS) and Schwann cells in the peripheral nervous system (PNS) (167). Two alternatively spliced isoforms of the molecule exist which are termed L-MAG and S-MAG. Their expression is regulated differentially throughout development (7,43,96,149,181). MAG is thought to mediate the interactions between glial cells and neurons during and subsequent to the process of myelination (9,105,177,180). Indeed it has been shown that liposomes expressing the MAG molecule can adhere specifically to neurons in culture and that this adhesion can be partially inhibited by MAG specific antibodies (133,145). Furthermore, MAG expressed in NIH 3T3 fibroblast cells promote neurite outgrowth from dorsal root ganglia

in cell culture, which can be partially blocked by anti-MAG antibodies (83). In order to characterize the cell adhesion function of MAG in a cell culture system we expressed both MAG isoforms in L cells, which do not aggregate when grown in suspension (117). During the course of our experiments we determined that MAG is capable of heterotypic intercellular binding and cell sorting, unlike the homotypic interactions observed for neural cell adhesion molecule (N-CAM) (144) and carcinoembryonic antigen (CEA) (13), other members of the immunoglobulin supergene family.

3.2 Results

3.2.1 Expression of L-MAG in L Cells

The L-MAG cDNA was introduced into L cell fibroblasts by retroviral infection. Immunofluorescent cytochemistry and immunoblot analysis with a MAG specific antibody (133) was used to identify clones expressing differing amounts of MAG on their surfaces. A cell line designated C5 expressed the highest levels of L-MAG (figure 3.1,lane D), while cell lines D2 and C3 exhibited intermediate to low levels of L-MAG (lanes B and C). The parental L cells do not display any immunoreactivity towards the anti-MAG antibodies used in these and all subsequent experiments (lane A). The protein band appearing below the major L-MAG containing band in the C5 sample is most likely partially glycosylated L-MAG.

Figure 3.1: Western blot analysis of L-MAG expressing L cell clones. Whole cell extracts from parental L cells (lane A) and G418 resistant L-MAG expressing L cell clones C3 (lane B), D2 (lane C), and C5 (lane D) were probed with anti-MAG monoclonal antibodies Gen 3 S1 and Gen 3 S3.

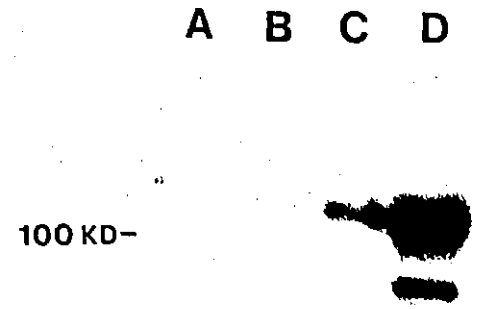
A B C D
100 KD–

3.2.2 Aggregation of L Cells Expressing L-MAG

Earlier work (133,145) had suggested that purified MAG molecules may be capable of cell adhesion events in cultured CNS cells. To directly test the ability of MAG to act as a cell adhesion molecule (CAM) when expressed in live cells, fibroblasts expressing different levels of the L-MAG isoform were subjected to a cell aggregation assay as described in Materials and Methods. Parallel cultures of non-expressing fibroblasts were subjected to the same regime. As shown in Figure 3.2A, C5 cells rapidly began to aggregate while D2, C3 and the parental L cells showed little aggregation over the same time period. Furthermore C5 cells tended to form aggregates of 5-10 cells while the clumps in the control cultures appeared to be mostly doublets or triplets of cells. After 18 hours large aggregates are formed from C5 cells (Figure 3.2B), while parental L cells remain virtually all single cells (Figure 2C). These results suggest that L-MAG can mediate cell adhesion and the adhesion is dependent upon the level of L-MAG expressed on the cell surface.

3.2.3 Aggregation of L Cells Requires a Threshold Level of MAG Expression

We wanted to determine whether a linear relationship exists between L-MAG expression and the ability to aggregate. We quantified the relative amount of L-MAG expressed in five independent L cell clones using ^{35}S-methionine labelled cells. The relative amount of L-MAG in each clone was expressed as a percentage of the highest expressing clone, C5, and was compared to the degree of aggregation of each clone after 30 minutes.

Figure 3.2: Cell aggregation behaviour of L-MAG L cell clones. L-MAG expressing L cells were subjected to aggregation analysis as described in Materials and Methods. (A) At the indicated time intervals samples were removed and the degree of aggregation was calculated as $(S_0-S_t)/S_0$. The results are expressed as the mean+/- standard error from 3 determinations for L parental cells [L(CNT), open circles], clones C3 [L(MAG-C3), open triangles] and D2 [L(MAG-D2), asterisks], and from 7 determinations for clone C5 [L(MAG-C5), closed squares]. Light microscopy of L(MAG-C5) cells (B) and L(CNT) cells (C) after 24 hours on an orbital shaker shows typical aggregates formed when L-MAG is expressed in L cells.

A

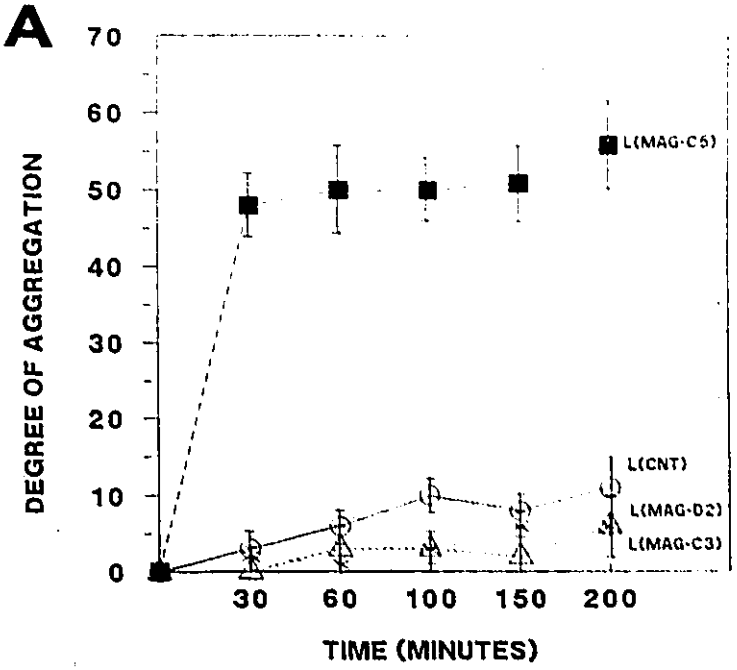
70
60
50
40
30
20
10
0
DEGREE OF AGGREGATION
L(MAG-C5)
L(CNT)
L(MAG-D2)
L(MAG-C3)
30
60
100
150
200
TIME (MINUTES)

B

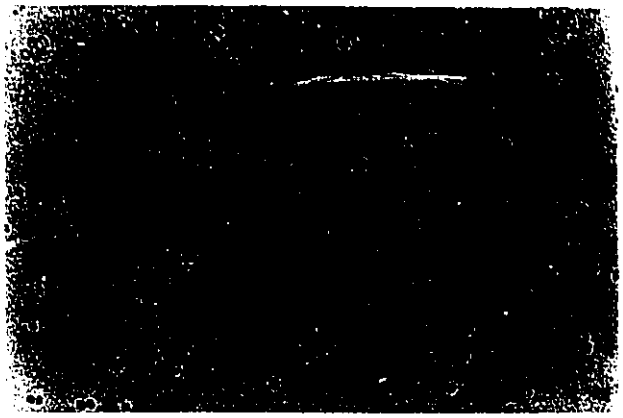

C

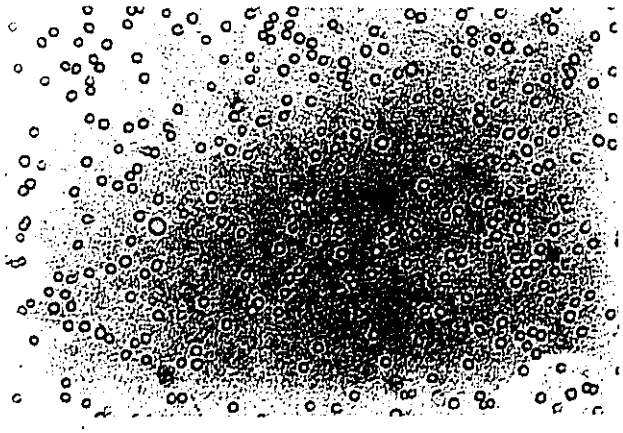

The results demonstrate that the ability to aggregate does not correlate in a linear fashion with the level of L-MAG expression (Figure 3.3). Rather, a threshold level of expression seems to be necessary in order for MAG-mediated aggregation to occur.

3.2.4 S-MAG Expression Level in L cells Determines Degree of Aggregation L cells transfected with the cDNA to S-MAG were screened by immunoblot analysis using anti-MAG antibodies (Figure 3.4). Several cell lines with varying amounts of S-MAG expression were generated and then assayed for cell aggregation. In order to accurately quantify MAG expression on the cell surface, these cell lines were subjected to flow cytometry. Figure 3.5 compares the ability of these cells to aggregate to the intensity of cell surface fluorescence. Similar to L-MAG, a certain threshold level of expression was necessary for cell aggregation to occur. Clone SM23 seems to express S-MAG at a level just above the threshold needed for aggregation, since clones which express only 15% less S-MAG do not adhere to each other. In general, above that threshold level all cell lines exhibited comparable degrees of adhesion. Clone SM32 was then chosen for further studies, since it provided for consistent cell aggregation results. Moreover, the cell surface expression of S-MAG in this line is similar to that of L-MAG in the C5 cell line.

Figure 3.3: Relationship between L-MAG expression and cell aggregation. L-MAG expressing L cell clones were labelled with ^{35}S-methionine, solubilized in SDS and immunoprecipitated with anti-MAG antibodies. The samples were resolved on SDS-PAGE and quantified by laser densitometry of the autoradiographs. The degree of aggregation of each clone was determined after 30 minutes of incubation. The results are expressed as the mean+/- standard error from 3-7 determinations.

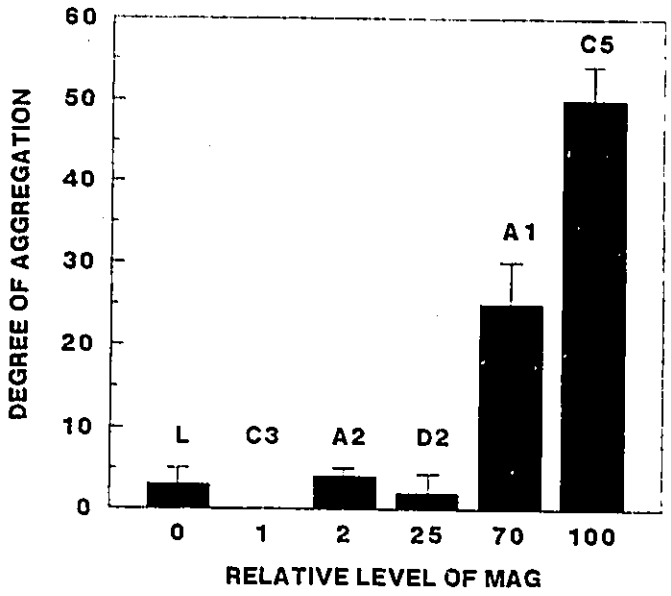
60
50
40
30
20
10
0
DEGREE OF AGGREGATION
L
C3
A2
D2
A1
C5
0
1
2
25
70
100
RELATIVE LEVEL OF MAG

Figure 3.4: Western blot analysis of S-MAG expressing L cell clones. Whole cell extracts from L-MAG C5 (lane 1), parental L cells (lane 2) and G418 resistant S-MAG expressing L cell clones SM25 (lane 3), SM2 (lane 4), SM27 (lane 5), SM31 (lane 6), SM34 (lane 7), SM38 (lane 8), SM36 (lane 9), SM48 (lane 10), SM23 (lane 11), SM1 (lane 12), SM3 (lane 13), SM9 (lane 14), SM32 (lane 15) and SM33 (lane 16) were probed with anti-MAG monoclonal antibodies Gen 3 S1 and Gen 3 S3.

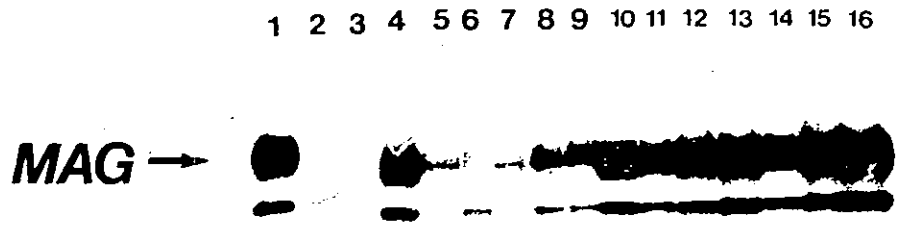
1 2 3 4 5 6 7 8 9 10 11 12 13 14 15 16
MAG

Figure 3.5: Relationship between S-MAG expression and cell aggregation. S-MAG expressing L cell clones were incubated with anti-MAG monoclonal antibody 513 and subsequently with an FITC conjugated secondary antibody. The cells were then assayed for cell surface fluorescence by flow cytometry. MAG levels in each clone was expressed as mean fluorescence and compared to the degree of aggregation after 30 minutes of incubation. Numbers associated with the triangles in the figure correspond to the SM clones. C5 corresponds to the L-MAG expressing L cell line. The results are expressed as the mean+/- standard error from 3-7 determinations.

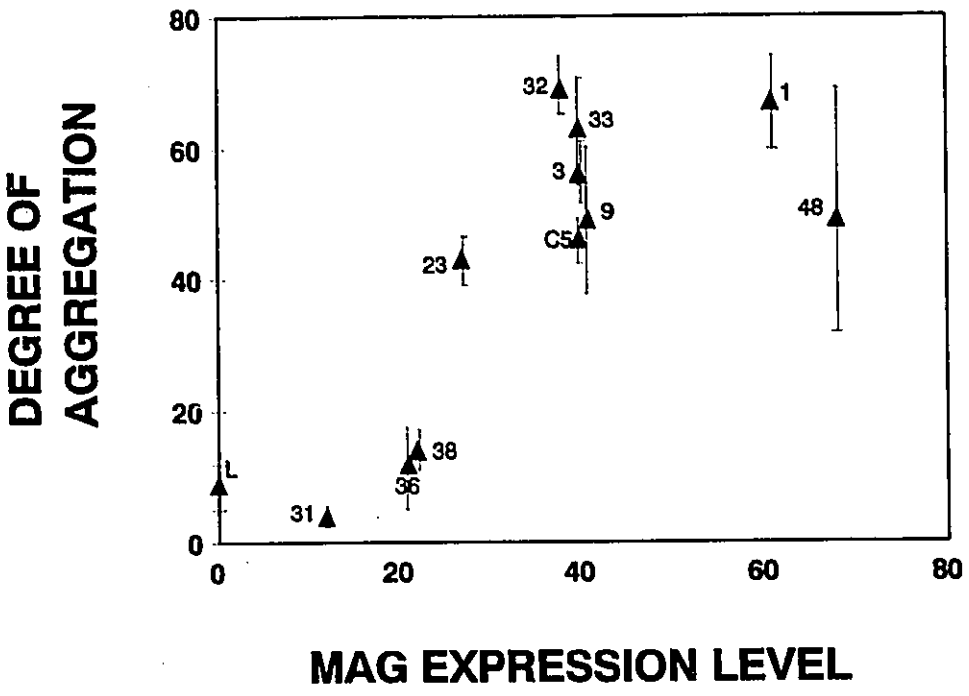
DEGREE OF AGGREGATION
MAG EXPRESSION LEVEL
0
20
40
60
80
L
31
36
38
23
32
33
3
9
C5
1
48

3.2.5 Antibody Mediated Inhibition of Aggregation

The specificity of the adhesion observed in these experiments was tested using a monoclonal antibody specific for MAG (Mab 513). This monoclonal antibody has previously been shown to inhibit the interactions between MAG and neurons (83,133). As is shown in Figures 3.6 and 3.7 the adhesion of MAG expressing cells is completely inhibited by the addition of Mab 513, while an irrelevant monoclonal (Mab 1G2) prepared in the same way had no effect on the adhesion. As a further control, the MAG cDNA was transfected into a subclone of NIH 3T3 cells which under the conditions of this assay, aggregate independently of the expression of L-MAG. When these L-MAG expressing cells were incubated with Mab 513 their normal aggregation was not inhibited (data not shown). Thus the inhibitory effect of the antibody was specific to cells which depend upon MAG expression for their aggregation. Using immunofluorescent cytochemistry we determined that the inhibitory effect of Mab 513 is not due to a clearing of MAG from the cell surface. After 200 minutes of incubating L(MAG-C5) cells with Mab 513 at 37°C, the fluorescent staining pattern is identical to cells stained at 0°C (data not shown). It is likely, therefore, that Mab 513 inhibits aggregation by steric hindrance, suggesting that the antibody recognizes an epitope at or in the vicinity of the MAG binding domain. The amount of antibody needed to saturate the MAG binding sites on the cells, as determined by immunofluorescent staining, is 4 μg/ml. This concentration of Mab 513 is also sufficient to inhibit MAG-mediated aggregation.

Figure 3.6: Inhibition of L-MAG-mediated aggregation by antibody. Cell aggregation assays of L(MAG-C5) cells were performed in the presence of 12ug/ml of medium of either anti-MAG monoclonal antibody 513 (closed triangles) (provided generously by M. Schachner) or monoclonal antibody 1G2 (open circles) (which does not recognize L-MAG by immunofluorescent cytochemistry). The results are expressed as the mean+/- standard error from 4 determinations.

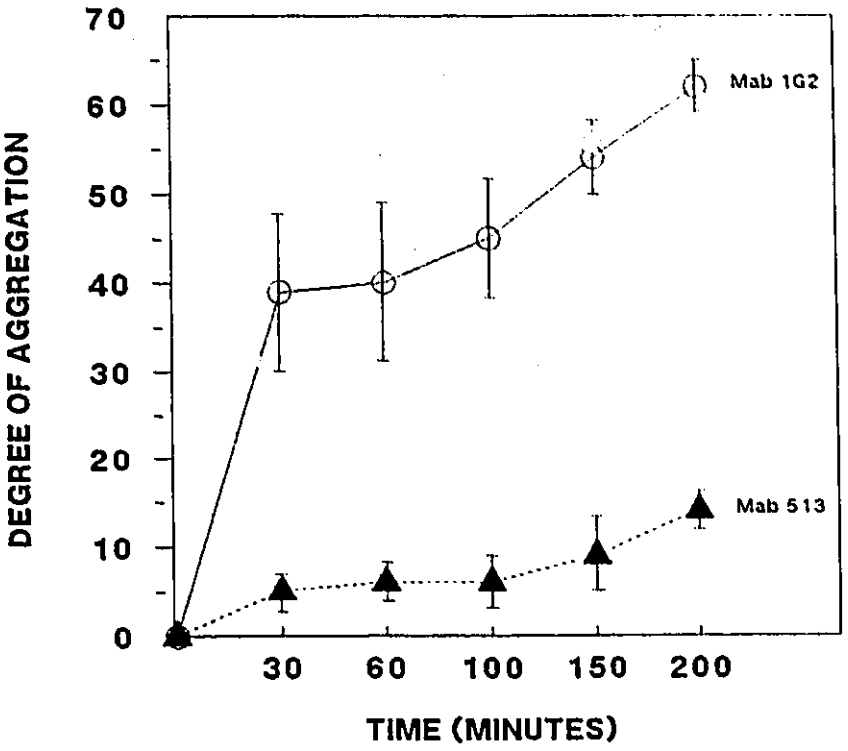
70
60
50
40
30
20
10
0
DEGREE OF AGGREGATION
Mab 1G2
Mab 513
30
60
100
150
200
TIME (MINUTES)

Figure 3.7: Inhibition of S-MAG-mediated aggregation by antibody. Cell aggregation assays of SM32 cells were performed in the presence of 12ug/ml of medium of either anti-MAG monoclonal antibody 513 (dotted line) or monoclonal antibody 1G2 (solid line), which does not recognize S-MAG by immunofluorescent cytochemistry. The results are expressed as the mean+/- standard error from 3 determinations.

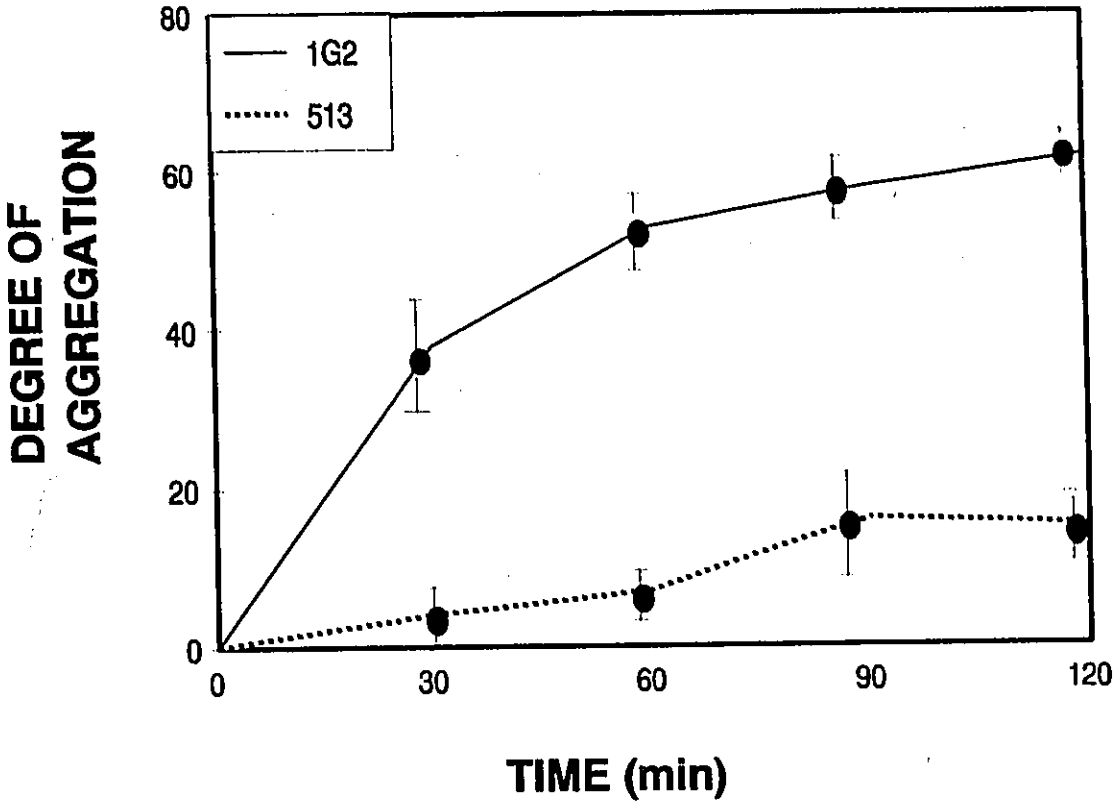
80
60
40
20
0
1G2
513
DEGREE OF AGGREGATION
0
30
60
90
120
TIME (min)

3.2.6 Effect of Calcium and Temperature on L-MAG Specific Aggregation

While cadherins have been shown to depend on calcium for their binding activity (117), the members of the immunoglobulin super gene family are generally thought to act in a calcium independent manner (82). To investigate the importance of calcium for L-MAG-specific cell binding activity, L(MAG-C5) cells were allowed to aggregate in the absence of calcium at 37°C and 4°C. The results demonstrate that C5 cells aggregate independently of calcium at both temperatures (Figure 3.8). Similar results were obtained with SM32 cells, implying that the binding properties of L-MAG and S-MAG are comparable. The aggregation of C5 cells at 4°C can also be inhibited by incubation with the anti-MAG monoclonal antibody (data not shown).

3.2.7 Heterotypic Binding of MAG

In the CNS L-MAG mediates the interaction of oligodendrocytes with neurons that do not express MAG molecules on their cell surface. Therefore, it has been suggested that L-MAG binds to a neuronal receptor molecule in a heterotypic manner. A cell sorting experiment was performed to test the binding specificity of L-MAG in L cell fibroblasts. In order to distinguish between the parental [L(CNT)] and transfected cells [L(MAG-C5)] in a mixed aggregation experiment, cells of one line were pre-labeled with fluoresceine iso-thiocyanate (FITC). Mixed populations of cells were aggregated for several hours and then examined using epifluorescent microscopy. If L(MAG-C5) cells were capable only of homotypic interactions we would expect that in the subsequent aggregates, either all or none of the cells would be labeled with the fluorescent dye.

Figure 3.8: Effect of calcium and temperature on cell aggregation. Cell aggregation was assayed for L(MAG-C5) cells essentially as described in Materials and Methods, except that the cells were resuspended in calcium free Puck's saline (13). The assay was then performed at 37°C (open circles) and at 4°C (closed triangles). The results are expressed as the mean+/- standard error from 3 determinations.

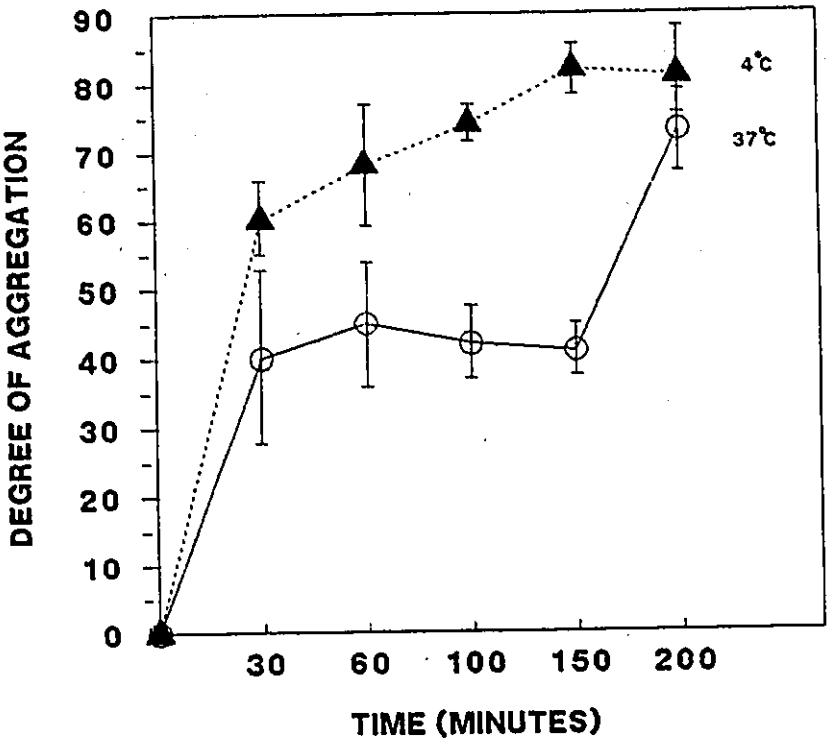
DEGREE OF AGGREGATION
90
80
70
60
50
40
30
20
10
0
30
60
100
150
200
TIME (MINUTES)
4°C
37°C

If on the other hand there were heterotypic interactions between the two cell types, the aggregates should contain both fluorescent and non-fluorescent cells. When L(MAG-C5) cells were labeled, the majority of aggregates contained fluorescent cells in association with equal numbers of non-fluorescent cells (Figure 3.9A-C). When the experiment was reversed the results were virtually identical (Figure 3.9D), indicating that L-MAG binds in a heterotypic fashion.

In an analogous experiment parental L cells were pre-labeled with FITC and mixed in a 1:1 fashion with un-labeled SM32 cells. After only 2 hours of incubation in culture SM32 cells formed heterotypic aggregates with parental L cells (Figure 3.10). These results suggest that similar to L-MAG, S-MAG functions as a heterotypic CAM. Additionally, these findings demonstrate the presence of a MAG receptor in L cell fibroblasts.

3.2.8 L-MAG Can Mediate Selective Cell Sorting

It has been previously shown that differential expression of CAMs can mediate selective adhesion and sorting of cells (38,117). We performed a cell mixing experiments with SP10 cells, a myeloma cell line that exhibits no endogenous cell adhesion activity. When L(MAG-C5) cells were mixed with SP10 cells, the majority of aggregates contained cells that were predominantly of the L(MAG-C5) type (80%-100% of cells) (Figure 3.11A). Most of the SP10 cells remained as single cells and did not incorporate into clumps. Equivalent results were obtained when L(MAG-C5) cells were mixed with the human promyelocytic leukaemia cell line HL60 (data not shown).

Figure 3.9: Cell sorting behaviour of L(MAG-C5) cells with L(CNT) cells. L(MAG-C5) cells were labeled with FITC, mixed in a 1:1 ratio with unlabeled L(CNT) cells and were allowed to aggregate for 18 hours. The aggregates were observed by light (A) and fluorescent light microscopy (B), and photomicrographs were taken of the same fields. Aggregates that were composed of 10 to 100 cells were randomly selected, and the percentage of labeled cells within each aggregate was determined. The cumulative quantification of three separate experiments are depicted as follows: (C) labeled L(MAG-C5) cells mixed with unlabeled L(CNT) cells; (D) labeled L(CNT) cells mixed with unlabeled L(MAG-C5) cells. In each case, the cells labelled with FITC are marked with an asterisks.

A

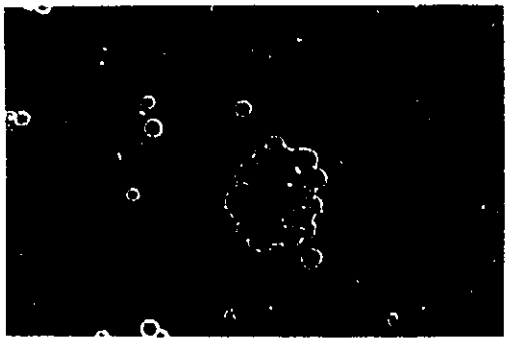

B

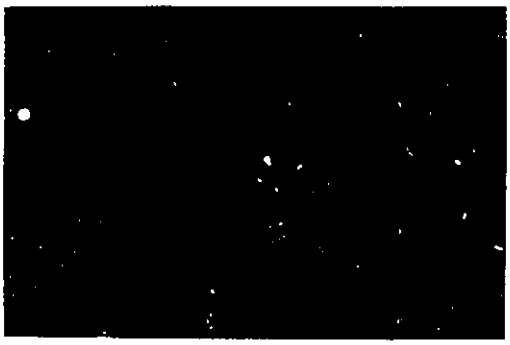

C

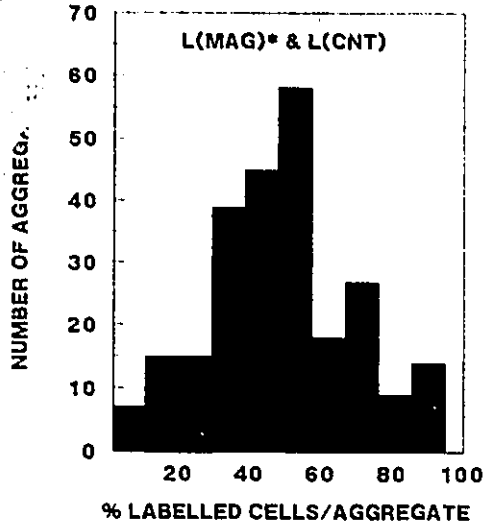
L(MAG)* & L(CNT)
NUMBER OF AGGREG
70
60
50
40
30
20
10
0
20
40
60
80
100
% LABELLED CELLS/AGGREGATE

D

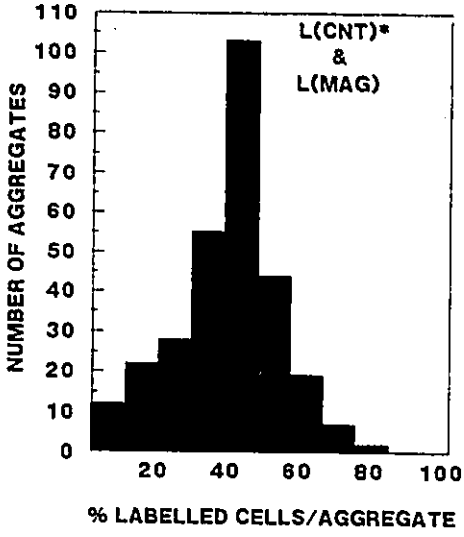
L(CNT)*
&
L(MAG)
NUMBER OF AGGREGATES
110
100
90
80
70
60
50
40
30
20
10
0
20
40
60
80
100
% LABELLED CELLS/AGGREGATE

Figure 3.10: Cell sorting behaviour of SM32 cells with parental L cells. Parental L cells were labelled with FITC, mixed in a 1:1 ratio with unlabeled SM32 cells and were allowed to aggregate for 2 hours. The aggregates were observed by light (a) and fluorescent light microscopy (b), and photomicrographs were taken of the same fields.

a

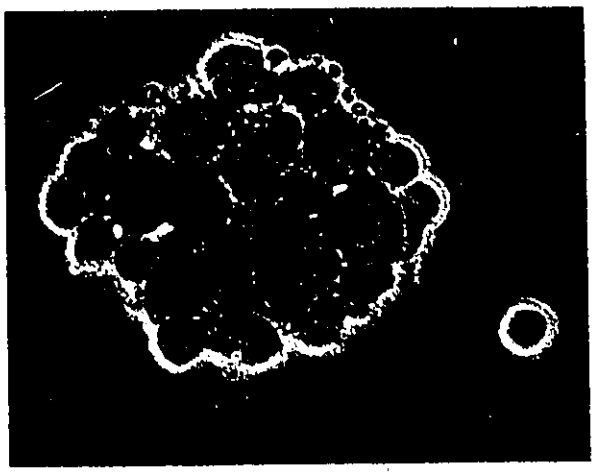

b

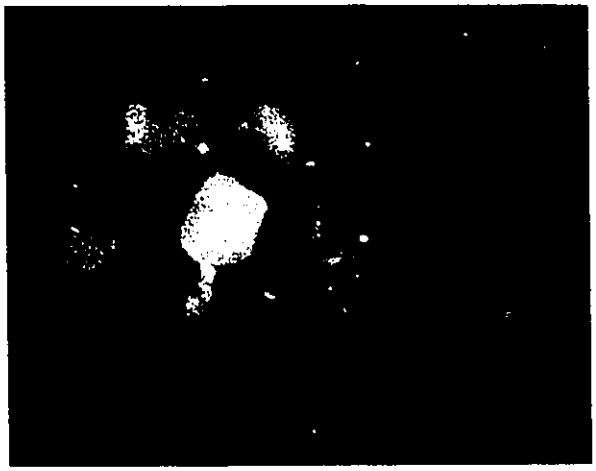

Figure 3.11: Segregation of L(MAG-C5) from SP10 myeloma and P19 embryonic carcinoma cells during cell sorting experiments. L(MAG-C5) cells were labeled with FITC, mixed in a 1:1 ratio with unlabeled SP10 or P19 cells and were allowed to aggregate for 18 hours. Aggregates that were composed of 10 to 100 cells were randomly selected, and the percentage of labeled cells within each aggregate was determined. The cumulative quantification of three separate experiments are depicted as follows: (A) labeled L(MAG-C5) cells mixed with unlabeled SP10 cells; (B) labeled L(MAG-C5) cells mixed with unlabeled P19 cells. In each case, the cells labeled with FITC are marked with an asterisks.

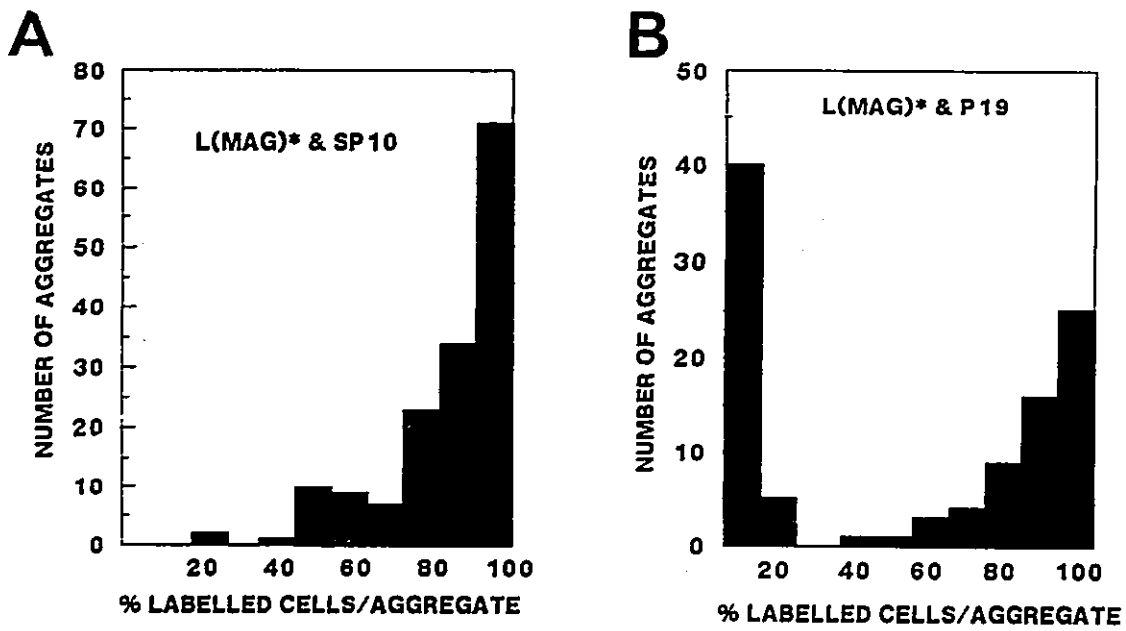
A
L(MAG)* & SP10
NUMBER OF AGGREGATES
0
10
20
30
40
50
60
70
80
20
40
60
80
100
% LABELLED CELLS/AGGREGATE
B
L(MAG)* & P19
NUMBER OF AGGREGATES
0
10
20
30
40
50
20
40
60
80
100
% LABELLED CELLS/AGGREGATE

In a related experiment we aggregated L(MAG-C5) cells in the presence of P19 embryonic carcinoma cells which express E-Cadherin, a calcium dependent homotypic CAM (117,195). Two types of aggregates were obtained. One class of aggregates contained mainly unlabelled P19 cells, while the majority of cells in the other group of aggregates were FITC labeled L(MAG-C5) cells (Figure 3.11B). Thus our results indicate that while the L-MAG receptor is expressed on the surface of L cells, it is absent from two lymphocytic cell lines and embryonic stem cells. Furthermore, the interaction of MAG with its receptor can mediate cell sorting in the presence of cells that are capable of homotypic interactions.

3.3 Discussion

In this chapter it is documented that MAG can participate in cell adhesion and cell sorting when expressed on the surface of fibroblasts. The finding that this binding can occur in the absence of calcium and at a low temperature is consistent with the adhesion properties observed for other CAMs that are members of the immunoglobulin supergene family (13,144). Since MAG mediated aggregation can occur at 4°C, the initial recognition and binding of MAG molecules to their receptors is independent of metabolic activity. This is in contrast to the binding activity of the cell adhesion molecule ICAM (104).

In the CNS and PNS, the expression of MAG appears prior to and during the first stages of oligodendrocyte-neuron and Schwann cell-neuron contact (9) and peaks around the time of maximum myelin formation (181). These and other observations (83,133,145)

have led to the speculation that MAG may bind to a receptor molecule present on the axonal surface and thus mediate the initial recognition event between oligodendrocytes and neurons. Since neurons do not express MAG themselves (9) it is likely that MAG functions as a heterotypic CAM. Our results support this idea and further suggest that a MAG receptor is expressed on the surface of L cell fibroblasts. Whether this represents an abnormal expression of a neuronal molecule on the surface of a transformed cell or simply expression of a related fibroblast cell surface molecule is not known. It is of interest to note however, that the MAG receptor is absent from lymphocytic cells and pluripotent embryonic stem cells.

L cells expressing low to moderate levels of MAG on their surfaces do not detectably associate in suspension whereas L cells expressing high levels of MAG readily aggregate. This was demonstrated for both L-MAG and S-MAG and suggests that there is a threshold level of MAG expression needed in order for cell adhesion to take place. Experiments performed with NCAM demonstrate that its biological activity is also subject to a threshold effect (32). NIH 3T3 cells expressing high levels of NCAM on their surface promoted cerebellar neurite outgrowth. The cerebellar neurites grew to only half the length if they were plated onto NIH 3T3 cells with 20% less NCAM expression on the cell surface. A similar decrease in L-MAG expression, reduced the ability of L cells to aggregate by 50%. The description of this phenomena was more comprehensive with respect to S-MAG, since more clones were analyzed for cell adhesion. In this case, a 15% decrease in S-MAG expression (compare clones SM36 and SM38 to clone SM23) completely abolished the ability of the cells to aggregate, suggesting that clone SM23

expresses S-MAG at a level just above the threshold. CEA has also been shown to mediate cell adhesion events in a concentration dependent fashion (13). These observations suggest that intercellular adhesion may be regulated in vivo by relatively small changes in CAM expression, binding properties and/or subcellular localization. We have previously shown that the L-MAG isoform is extensively phosphorylated in its cytoplasmic domain (4,36). This reversible post-translational modification could provide a mechanism for the regulation of L-MAG adhesion.

The present study has demonstrated that MAG confers cell adhesion properties to an anchorage independent fibroblast cell line. As mentioned above, other investigators have incorporated MAG purified from brain into liposomes to study its cell adhesion properties (133,145). While our results are in general agreement with the liposome studies, fibroblasts expressing MAG have several added advantages. We were able to demonstrate that MAG binding occurs in a heterotypic fashion and is governed by a threshold effect. It is, therefore, possible and perhaps more relevant to study the binding properties of MAG in the context of the normal cellular milieu. This is particularly important if one is attempting to determine the contribution of post-translational modifications and/or accessory molecules (i.e. cytoskeletal components) to the regulation of MAG binding properties. Furthermore, the mapping of binding and regulatory domains in the MAG molecule can now be directly determined using site directed mutagenesis of the MAG cDNA along with the expression of mutant proteins in fibroblast lines. Finally the identification of cell lines which do and do not express the MAG receptor should facilitate the identification and cloning of this molecule.

CHAPTER 4

DIFFERENTIAL PHOSPHORYLATION OF MYELIN-ASSOCIATED GLYCOPROTEIN ISOFORMS IN CELL CULTURE

SUMMARY

The alternative splicing of myelin-associated glycoprotein (MAG) mRNA generates two isoforms that harbour distinct potential phosphorylation sites in their cytoplasmic tails. Here we characterize the in vivo phosphorylation of MAG isoforms in fibroblasts transfected with the cDNAs encoding the two isoforms of MAG and in primary rat oligodendrocyte cultures. Our results demonstrate that L-MAG is phosphorylated constitutively mainly on serine, but also on threonine and tyrosine residues. S-MAG contains mainly phosphoserine, with low detectable amounts of phosphotyrosine. This isoform displays a 10 fold lower stoichiometry of phosphorylation compared to L-MAG. Tryptic digest analysis of both isoforms demonstrates that all the phosphorylation sites in S-MAG are represented in L-MAG. The identity of tyrosine 558 has been confirmed in both isoforms by further analysis of tryptic phosphopeptides. The same phosphorylation sites were identified in primary rat oligodendrocytes. Phosphorylation of tyrosine 558 is induced several fold with ammonium vanadate in L-MAG, but not in S-MAG, implying a difference in the regulation of tyrosine phosphorylation of these isoforms. Furthermore, ^{32}P labeling of v-src transformed NIH 3T3 cells that express L-MAG also show that L-MAG is likely to be an in vivo substrate for $pp60^{v\text{-}src}$ tyrosine kinase activity. S-MAG is phosphorylated to a lower stoichiometry in these cells, suggesting that even in systems with constitutively activated PTKs, S-MAG is an inferior kinase substrate. These results demonstrate that both MAG isoforms are phosphorylated, albeit to a different extent, suggesting a regulatory influence of the cytoplasmic domain on interacting signal transduction molecules.

4.1 Introduction

The characterization of molecules involved in cell adhesion is basic to the understanding of developmental events. Certain types of cell surface glycoproteins have been demonstrated to play a fundamental role in this process. One group of cell adhesion molecules has been included in the immunoglobulin (Ig) supergene family by virtue of their sequence and structural features (189). Among these molecules is myelin-associated glycoprotein (MAG), a transmembrane glycoprotein involved in neuron-glia and glia-glia interactions in the developing nervous system (189). MAG is expressed on the surface of oligodendrocytes in the CNS and Schwann cells in the PNS (167). MAG mRNA is alternatively spliced into two developmentally regulated isoforms, suggesting that L-MAG and S-MAG perform functionally different roles in myelin formation (43,181). The early appearance of L-MAG at the onset of the myelin program suggests a potential role for the cytoplasmic domain of this isoform in the initial processes of intercellular recognition and signal transduction. S-MAG mRNA, which is maximally expressed in mature myelin may play a structural role in maintaining the integrity of the myelin sheath. L-MAG and S-MAG exhibit identical external and transmembrane domains, but differ in their cytoplasmic carboxyl-termini (7,96,149). Both isoforms contain several potential phosphorylation sites in the carboxyl terminal region, among which is a region identified as a potential protein kinase C (PKC) phosphorylation site by Arquint et al. (7). In addition, L-MAG contains a segment potentially phosphorylated by protein kinase A (7) and PKC (149), as well as a region homologous to the epidermal growth factor (EGF) receptor autophosphorylation site (7,149). Previously, phosphorylation of L-MAG was

detected in myelinating rodent brain in vivo as well as in myelin in vitro on serine, threonine and tyrosine residues (36,37). Phosphorylation of S-MAG was never detected in myelinating brain.

Here, we report the isolation and characterization of fibroblast cell lines expressing the MAG cDNAs. The results demonstrate that L-MAG is phosphorylated on serine, threonine and tyrosine residues in cell culture, whereas S-MAG is constitutively phosphorylated only on serine residues. While growth factors are unable to modulate MAG phosphorylation, the v-src encoded kinase constitutively phosphorylates L-MAG on tyrosine residues. The results presented here are consistent with phosphorylation of the cytoplasmic domains of both molecules playing a role in the regulation of MAG activity in developing and mature myelin.

4.2 Results

4.2.1 Characterization of MAG Expression in 3T3 Cell Fibroblasts

Live MAG expressing cells were examined by immunofluorescent cytochemistry using a monoclonal anti-MAG antibody (513). The results indicate that L-MAG and S-MAG are both expressed uniformly on the cell surface (Figure 4.1). Immunoblot analysis of membrane extracts of these cells confirms that the antibody recognizes L-MAG and S-MAG in LM and SM cells respectively (Figure 4.2, lanes a and b). It should be noted that glycosylated S-MAG exhibits a slightly lower molecular weight than glycosylated L-MAG.

4.2.2 Phosphorylation of MAG

MAG phosphorylation was assessed by labeling the cells in phosphate free medium containing ^{32}P-orthophosphate and immunoprecipitating MAG from a cell extract with monoclonal anti-MAG antibodies (Gen S1 and Gen S3). The immunoprecipitations were performed on cell lysates from equal numbers of cells and the results demonstrate that L-MAG and S-MAG are both phosphorylated (Figure 4.2). Using differential labeling with ^{35}S-methionine and ^{32}P-orthophosphate L-MAG protein was shown to contain 10 moles of phosphate per mole of polypeptide. In parallel experiments we determined that the half life of MAG is approximately four hours in NIH 3T3 cells (Figure 4.3). For phosphate stoichiometry determinations, cells were incubated overnight (18 hours) with ^{32}P orthophosphate and ^{35}S-methionine and therefore contain MAG molecules which have been uniformly labeled with both isotopes. Thus, our calculation of the extent of phosphorylation will not be biased by long lived MAG molecules which do not contain ^{35}S methionine but are post-translationally modified with ^{32}P. Taken together these results indicate that L-MAG is in fact a formidable protein kinase substrate. Although SM cells express high levels of S-MAG on the cell surface, the stoichiometry of S-MAG phosphorylation was determined to be approximately one tenth the amount of L-MAG phosphorylation (Figure 4.2).

Figure 4.1: Immunofluorescent cytochemistry on MAG expressing fibroblasts. Live LM (a), SM (b) and PVsrcLM (c) cells were stained with monoclonal anti-MAG antibody (Mab 513) and subsequently with fluoresceine conjugated goat anti-mouse secondary antibody. No fluorescence was observed with cells stained with secondary antibody alone. The exposure times and magnification are the same for all pictures (magnification bar represents 20μm).

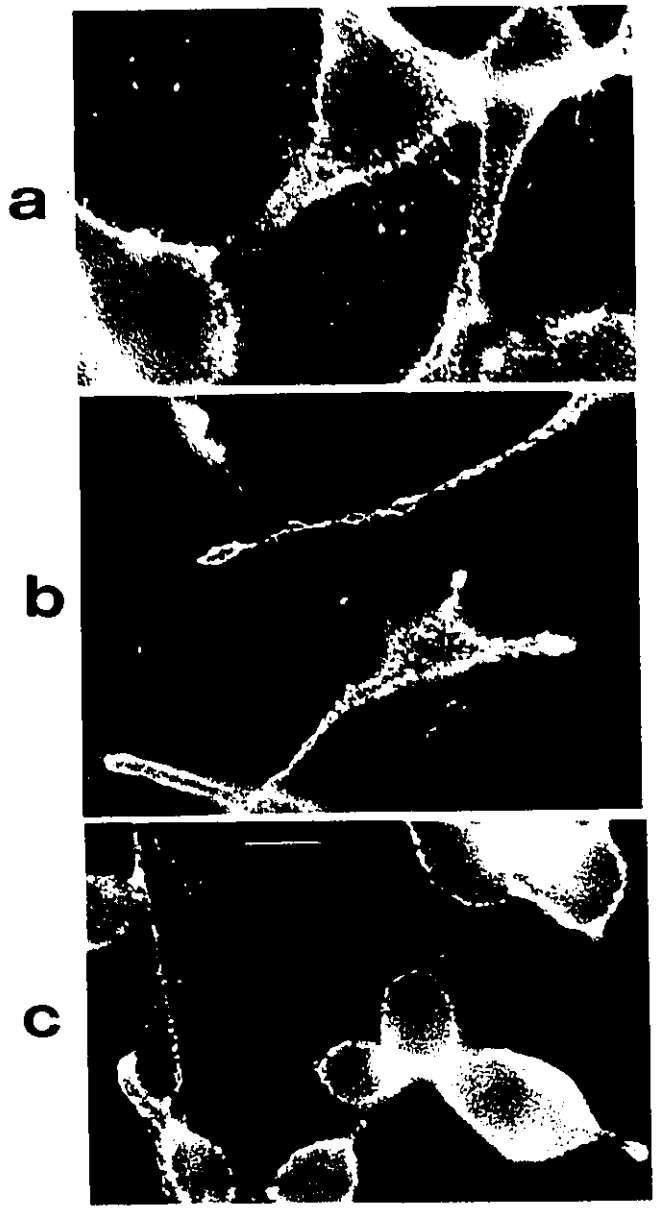
a
b
c

Figure 4.2: Phosphorylation of MAG isoforms in LM and SM cells. Immunoblot analysis of membrane extracts from LM (lane a) and SM (lane b) cells were probed with a mixture of monoclonal anti-MAG antibodies Gen S1 and Gen S3 and detected using an ^{125}I- labeled sheep anti mouse antibody. Cell extracts from 32P labeled LM cells (lane c), SM cells (lane d) and NIH 3T3 cells (lane e) were immunoprecipitated using anti-MAG antibodies as described in materials and methods. A sample containing a mixture of LM and SM cell extract was immunoprecipitated with non-immune serum (lane f). The samples were analyzed using SDS-PAGE and detected by autoradiography.

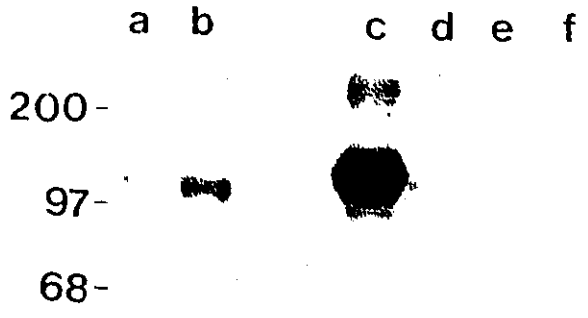
a b c d e f
200-
97-
68-

Figure 4.3: Metabolic half-life determination of L-MAG in 3T3 cell fibroblasts. LM cells were metabolically labeled for 18 hours with ^{35}S-methionine. The samples were harvested immediately after ^{35}S-methionine labeling (lane p), 4 hours (lane 4) and 9 hours (lane 9) after removal of label and replacement with unlabeled αMEM. L-MAG was immunoprecipitated using a mixture of monoclonal anti-MAG antibodies Gen S1 and Gen S3 and analyzed using SDS-PAGE (7.5% polyacrylamide) with subsequent autoradiography. To calculate the half-life, the bands corresponding to L-MAG were cut out from the gel and analyzed using liquid scintillation counting.

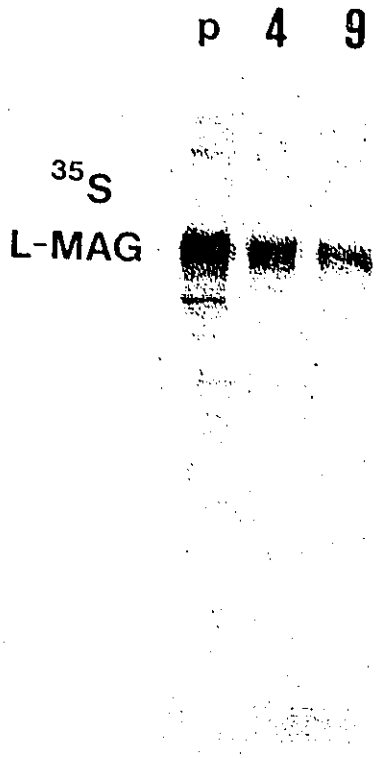
p 4 9
^{35}S
L-MAG

4.2.3 Phosphoamino Acid Content of L-MAG

Phosphoamino acid analysis of L-MAG phosphorylated in metabolically labeled fibroblasts shows that it is constitutively phosphorylated mainly on serine, but also on threonine and tyrosine residues (Figure 4.4B), thereby mimicking the phosphorylation pattern in brain. Ammonium vanadate, a phosphotyrosine phosphatase inhibitor, increases phosphotyrosine levels in cells (90). Although no quantitative change occurred in phosphorylated L-MAG protein from vanadate treated cells (compare lanes a and b, Figure 4.4A and Figure 4.5), there was a dose dependent increase in the amount of phosphotyrosine present in the protein (Figure 4.6). Phosphothreonine and phosphoserine levels increased with 50 μM ammonium vanadate, but decreased with higher concentrations of vanadate (Figure 4.6). While ammonium vanadate did not change the amount of L-MAG in the membrane of these cells as detected by immunoblot analysis (Figure 4.7A) and immunofluorescent cytochemistry (data not shown), it significantly elevated its phosphotyrosine content (Figure 4.7B). In fact, L-MAG was determined to be the major tyrosine phosphorylated protein in these cells. Control experiments determined that the faint appearing protein bands on the immunoblots are non-specific proteins reacting with the secondary antibody (data not shown).

Figure 4.4: The effect of vanadate and v-src transformation on phosphorylation of L-MAG <u>in vivo</u>. (A) Phosphorylated L-MAG was immunoprecipitated from LM cells ^{32}P labeled in the absence (lane a) or presence (lane b) of 500 μM ammonium vanadate, and from ^{32}P-labeled PVsrcLM cells (lane c). The samples were resolved on SDS-PAGE and detected by autoradiography. (B) Phospho-amino acid analysis on electroeluted L-MAG protein was performed using two-dimensional thin-layer electrophoresis as described in Materials and Methods: (a) L-MAG from untreated LM cells; (b) L-MAG from vanadate treated LM cells; (c) L-MAG from PVsrcLM cells. The positions of phosphoserine (S), phosphothreonine (T) and phosphotyrosine (Y) are indicated for reference in sample (a).

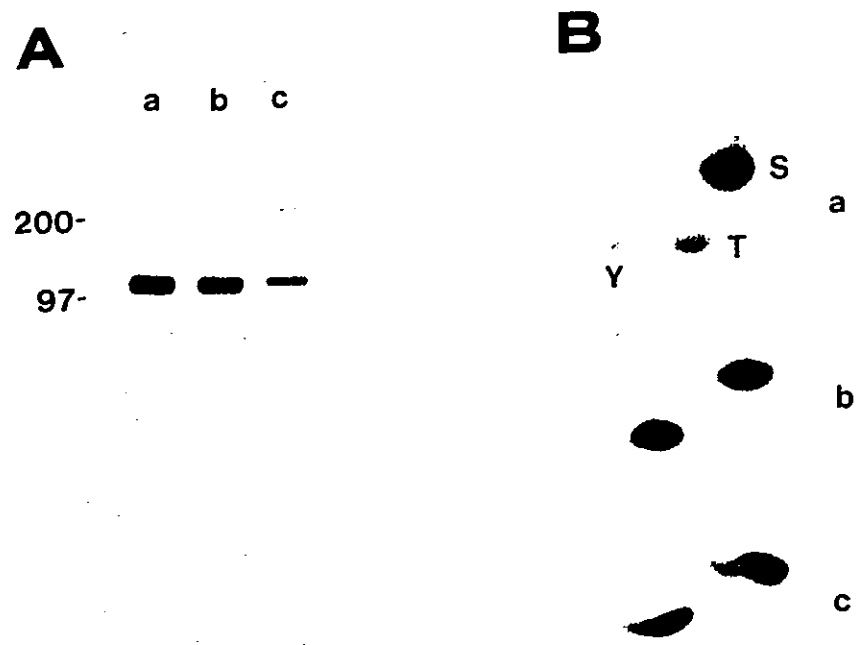
A
a b c
200-
97-
B
S
a
T
Y
b
c

Figure 4.5: Effect of increasing doses of ammonium vanadate on L-MAG phosphorylation- SDS-PAGE analysis. LM cells were labeled with ^{32}P in the presence of increasing concentrations of ammonium vanadate. L-MAG was immunoprecipitated from lysates of cells labeled in the presence of 10 μM (lane 10), 50 μM (lane 50), 100 μM (lane 100), 200 μM (lane 200) and 500 μM (lane 500) vanadate. Analysis was by SDS-PAGE (10% polyacrylamide) with subsequent autoradiography.

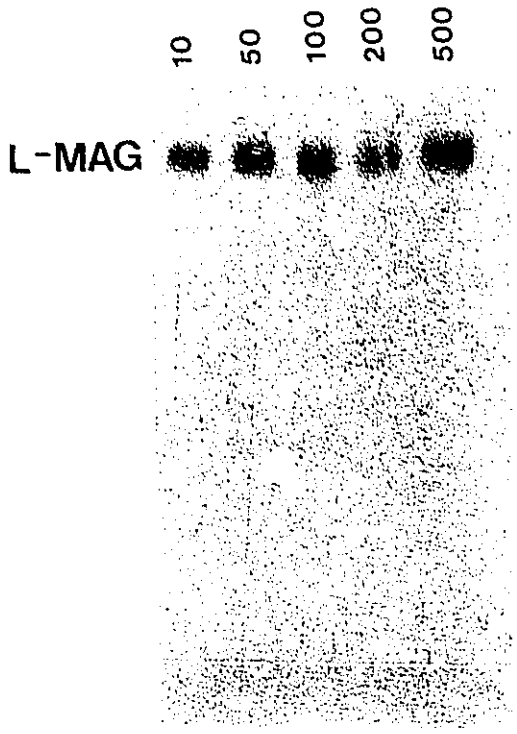
10
50
100
200
500
L-MAG

Figure 4.6: Effect of increasing doses of ammonium vanadate on L-MAG phosphorylation- phosphoamino acid analysis. LM cells were labeled with ^{32}P in the presence of increasing concentrations of ammonium vanadate. Phosphoamino acid analysis was performed on immunoprecipitated phosphorylated L-MAG protein using two dimensional thin layer electrophoresis as described in Materials and Methods. Samples are shown in order of increasing concentrations of ammonium vanadate: (a) 10μM, (b) 50 μM, (c) 100 μM, (d) 200 μM, (e) 500 μM. The positions of phosphoserine (S), phosphothreonine (T), and phosphotyrosine (Y) are shown for reference in sample (b).

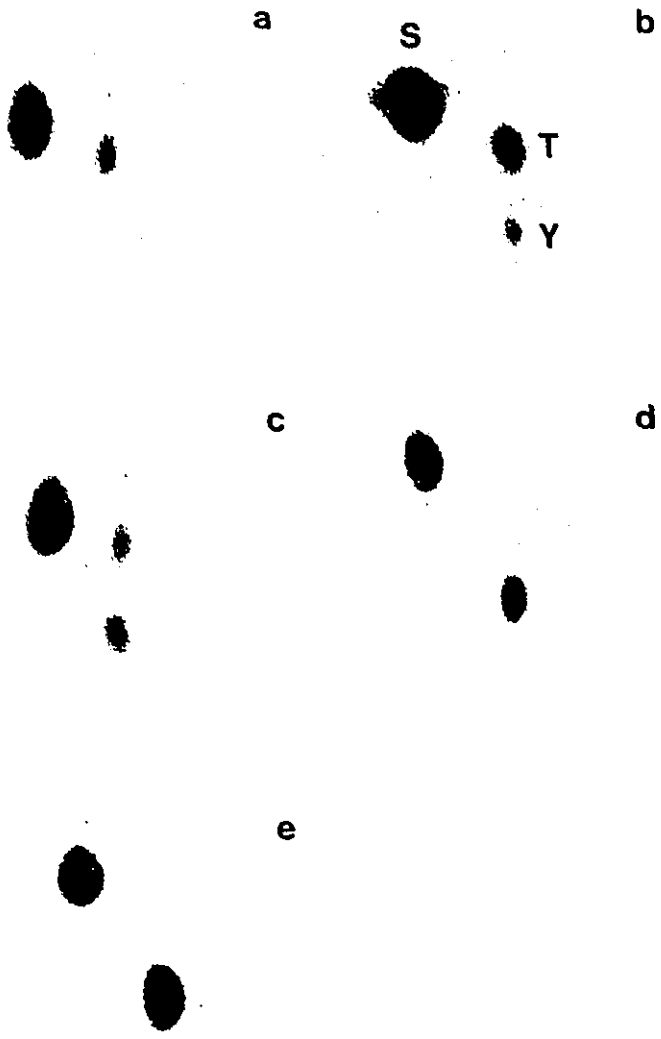
a
S
b
T
Y
c
d
e

Figure 4.7: L-MAG is the major tyrosine phosphorylated membrane protein in LM cells. LM cells were left untreated or pre-treated with 500 μM vanadate for three hours. Membrane extracts were prepared and were either left untreated or were subjected to chemical deglycosylation with TFMS as described in Materials and Methods. Immunoblot analysis was performed using a polyclonal anti-MAG antibody (panel A) or using the PY20 antiphosphotyrosine antibody (panel B). Samples were as follows: LM membranes from untreated cells (lane a) and deglycosylated (lane b), LM membranes from vanadate pre-treated cells (lane c) and deglycosylated (lane d). Molecular weight standards are indicated in kilodaltons.

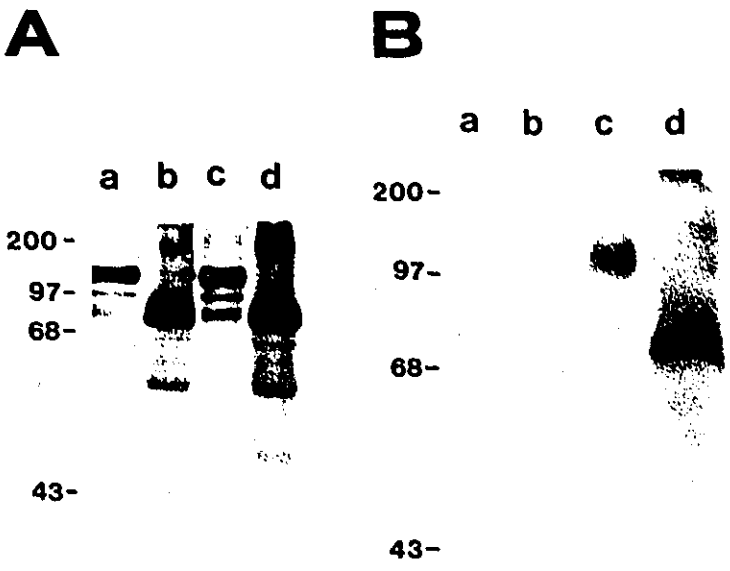
A
a b c d
200-
97-
68-
43-
B
a b c d
200-
97-
68-
43-

4.2.4 Tryptic Digest Analysis of L-MAG

The L-MAG cDNA sequence revealed the presence of potential phosphorylation sites for PKC, cAMP dependent kinase and an EGF-receptor autophosphorylation site (7,149). We examined the effects of various kinase activators on L-MAG phosphorylation and found that EGF, IGF-1 and insulin had no detectable effect on the phosphoamino acid content in phosphorylated L-MAG (Figure 4.8). Treatment of LM cells with dbcAMP, an activator of a different class of serine\threonine kinase quantitatively increased the phosphorylation of L-MAG in some experiments (data not shown). However, this result was not obtained consistently and dbcAMP did not alter L-MAG phosphorylation significantly in a qualitative sense, as determined by phosphoamino acid analysis and tryptic peptide mapping (data not shown).

Two-dimensional tryptic digest mapping of phosphorylated L-MAG revealed the presence of 7-10 phosphopeptides (Figures 4.9 and 4.13c). TPA, a known activator of the serine\threonine specific protein kinase-PKC (115), stimulated the phosphorylation of peptide 6 and decreased the phosphorylation of peptide 5 (Figure 4.9c). The inactive phorbol ester 4α Phorbol served as a control for TPA stimulation and did not affect constitutive L-MAG phosphorylation (data not shown). Identical phosphorylation patterns were observed, whether MAG was expressed in 3T3 cells (LM cells) or in L cell fibroblasts (C5 cell clone).

Figure 4.8: Effect of growth factors on L-MAG phosphorylation. LM cells were labeled with ^{32}P and then stimulated with different growth factors. Phosphoamino acid analysis was performed on immunoprecipitated phosphorylated L-MAG protein using two dimensional thin layer electrophoresis as described in Materials and Methods. The samples were either left untreated (NT), treated with 500 μM vanadate (VO_4), insulin (INS) and epidermal growth factor (EGF). PS= phosphoserine, PT= phosphothreonine, PY= phosphotyrosine.

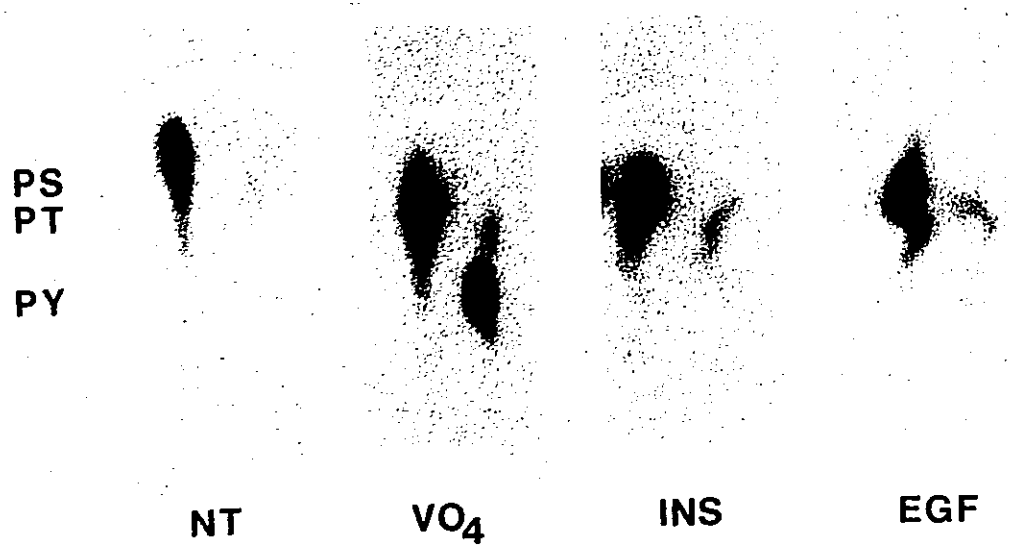
PS
PT
PY
NT
VO4
INS
EGF

Figure 4.9: Tryptic digestion of L-MAG phosphorylated in C5 L cells. C5 cells were ^{32}P- labeled and were left untreated (a) or were treated with 500μM ammonium vanadate (b), TPA (c) as described in Materials and Methods. Panel (d) represents phosphorylated L-MAG derived from PVsrcLM cells. Phosphorylated L-MAG was purified and digested with trypsin. The tryptic fragments were resolved by thin-layer chromatography (TLC) and electrophoresis (TLE), as described in Materials and Methods. The tryptic fragments were detected by autoradiography and were numbered 1-7. Phosphopeptides that were affected during TPA and vanadate treatment are identified with arrows.

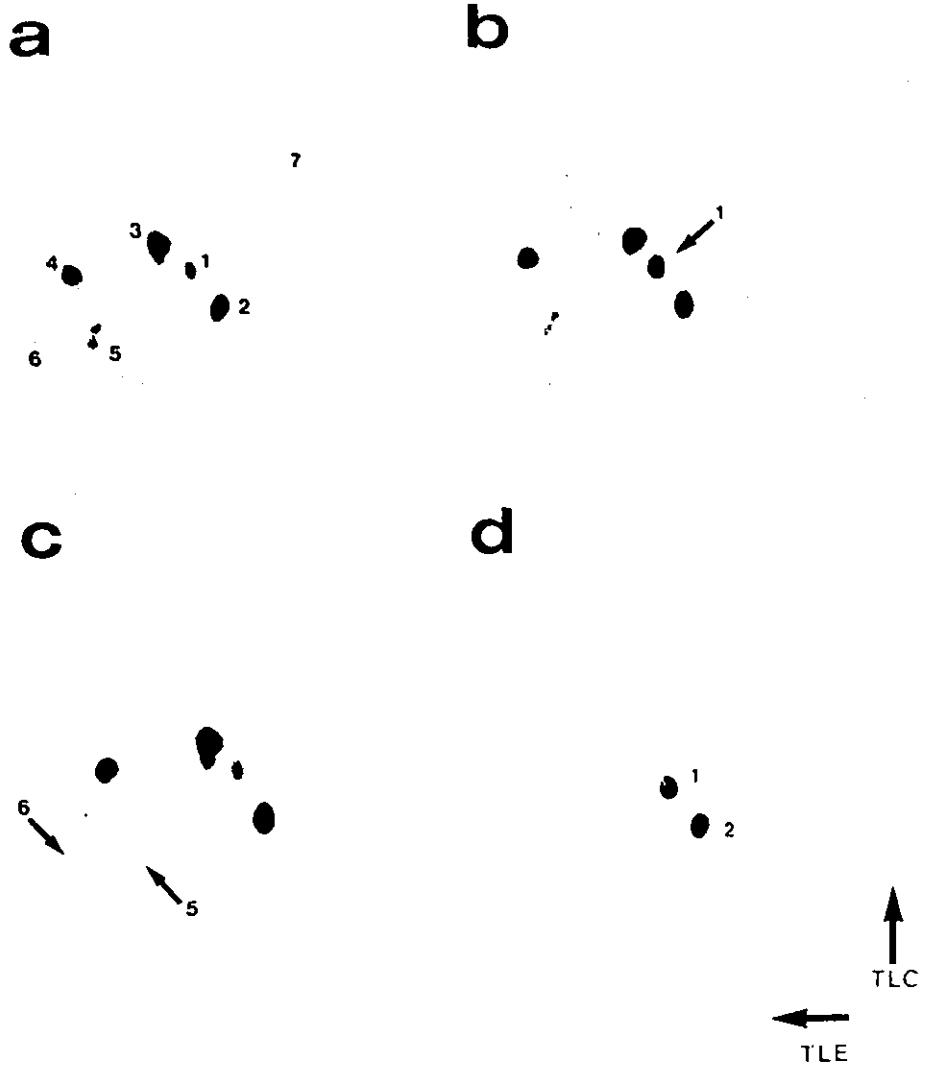
a
b
c
d
7
3
4
1
2
6
5
1
6
5
1
2
TLC
TLE

Vanadate treatment stimulates the phosphorylation of peptides 1, 8, 9 and 10. Phosphoamino acid analysis reveals the presence of phosphotyrosine in tryptic phosphopeptides 1, 8, 9, and 10 (Figure 4.10), where peptide 1 is considered to harbour the major tyrosine phosphorylation site. All other peptides contain only phosphoserine, with the exception of peptide 5, which is phosphorylated on threonine residues (Figure 4.10). The phosphotyrosine content in peptides 1, 8 and 10 is confirmed by immunoprecipitating these peptides from a tryptic digest using an anti-phosphotyrosine specific antibody (Figure 4.11b). The peptides were eluted with phenyl phosphate and analyzed by two dimensional mapping. Peptide 9 was not enriched with this procedure. A possible explanation is that anti-phosphotyrosine antibodies react with different affinities towards various tyrosine phosphorylated epitopes. It is possible that peptide 9 is among those not recognized by the antibody. Alternatively, peptide 9 has extremely high affinity towards the antibody and was not eluted with phenyl phosphate.

In order to determine whether tyrosine and serine phosphorylation occurs on matching L-MAG molecules, phosphorylated MAG from ^{32}P-labeled C5 cells was immunoprecipitated with an anti-phosphotyrosine antibody. SDS-PAGE analysis showed that L-MAG was the major tyrosine phosphorylated protein immunoprecipitated from these cells (data not shown), confirming earlier immunoblot data (see Figure 4.7B). Intriguingly, tryptic digest analysis of tyrosine phosphorylated L-MAG revealed a marked under-representation of peptide 2 with respect to peptide 1, but no change in the ratio of peptide 1 to 3 (Figure 4.11a).

Figure 4.10: Phosphoamino acid analysis of tryptic phosphopeptides derived from L-MAG. Phospho-tryptic fragments were eluted from thin-layer plates, lyophilized and digested in 6N HCl. Phospho-amino acids were resolved using one-dimensional electrophoresis (pH 3.5). The analyzed samples represent tryptic phosphopeptides 1 (a), 2 (b), 3 (c), 4 (d), 5 (e), 6 (f), 7 (g), 8 (h), 9 (i), 10 (j). PS= phosphoserine, PT= phosphothreonine, PY= phosphotyrosine.

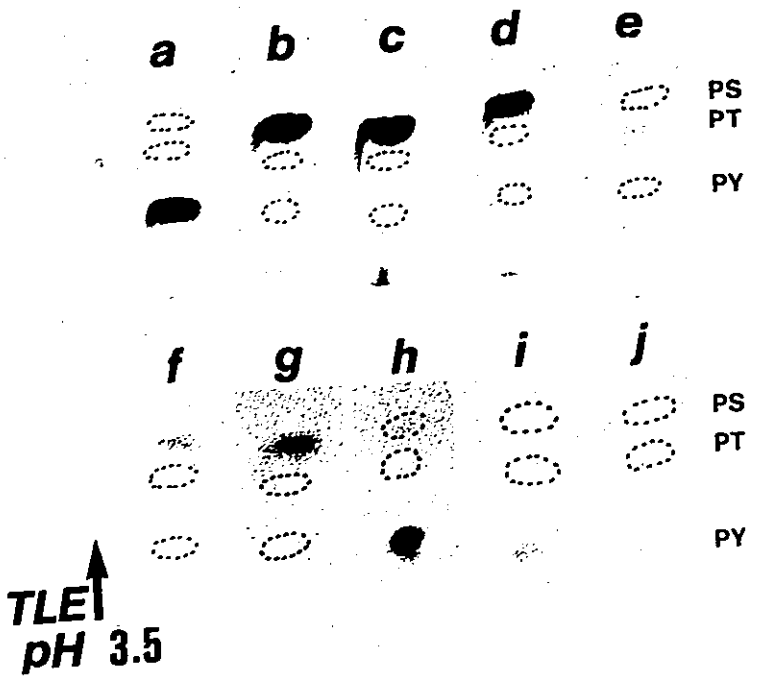
a
b
c
d
e
PS
PT
PY
f
g
h
i
j
PS
PT
PY
TLE
pH 3.5

Figure 4.11: Isolation of phosphotyrosine containing tryptic phosphopeptides. (a) Anti-phosphotyrosine antibodies were used to immunoprecipitate tyrosine phosphorylated proteins from vanadate (500 μM) treated C5 cells that were labeled with ^{32}P-orthophosphate. Immunoprecipitated protein corresponding to L-MAG was digested with trypsin and resolved on TLC and TLE as described in Materials and Methods. The autoradiograph shows peptides derived from tyrosine phosphorylated L-MAG. (b) A tryptic digest obtained from phosphorylated MAG was immunoprecipitated with anti-phosphotyrosine antibodies and analyzed by TLC and TLE. The autoradiograph reveals peptides that were reactive with anti-phosphotyrosine antibodies. The identities of the phosphopeptides are indicated by the numbers assigned to them in Figures 4.9a and 4.13c.

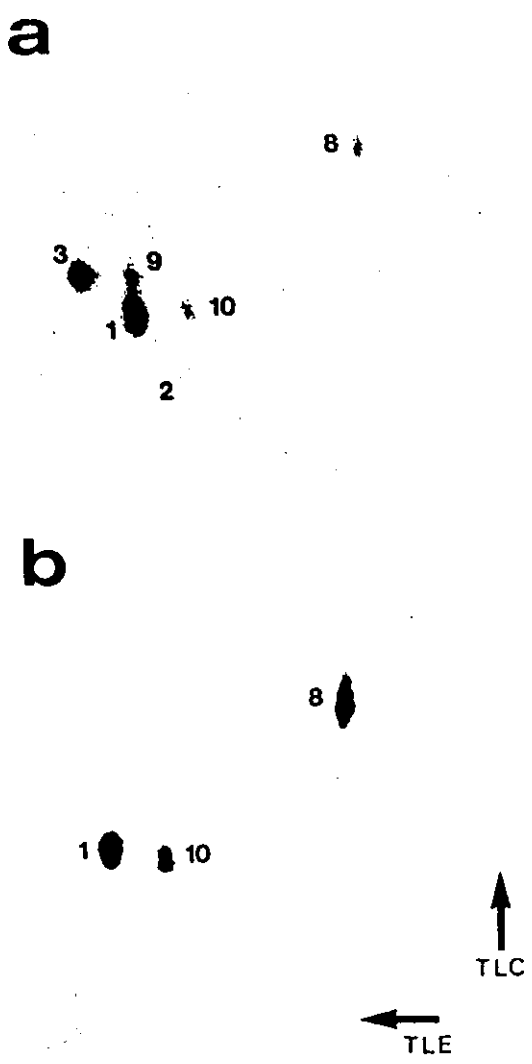
a
8
3
9
10
1
2
b
8
1
10
TLC
TLE

Tyrosine phosphorylated peptides 8, 9 and 10 were enriched (their identity confirmed by phosphoamino acid analysis), whereas peptides 4-7 (all serine/threonine phosphorylated peptides) were conspicuously absent. Therefore, with the exception of the phosphorylated residue in peptide 3, all other serine and threonine phosphorylated sites reside in L-MAG molecules that are, by default, not tyrosine phosphorylated. This result implies that tyrosine and serine/threonine phosphorylation events of L-MAG are regulated in a reciprocal manner.

4.2.5 L-MAG Phosphorylation in PVsrcLM Cells

Previously we demonstrated that partially purified MAG can be phosphorylated by $pp130^{gag\text{-}fps}$ and $pp60^{v\text{-}src}$ in vitro, two cytoplasmic tyrosine kinases encoded by the v-fps and v-src oncogenes respectively (36). In order to investigate whether L-MAG can be a substrate for $pp60^{v\text{-}src}$ in vivo, the L-MAG cDNA was introduced into v-src transformed NIH3T3 cells by retroviral infection. In PVsrcLM cells the cell surface distribution of L-MAG appears uniform (Figure 4.1). Thus, v-src transformation does not affect the transport of MAG to the cell surface, nor its distribution on the cell membrane. Phospho-amino acid analysis of L-MAG protein immunoprecipitated from ^{32}P labeled PVsrcLM cells demonstrates that L-MAG is constitutively phosphorylated mainly on serine and tyrosine residues, with a small amount of phosphothreonine being present (Figure 4.4). The high level of phosphotyrosine present in L-MAG isolated from these cells is not due to $pp60^{v\text{-}src}$ activity during the isolation procedure, since the cells were lysed in hot 2% SDS. Labeling PVsrcLM cells in the presence of ammonium vanadate did not change the

constitutive phosphorylation of L-MAG (data not shown).

Examination of L-MAG derived tryptic fragments from PVsrc1.M cells reveals the presence of peptides 1 and 2 as the major phosphorylation sites (Figure 4.9d). This confirms the results of the phosphoamino acid analysis, as peptide 1, the major tyrosine phosphorylation site, is present at a 1:1 ratio to peptide 2, the major serine phosphorylation site.

4.2.6 Analysis of S-MAG Phosphorylation

Phospho-amino acid analysis of phosphorylated S-MAG demonstrated that constitutive phosphorylation occurred primarily on serine residues. While TPA and dbcAMP had no detectable effect on S-MAG phosphorylation as determined by SDS-PAGE analysis (Figure 4.12A) and tryptic digest analysis (data not shown), vanadate treatment induced low but detectable levels of phosphotyrosine and phosphothreonine in this isoform (Figure 4.12B). Tryptic digest analysis of phosphorylated S-MAG revealed the presence of one major and two minor peptides (Figure 4.13a). Vanadate treatment, however, had no major effect on the tryptic map pattern (Figure 4.13b). Interestingly, the migration of S-MAG peptides a, b and c resembled closely the migration of L-MAG peptides 1, 2 and 7 respectively. To determine whether these peptides representing the major phosphorylation sites in S-MAG are identical to the ones in L-MAG, the peptides were eluted from the thin-layer plates and mixed together.

Figure 4.12: S-MAG phosphorylation. Phosphorylated S-MAG was immunoprecipitated from ^{32}P- labeled SM cells, resolved on SDS-PAGE and detected by autoradiography. SM cells were either left untreated (lane a), labeled in the presence of 500 μM ammonium vanadate (lane b), 4α Phorbol (lane c), TPA (lane d), sodium butyrate (lane e) or dbcAMP (lane f). The radioactive material at the top of the gel in each lane is labeled nucleic acid that associates non-specifically to protein A-sepharose. The amount of this material varies randomly between samples in different experiments. (B) Phospho-amino acid analysis on phosphorylated S-MAG immunopurified from vanadate treated SM cells. S= phosphoserine, T= phosphothreonine, Y= phosphotyrosine.

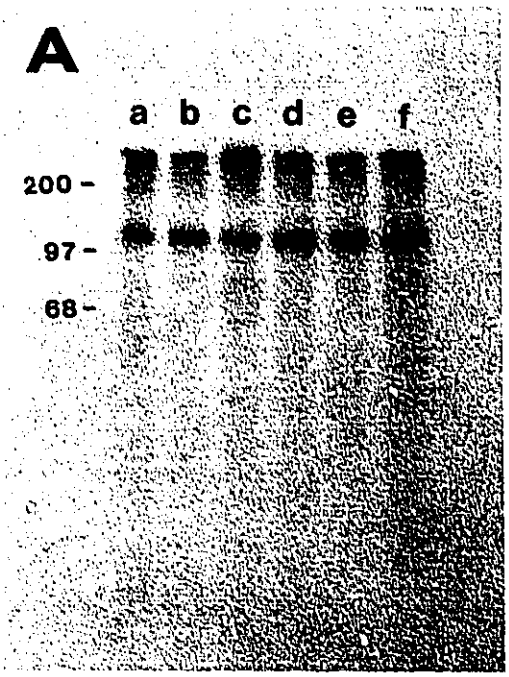
A
a b c d e f
200 -
97 -
68 -

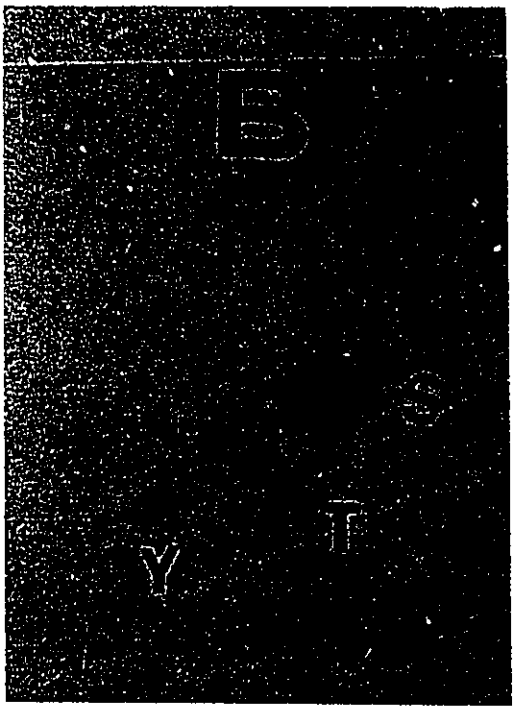
B

Figure 4.13: Tryptic digest analysis of phosphorylated S-MAG. Tryptic digests were performed on S-MAG immunoprecipitated from ^{32}P-orthophosphate labeled cells that were left untreated (a) or treated with 500 μM vanadate (b). The resultant thin-layer maps were visualized by autoradiography (3 day exposure) and compared to a peptide map derived from phosphorylated L-MAG (c) (18 hours exposure). S-MAG peptides a, b and c were eluted from the thin-layer plates and mixed with L-MAG peptides 1 or 9 (d), 7 or 8 (e), and 2 or 10 (f) respectively (peptides 1,2 and 7 are labeled as described in Figure 9a). The peptide mixtures were resolved on TLC and TLE as described in Materials and Methods.


a
c
b
b
c
b
b
c
d
8
7
a
1
c
10
2
1 + a
a
e
7 + c
b
c
f
2 + b
10
b
TLC
TLE

Since peptides 9, 10 and 8 migrate proximal to peptides 1, 2 and 7 in an L-MAG tryptic map (Figure 4.13c), these peptides were also mixed with the S-MAG peptides. Figure 4.12, panel d shows that S-MAG peptide a comigrates with peptide 1 from L-MAG, but not with peptide 9. Similarly, peptide c comigrates with peptide 7 (Figure 4.13e) and peptide b comigrates with peptide 2 (Figure 4.13f). These results demonstrate that all the phosphorylation sites in S-MAG are also present in L-MAG. Furthermore, the major vanadate inducible tyrosine phosphorylation site in L-MAG is also phosphorylated in S-MAG.The phosphorylation of this tyrosine residue in S-MAG, however, is insensitive to vanadate stimulation.

4.2.7 S-MAG Phosphorylation in Src-transformed Cells

The results discussed above indicate that, while S-MAG is phosphorylated on the same tyrosine residue as L-MAG, the stoichiometry of phosphorylation is many fold lower and cannot be increased with vanadate treatment. In order to determine whether this phenomena also holds true in cells with high intrinsic PTK activity, S-MAG was expressed in PVsrc cells. The resultant PVsrcSM12 cells were labeled in tissue culture with ^{32}P-orthophosphate along with PVsrcLM, C5 and SM32 cells. Immunoprecipitated MAG isoforms were then analyzed for phosphorylation by SDS-PAGE (Figure 4.14a) and MAG content by immunoblotting (Figure 4.14b). The results confirm that L-MAG expressed in L cells exhibits a higher degree of phosphorylation than S-MAG in L cells (Figure 4.14a, compare lanes 1 and 2), while the amount of MAG in each sample is comparable (Figure 4.14b, lanes 1, 2).

Figure 4.14: Comparison of L-MAG and S-MAG phosphorylation in fibroblasts and in PVsrc cells. MAG isoforms were immunoprecipitated from ^{32}P-labeled cells. (a) MAG originating from C5 L cells (lane 1), SM cells (lane 2), PVsrcLM cells (lane 3), PVsrcSM12 cells (lane 4) were analyzed by SDS-PAGE (7.5% polyacrylamide) and by (b) immunoblotting using anti-MAG antibodies. Molecular weight standards are indicated in kilodaltons. Tryptic digestion was then performed on L-MAG (c) and S-MAG (d) derived from PVsrc cells and resolved using TLC and TLE. Both peptide maps were autoradiographed for 2 days.

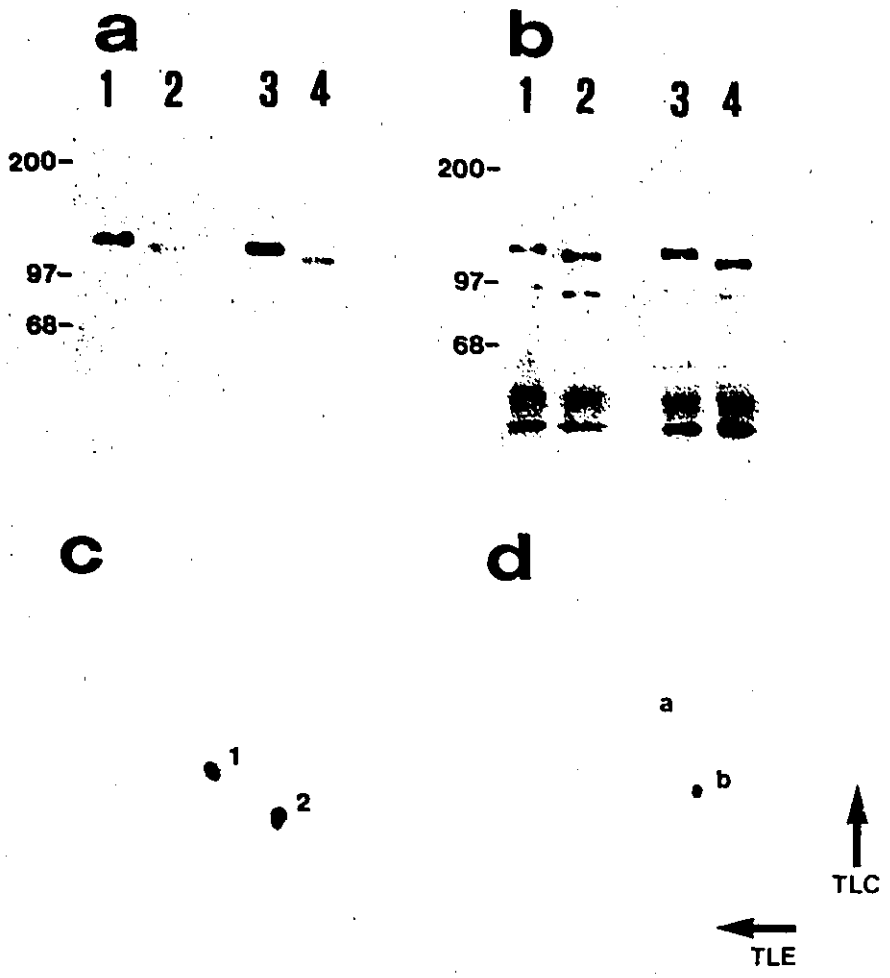
a
1 2 3 4
200-
97-
68-
b
1 2 3 4
200-
97-
68-
c
1
2
d
a
b
TLC
TLE

Unexpectedly, analogous results were obtained with PVsrc cells. L-MAG phosphorylation was distinctly higher than S-MAG phosphorylation (Figure 4.14a, compare lanes 3 and 4), despite having similar amounts of MAG in the samples (Figure 4.14b, lanes 3 and 4). Tryptic digest analysis of phosphorylated MAG in PVsrc cells demonstrates prominent phosphorylation of peptides 1 and 2 in L-MAG (Figure 4.14c, compare to Figure 4.9d), while peptides a and b in S-MAG are phosphorylated to a lesser extent (Figure 4.14d). Furthermore, the ratio of phosphorylation of peptide 1 to peptide 2 appears to be 1:1 in L-MAG, whereas the ratio of peptide a to peptide b in S-MAG seems to be in favour of peptide b by at least five fold. These findings suggest that even in src-transformed cells, S-MAG emerges as an inferior PTK substrate. However, it should be noted that tyrosine phosphorylation of S-MAG expressed in PVsrc cells is improved over S-MAG phosphorylation in L cells or 3T3 cells.

4.2.8 Characterization of Phospho-tryptic Peptides

In order to characterize MAG phosphorylation sites further, V8 protease and thermolysin digestions were performed on several of the tryptic phosphopeptides. Thermolysin cuts proteins at the amino-termini of Leu, Phe, Ile, Val, Met, and Ala. Under the conditions used in this study V8 protease attacks peptide bonds carboxyl-terminal to Glu residues (15). Figure 4.15 summarizes the results. Peptides 1 (panel a), 7 (panel c), 8 (panel d) and 9 (panel e) are susceptible to both V8 and thermolysin digestion. While peptide 2 is resistant to both proteases (panel b), peptide 10 is resistant to only V8 protease (panel f).

Figure 4.15: V8 protease and thermolysin digestion of tryptic phosphopeptides. L-MAG derived tryptic phosphopeptides 1 (a), 2 (b), 7 (c), 8 (d), 9 (e) and 10 (f) were eluted from thin-layer plates and re-digested with V8 protease or thermolysin. The digests were analyzed by chromatography. The samples in each panel correspond to: thermolysin digested (lane 1), thermolysin digested mixed with undigested (lane 2), undigested (lane 3), undigested mixed with V8 protease digested (lane 4), V8 protease digested (lane 5).

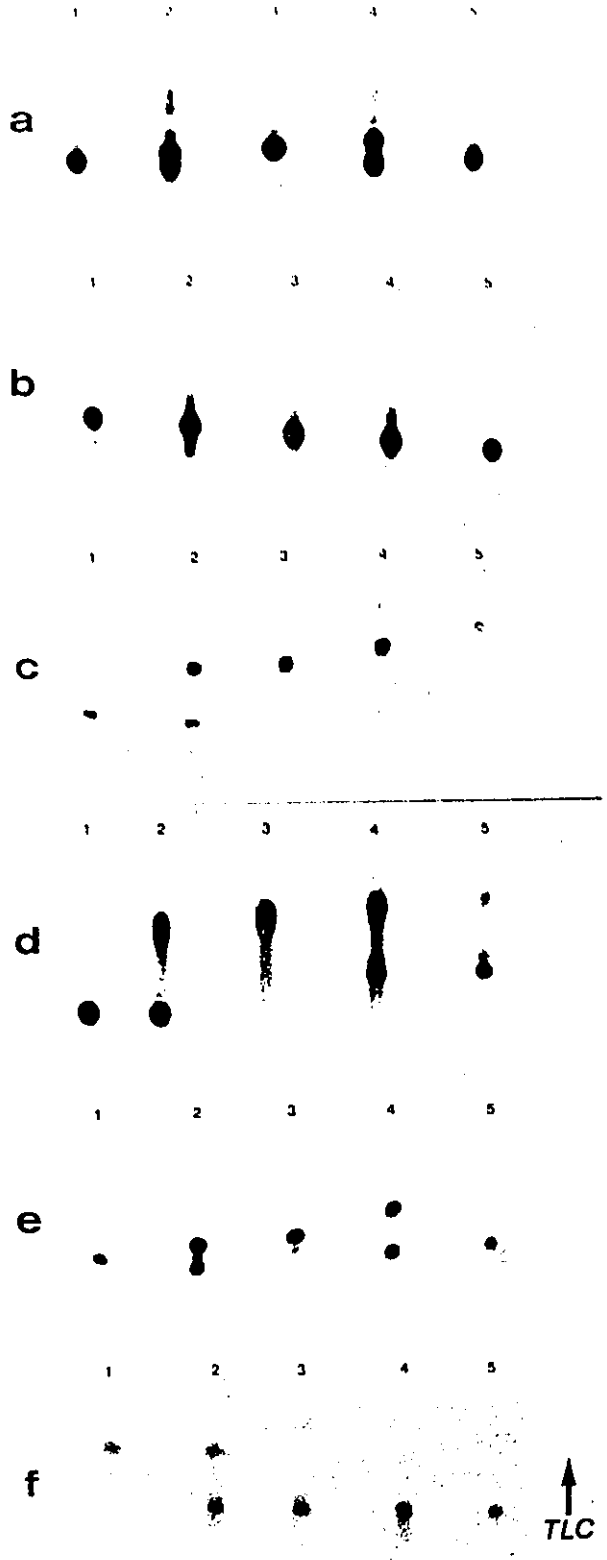
a
b
c
d
e
f
TLC

4.2.9 Phosphorylation of MAG in Oligodendrocytes

To determine whether the identification of MAG phosphorylation sites in heterologous cells is physiologically relevant, primary rat oligodendrocytes were analyzed for MAG phosphorylation. Oligodendrocyte precursors were differentiated for 12-14 days in SFM prior to ^{32}P-orthophosphate labeling. At this point in time the cultures are comprised of 100% MAG positive oligodendrocytes as determined by immunofluorescent cytochemistry (data not shown). ^{32}P-labeled MAG was then immunoprecipitated from untreated versus vanadate treated cells and analyzed by SDS-PAGE (Figure 4.16a). The results show that phosphorylation of MAG in oligodendrocytes is enhanced 2-3 fold with vanadate. This is in contrast to fibroblasts, were vanadate treatment results in only a qualitative change of MAG phosphorylation. MAG in untreated oligodendrocytes is phosphorylated mainly on serine residues (Figure 4.16b, panel 1). Vanadate stimulates the phosphorylation of both serine and tyrosine (Figure 4.16b, panel 2). Furthermore, tryptic digest analysis demonstrates the presence of peptides 1, 2 and 3 in untreated cells (Figure 4.16c, panel 1). During vanadate stimulation, phosphopeptide 7 appears and the phosphorylation of peptides 1 and 2 increase dramatically (Figure 4.16c, panel 2). The identity of these peptides was confirmed by mixing trypsin digested MAG from vanadate treated oligodendrocytes with L-MAG tryptic fragments derived from vanadate treated fibroblasts (Figure 4.16c, panel 2 + L-MAG). Other phosphopeptides identified in fibroblasts were not detected in oligodendrocytes, raising doubt as to their possible physiological significance.

The tryptic map data suggests that the phosphorylated MAG in oligodendrocytes is

identical to L-MAG. Consistent with this suggestion is the identification of peptide 3 (albeit faint), which is not present in S-MAG, and the increase in phosphorylation of peptide 1 with vanadate treatment, which does not happen to S-MAG in fibroblasts. Interestingly, the phosphorylation pattern of MAG from vanadate treated oligodendrocytes is reminiscent of the pattern observed in PVsrcLM cells (compare Figure 4.16c, panel 2 to Figures 4.9d and 4.14c). However, the possibility remained that S-MAG phosphorylation is different in oligodendrocytes compared to fibroblasts, especially in light of the absence of peptides 4, 5 and 6 which are characteristic of L-MAG phosphorylation in fibroblasts. To conclusively demonstrate that phosphorylated MAG in oligodendrocytes is analogous to L-MAG and not S-MAG, immunoprecipitated ^{32}P-labeled MAG from oligodendrocytes and from C5 cells were chemically deglycosylated using TFMS. Figure 4.17 demonstrates that MAG from both cell types comigrate on SDS-PAGE at a molecular weight of approximately 72 kd. This result confirms the identity of phosphorylated MAG in oligodendrocytes as L-MAG, since S-MAG when deglycosylated migrates at 67 kd. Moreover, the oligodendrocytes are used at an age corresponding to a period of active myelination in vivo, where the expression of L-MAG predominates over S-MAG.

Figure 4.16: Phosphorylation of MAG in primary rat oligodendrocyte cultures. Primary cultures of rat oligodendrocytes were labeled with ^{32}P-orthophosphate. (a) MAG was immunoprecipitated from lysates of cells that were untreated (lane 1) or treated with 500 μM vanadate (lane 2) and resolved on SDS-PAGE (7.5% polyacrylamide). Molecular weight standards are indicated in kilodaltons. (b) Phosphoamino acid analysis of immunoprecipitated MAG from untreated (panel 1) versus vanadate treated (panel 2) cells. S= phosphoserine, T= phosphothreonine, Y= phosphotyrosine. (c) Tryptic digest analysis of MAG from untreated (panel 1) versus vanadate treated (panel 2) cells. The identities of the phosphopeptides are indicated by the numbering used in Figure 4.9, and was verified by mixing MAG derived tryptic digests from vanadate treated oligodendrocytes with tryptic digests from L-MAG immunopurified from vanadate treated fibroblasts (panel 2 + L-MAG). The tryptic digests were analyzed by TLC and TLE as described in the Materials and Methods.

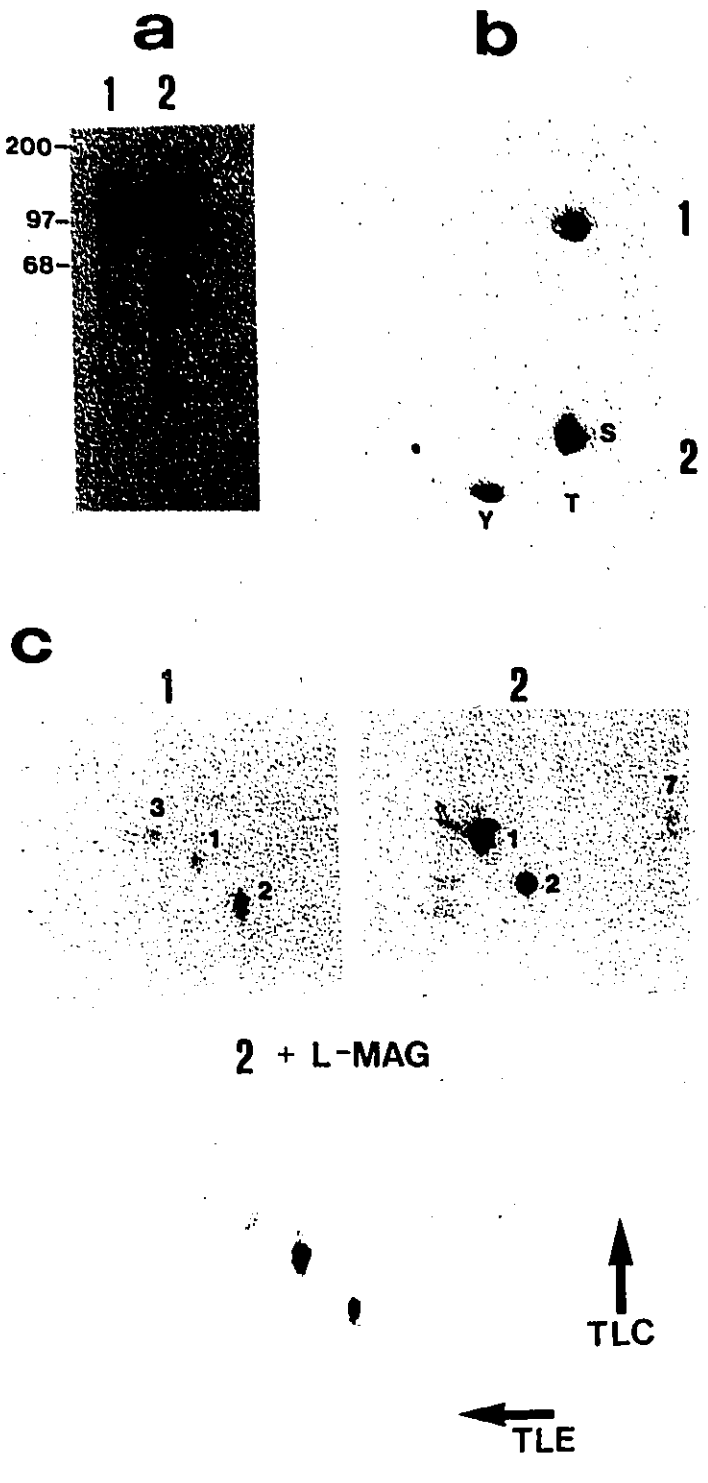
a
1 2
200
97
68
b
1
S
2
Y
T
c
1
2
3
1
2
1
2
7
2 + L-MAG
TLC
TLE

Figure 4.17: Deglycosylation of MAG in oligodendrocytes. MAG was immunoprecipitated from ^{32}P-orthophosphate labeled C5 L cells (lane 1) and oligodendrocytes (lane 2). The immunoprecipitates were subjected to chemical deglycosylation using TFMS as described in Materials and Methods. The samples were then resolved on SDS-PAGE (7.5% polyacrylamide) and visualized by autoradiography. Molecular weight standards are indicated in kilodaltons.

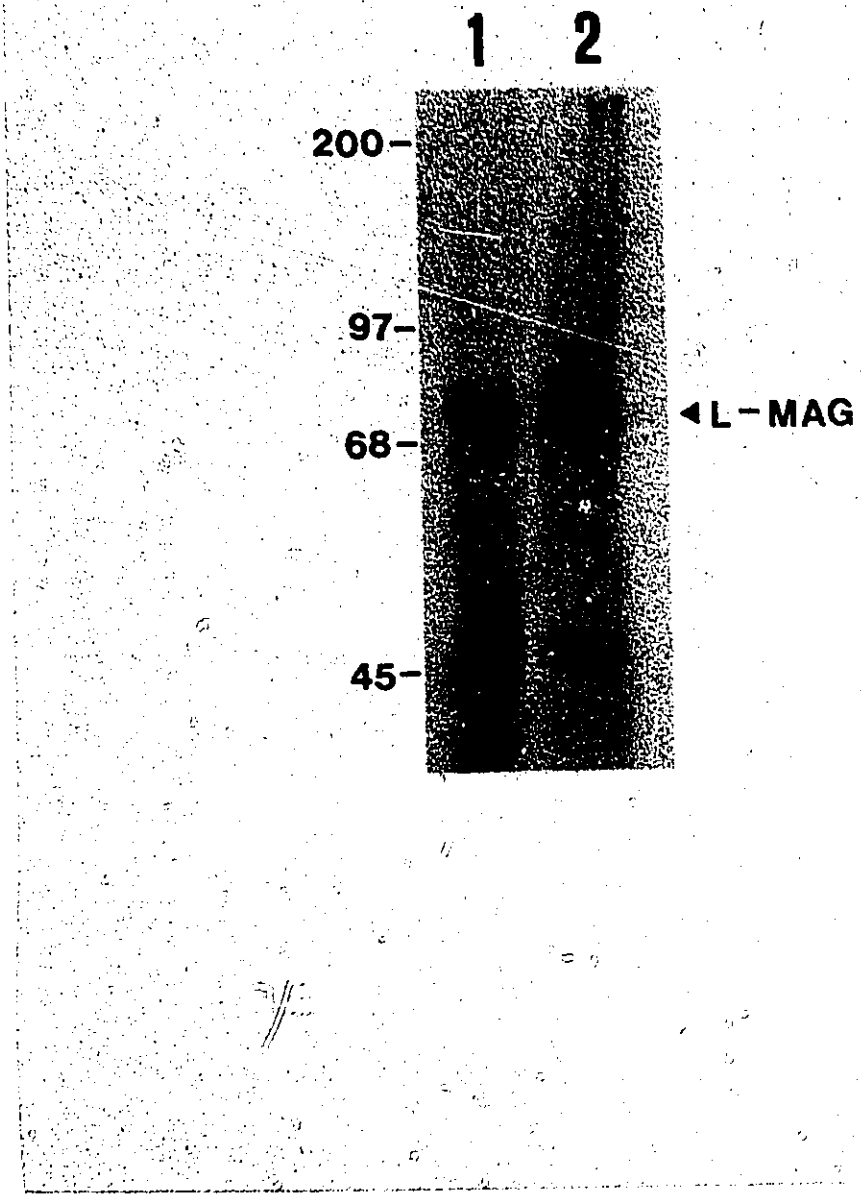
1
2
200–
97–
68–
45–
◀L–MAG

4.3 Discussion

In this study I demonstrate that both L-MAG and S-MAG are phosphorylated in a heterologous cell culture system. My present results were obtained with cells expressing high amounts of MAG and demonstrate that the stoichiometry of L-MAG phosphorylation is at least one order of magnitude greater than the phosphorylation of the S-MAG isoform. While previous observations had suggested that only L-MAG is an in vivo protein kinase substrate (36,37), it is likely that the inability to detect S-MAG phosphorylation in brain reflects its poor expression at the time of rapid myelination and its relatively lower stoichiometry of phosphorylation.

The protein kinases involved in MAG phosphorylation in brain are currently unknown. However, the phosphorylation of L-MAG in fibroblast cells is comparable to the pattern observed in oligodendrocytes in culture (this study) and in brain (with respect to phosphoamino acid content) (36), suggesting that common regulatory pathways are involved.

The tryptic cleavage sites in the cytoplasmic domains of L-MAG and S-MAG are outlined in figure 4.18. TPA, a PKC activator, can augment the phosphorylation of L-MAG, but not S-MAG in fibroblasts. TPA stimulation involves the minor peptide 6, which contains phosphoserine. Therefore, the potential PKC phosphorylation site that is common between L-MAG and S-MAG, threonine 543, is unlikely to be the site stimulated by TPA in tissue culture cells. A possible candidate sequence for a TPA inducible site may reside in the tryptic peptide LGSER (containing serine 579), which is part of a potential PKC phosphorylation site identified in L-MAG by Salzer et al.(149).

Figure 4.18: Schematic representation of the tryptic cleavage sites in L-MAG and S-MAG. The cytoplasmic domains of L-MAG and S-MAG are depicted as described previously in Figure 1.1. The arrows correspond to the positions of tryptic cleavage sites relative to the potential MAG phosphorylation sites. Tryptic fragments that are common to L-MAG and S-MAG are designated as peptides A and B.

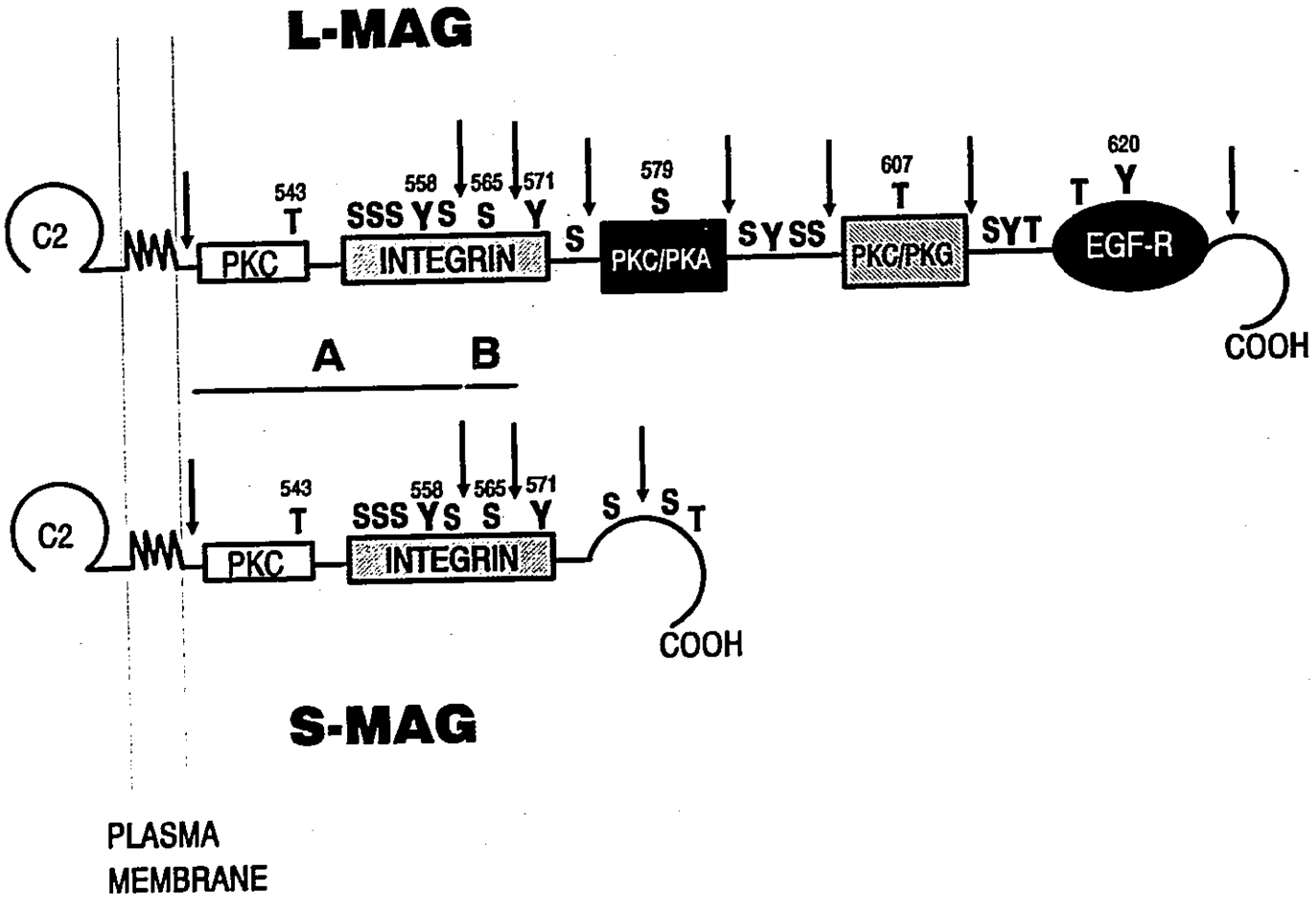
L-MAG
C2
PKC
543
T
558
565
571
SSS Y S S Y
INTEGRIN
S
579
S
PKC/PKA
S Y SS
607
T
PKC/PKG
SYT
620
T Y
EGF-R
COOH
A
B
C2
PKC
543
T
558
565
571
SSS Y S S Y
INTEGRIN
S S T
COOH
S-MAG
PLASMA
MEMBRANE

Peptide 6 is V8 protease labile and thermolysin resistant (data not shown), consistent with the LGSER sequence. TPA induced phosphorylation of L-MAG is relatively minor and its significance is, as yet, unclear. Nonetheless, it is intriguing that L-MAG, which is expressed concomitantly with the initiation of the myelin program appears to be a PKC substrate, since it has been previously shown that adherence of oligodendrocytes to a substratum causes a simultaneous activation of myelinogenesis and a PKC-mediated phosphorylation of myelin basic protein (183).

PTKs have been implicated in regulatory processes during development and differentiation (49,58,59,108). They can be divided into two major classes: (a) the growth factor receptor-type PTK, such as the EGF and insulin receptors; and (b) the cytoplasmic PTK's, such as the protein products of the c-src and c-abl proto-oncogenes (75). While EGF, IGF-1 and insulin had no effect on the phosphorylation of MAG, v-src transformation significantly increased L-MAG phosphotyrosine levels. Vanadate treatment significantly elevated phosphotyrosine levels in fibroblasts and oligodendrocytes, but had no major effect on the constitutive tyrosine phosphorylation of L-MAG in v-src transformed cells. Tryptic digest analysis of L-MAG from all four cell types (3T3 cells, L cells, oligodendrocytes and PVsrc cells), revealed that phosphopeptide 1 accounts for most of the phosphotyrosine content in MAG, suggesting that $pp60^{v\text{-}src}$ phosphorylates the same tyrosine residues as the endogenous oligodendrocyte and fibroblast MAG protein tyrosine kinase. It may be that L-MAG is phosphorylated by the cellular homologue of the protein product of v-src, $pp60^{c\text{-}src}$, which has been detected in myelin (69).

The identification of some of the important phosphorylation sites in MAG was

facilitated by the fact that all the phosphorylation sites in S-MAG were also present in L-MAG. Analysis of the protein sequence of L-MAG and S-MAG reveals that they share two cytoplasmic domain derived tryptic phosphopeptides- A and B (Figure 4.18). While peptide A contains several serine, one threonine and one tyrosine residue, peptide B contains a single serine residue. The analysis of the phospho-tryptic fragments generated from MAG are summarized in Table 4.1. The major tyrosine phosphorylation site in L-MAG (phosphopeptide 1) is also present in S-MAG (as peptide a). L-MAG and S-MAG share two tyrosine residues in their cytoplasmic domains, tyrosines 558 and 571 (Figure 4.18). Tyrosine 571 is unlikely to correspond to the phosphorylated residue in peptide 1/a, since it resides in a tryptic fragment spanning the junction at which S-MAG and L-MAG diverge in amino acid sequence (Figure 4.18). Therefore, by default, the tryptic fragment (peptide A in Figure 4.18) containing tyrosine 558 must be identical to peptide 1/a. Results of V8 protease and thermolysin digestions of this peptide corroborate this conclusion.

The identity of the major serine phosphorylation site(s) common to L-MAG and S-MAG and residing in phosphopeptide 2/b is less clear. Peptide 2/b is resistant to both V8 protease and thermolysin digestion. The candidate sequence ISGAPDK (peptide B in Figure 4.18), with serine 565 as the phosphorylation site is compatible with the data. However, in the absence of further diagnostic tests, the site of phosphorylation in peptide 2 cannot be definitively assigned.

Table 4.1: Summary of MAG tryptic phosphopeptide analysis. Tryptic peptides (1-10) derived from L-MAG have been analyzed for susceptibility to V8 protease (V8) and thermolysin (X) digestion. Phospho-amino acid content (Paa) and presence in S-MAG were determined. The candidate amino acid sequence from the L-MAG cytoplasmic region is presented for each tryptic peptide, where the putative phosphorylation sites are marked in bold. PS= phosphoserine, PT= phosphothreonine, PY= phosphotyrosine, ND= not determined.

Peptide	V8	X	Paa	S-MAG	Candidate sequence
1	+	+	PY	+	NVTEESPSFSAGDNPHVLYSPEFR
2	-	-	PS	+	I S G A P D K , NVTEESPSFSAGDNPHVLYSPEFR
3	-	-	PS	-	unknown
4	-	-	PS	-	"
5	ND	+	PT	-	"
6	+	-	PS	-	LGSER, YESEK
7	+	+	PS	+	NVTEESPSFSAGDNPHVLYSPEFR
8	+	+	PY	-	G E P P E L D L S Y H S D L G K , DSYTLTEELAEYAEIR
9	+	+	PY	-	G E P P E L D L S Y H S D L G K , DSYTLTEELAEYAEIR
10	-	+	PY	-	unknown

The minor serine phosphorylated peptide 7/c is labile to both V8 protease and thermolysin. Since this peptide is present in both L-MAG and S-MAG, it presumably corresponds to peptide A phosphorylated on a single serine residue (Figure 4.18, Table 4.1). The identities of the phosphorylation sites residing in the phosphopeptides particular to L-MAG are still unknown. Although one of the minor tyrosine phosphorylation sites present in peptides 8, 9 and 10 probably corresponds to the tyrosine homologous to the EGF-receptor autophosphorylation site (tyrosine 620), more information is needed to confirm this conclusion.

As described in figure 4.11, L-MAG molecules phosphorylated on tyrosine 558 display minimal phosphorylation on serines present in phosphopeptides 2/b and 7/c in particular, suggesting that tyrosine phosphorylation of MAG prevents phosphorylation of serine residues. The inability of serine/threonine kinases to recognize tyrosine phosphorylated MAG as a substrate may be due to a change in the conformation of the MAG cytoplasmic domain by tyrosine phosphorylation. Alternatively, access to the serines may be prevented by steric hindrance caused by the phosphotyrosine moiety. As a result of the reciprocal relationship between serine/threonine and tyrosine phosphorylation there exist two L-MAG populations, which potentially perform different functions.

Although phosphorylation sites are shared between L-MAG and S-MAG, the stoichiometry of phosphorylation differs dramatically between the two isoforms. In fact, the major vanadate inducible phosphorylation site in L-MAG, tyrosine 558, is insensitive to vanadate stimulation in S-MAG. This suggests that the reduced phosphorylation in S-MAG is not due to an increase in its turnover. Even when S-MAG is expressed in v-src-

transformed cells, the stoichiometry of phosphorylation is lower than that of L-MAG especially with respect to phosphorylation of tyrosine 558. A possible mechanism may involve an increase in the stability of phosphates in S-MAG, resulting in a decreased incorporation of ^{32}P during the labeling period of 4 hours. However, immunoblots of lysates from cells expressing either isoform reveal the presence of phosphotyrosine immunoreactivity only in L-MAG when probed with an anti-phosphotyrosine antibody (data not shown). Therefore, as this phenomena cannot be accounted for by either an increase or a decrease in the phosphate turnover in S-MAG, the serine and especially tyrosine phosphorylation in MAG is a function of the carboxyl terminus. In effect, the unique segments of the MAG cytoplasmic tails dictate the extent of phosphorylation.

The mechanism of regulation of phosphorylation is unknown, but it may involve one of four scenarios: (i) the unique 10 amino acid carboxyl terminus of S-MAG is inhibitory to kinases; (ii) the 54 amino acid carboxyl terminus unique to L-MAG is stimulatory to kinases or (iii) inhibitory to phosphatases; (iv) the secondary structure of the cytoplasmic domains of S-MAG and L-MAG are so different that they exhibit distinct properties as protein kinase substrates.

The first two models are not mutually exclusive. The L-MAG carboxyl tail may exhibit docking sites for protein kinases that would not be present in S-MAG. A stable intermolecular association between kinase and MAG is likely to be necessary for phosphorylation to occur. In the absence of these putative kinase binding sites, as would be the case for S-MAG, phosphorylation proceeds inefficiently. In addition, the unique carboxyl tail of S-MAG may prevent efficient recognition of the phosphorylation sites by

the kinases.

The third model is not likely to be the case, since vanadate treatment does not increase phosphotyrosine levels in S-MAG. All known phosphotyrosine-specific protein phosphatases are vanadate sensitive (54). Therefore, a simple protection of the phosphorylation sites by the carboxyl terminus of L-MAG is unlikely to account for the difference in the stoichiometry of phosphorylation between S-MAG and L-MAG.

The secondary structure of peptides and proteins has previously been known to influence their propensity as PTK substrates (139). It is, therefore, a possibility that the unique domains of L-MAG and S-MAG exert structural constraints on the common portion of their cytoplasmic domains, thereby altering their capacities as PTK substrates. To test any of the above described models, cytoplasmic deletion mutants of MAG need to be generated in order to determine the point at which the stoichiometry of mutant L-MAG phosphorylation drops down to the levels observed for S-MAG.

Regardless of the mechanism, the consequence of generating two isoforms, that are distinct only in their carboxyl termini, is to produce isoforms with different capabilities of interacting with signal transduction pathways. The most striking feature of this difference is the capacity of one isoform, L-MAG, to become extensively phosphorylated on tyrosine. A potential role for tyrosine specific protein phosphorylation in the regulation of cell-cell and/or cell-matrix interactions has been demonstrated for the sevenless homeotic gene of Drosophila (58), the platelet integrin- glycoprotein gpIIb-IIIa (41,51,52) and the fibronectin receptor (70,172). It was demonstrated that tyrosine phosphorylated integrins, isolated from Rous sarcoma virus-transformed chick embryo

fibroblasts, exhibited a decreased ability to bind fibronectin and talin, compared to non-phosphorylated receptor (172). The critical integrin phosphorylation site has been mapped to tyrosine 788, which is located in a domain responsible for binding the cytoskeleton (172). A homologous stretch of amino acids is found in the region common to both MAG isoforms (amino acids 551-573) (149,171). Interestingly, the major tyrosine phosphorylation site in MAG, tyrosine 558, is nested amongst amino acids similar to those surrounding tyrosine 788 of the fibronectin receptor. Therefore, this conserved region is a PTK target in two distinct cell adhesion molecules. We speculate that phosphorylation of the cytoplasmic domain may modify the interaction between MAG and certain cytoplasmic components thus regulating MAG specific cell adhesion functions.

L-MAG may function as a signal transducer as has been observed for other cell adhesion molecules that are members of the Ig gene superfamily (31,152,185). Sequences found in the unique domain of L-MAG may represent docking sites for protein kinases. Oligomerization of L-MAG molecules through ligand binding may result in kinase activation, generation of second messenger signals and ultimately alteration in gene expression. S-MAG, which lacks this domain and putative kinase binding sites, may have more restricted activities and serve only as an adhesive molecule.

CHAPTER 5

STUDIES ON MYELIN-ASSOCIATED GLYCOPROTEIN IN SIGNAL TRANSDUCTION

SUMMARY

The role of MAG in the bi-directional transmission of signals was investigated. Increasing the tyrosine phosphorylation of MAG had no detectable effect on its cell adhesion properties, implying an alternative function to MAG phosphorylation. During cell surface cross-linking experiments, the kinases that associate with MAG were not found to co-immunoprecipitate with MAG. This distinguishes MAG from CD4 and its interaction with the protein tyrosine kinase Lck. Similarly, no change in the phosphorylation pattern of L-MAG was detected during MAG cross-linking. Phosphorylation of MAG, however, may be important in linking MAG to certain signalling pathways, since tyrosine phosphorylated L-MAG associates with the SH2 domain of phospholipase C-gamma in an in vitro binding assay. This interaction was dependent on tyrosine phosphorylation and did not occur with other SH2 domains. This finding suggests a functional importance to the generation of two MAG isoforms. L-MAG can become tyrosine phosphorylated and interact with signalling molecules via specific protein motifs. Early in development this interaction may lead to the induction of messages important for the initiation of myelin synthesis. S-MAG, on the other hand, does not become tyrosine phosphorylated and may simply function as a cell adhesion molecule important for the maintenance of the myelin structure in the adult brain.

5.1 Introduction

The initiation of myelin synthesis correlates with the appearance of myelin-associated glycoprotein (MAG) (9,122), a major myelin specific glycoprotein which is expressed in oligodendrocytes in the CNS and Schwann cells in the PNS (167). MAG has properties of cell adhesion molecules (CAMs) (3,133,145) and belongs to the immunoglobulin (Ig) supergene family (7,96,149). Schwann cells which, by retroviral infection, express an antisense mRNA to MAG fail to initiate myelination of neurons in culture (124). Overexpression of MAG in Schwann cells, on the other hand, leads to the ensheathment of about ten times as many sensory neurons as compared to control cultures (121). These findings, as well as other in vivo studies (9), indicate that MAG is involved in the initial glia-neuron recognition event necessary for myelination to occur.

MAG exists as two alternatively spliced isoforms, L-MAG and S-MAG, that differ in their carboxyl termini (7,96,149). The expression patterns of both isoforms differ during development, suggesting that L-MAG and S-MAG play distinct roles during development (43,128,181). An interesting feature of L-MAG and S-MAG is that they are differentially phosphorylated on serine and tyrosine residues (4,36). The carboxyl terminus of L-MAG is longer than that of S-MAG and it contains several potential phosphorylation sites. The identification of the major tyrosine and serine phosphorylation sites, however, revealed that these sites reside in domains that are common to both isoforms (Chapter 4). Yet, the stoichiometry of phosphorylation of L-MAG is at least ten fold greater (4), suggesting that L-MAG has a greater ability to interact with protein kinases than S-MAG.

The biological functions of MAG may in part be regulated by phosphorylation. In

order to explore this possibility, the effect of phosphorylation on the cell adhesion properties of MAG were tested. Furthermore, since it has become apparent that cell adhesion processes are closely linked to signal transduction pathways (31,93,152,185,194), the involvement of MAG with signalling molecules was investigated.

5.2 Results and Discussion

5.2.1 Effect of tyrosine phosphorylation on the cell adhesion properties of MAG

L-MAG and S-MAG have both been shown to function as cell adhesion molecules when expressed in L cell fibroblasts (Chapter 3). Both isoforms conferred heterotypic, calcium and temperature independent adhesion to L cells in suspension cultures. A possible function of phosphorylation may be in the regulation of MAG-mediated cell adhesion. The differential phosphorylation of MAG isoforms would provide a mechanism for alternative modes of functional regulation at different times during development. In order to investigate this possibility L-MAG and S-MAG expressing L cells were pre-incubated with vanadate prior to a cell aggregation assay. Vanadate pretreatment results in a dramatic increase in tyrosine phosphorylation of L-MAG, but not of S-MAG. The findings of these cell adhesion assays are summarized in Figure 5.1. In the absence of vanadate pretreatment, L-MAG and S-MAG expressing cells displayed normal cell aggregation activity. Vanadate treatment, before and during the cell adhesion assay, caused a small decrease in both L-MAG and S-MAG mediated aggregation. Immunoblot analysis of cell extracts probed with an anti-phosphotyrosine antibody after the cell

adhesion assay confirmed that, while many proteins become tyrosine phosphorylated in vanadate treated L-MAG and S-MAG expressing cells, only the L-MAG isoform was tyrosine phosphorylated (data not shown). Since the decrease in aggregation was observed for both L-MAG and S-MAG, it was concluded to be unrelated to MAG phosphorylation. Similarly, TPA, which caused a change in the phosphorylation of L-MAG, but not S-MAG (Chapter 4), had no effect on the cell adhesion properties (data not shown).

These results lead to the conclusion that an increase in tyrosine phosphorylation does not affect MAG mediated cell aggregation of L cells in suspension. This is in contrast to studies on integrin mediated binding phenomena, in which tyrosine phosphorylated integrins do not bind their ligand fibronectin (172). The L cell system, may however, not be an ideal system to study the effects of tyrosine phosphorylation on MAG-ligand interactions, since a significant overexpression of MAG is required to observe cell adhesion. This may be due to the fact that MAG is not binding to its physiological ligand in L cells. MAG-mediated adhesion may be more sensitive to changes in phosphorylation in the context of oligodendrocyte-neuron interaction. Furthermore, since L-MAG displays constitutive phosphorylation on tyrosine, future experiments should assess the effect of decreasing MAG phosphorylation on cell adhesion. This could be achieved by incubating the cells with the kinase inhibitor genistein (Akiyama et al., 1987, J. Biol. Chem. 262: 5592-5595) during a cell aggregation assay. Alternatively, the tyrosine phosphorylation of MAG may have different role in MAG function as is addressed in the next two sections.

Figure 5.1: Effect of vanadate on MAG-mediated L cell aggregation. S-MAG (SM32) (panel A) and L-MAG (C5) (panel B) expressing L cells were left untreated or pre-treated with 500 μM vanadate for 3 hours. Single cell suspensions were then aggregated in the presence (dotted line) or absence (solid line) of vanadate. The degree of aggregation was determined at different time points and expressed as the mean +/- standard error from 4 determinations.

A

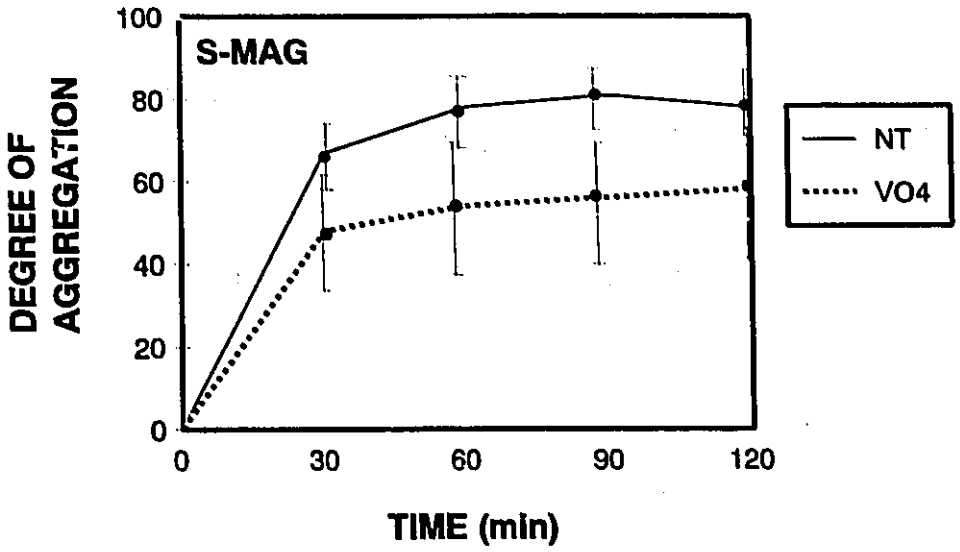
S-MAG
DEGREE OF AGGREGATION
100
80
60
40
20
0
0
30
60
90
120
TIME (min)
NT
VO4

B

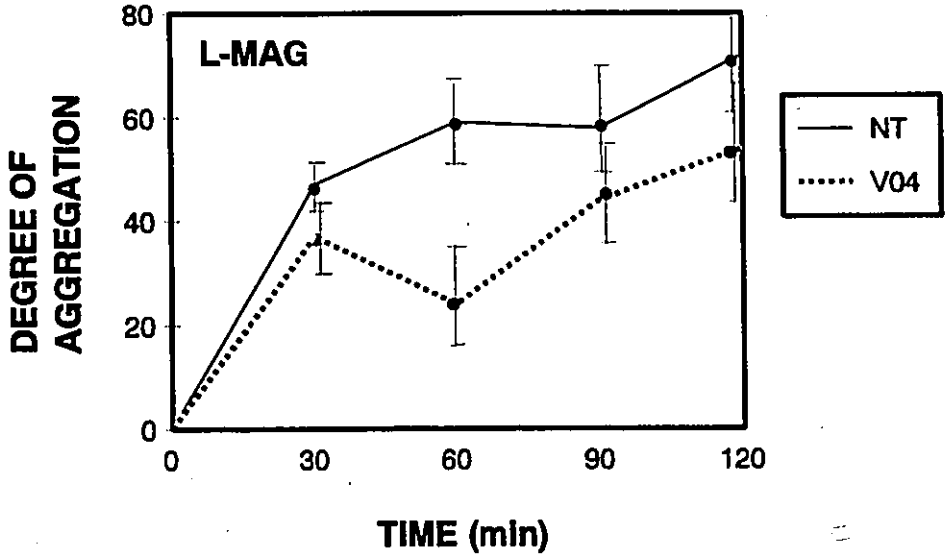
L-MAG
DEGREE OF AGGREGATION
80
60
40
20
0
0
30
60
90
120
TIME (min)
NT
V04

5.2.2 Effect of cross-linking MAG on signal transduction molecules

An important consequence of cell adhesion is the generation of second messengers and the activation of signal transduction pathways (31). In order to study the intracellular consequences of adhesive events, ligand-CAM binding interactions have been mimicked by cross-linking CAMs on the cell surface with specific antibodies (93,185). Using this methodology CD4, an Ig related CAM in T-cells, was cross-linked on the cell surface of HUT78 cells, a transformed T-cell line. CD4 was then immunoprecipitated and associated kinase activity was assessed. As has been described previously (185) CD4 cross-linking resulted in the activation of $p56^{lck}$ (Figure 5.2, lane 3), a protein tyrosine kinase (PTK) of the src family (1,184). Due to the similarities of MAG with CD4, analogous experiments were performed with L-MAG in fibroblasts and oligodendrocytes. The anti-MAG monoclonal antibody 513 was used for MAG cross-linking, since this antibody presumably recognizes the MAG-ligand binding site (3,133). The results showed no specifically associated kinase activity in anti-MAG immunoprecipitates (data not shown). The association of Lck with CD4 is a tight non-covalent metal ion coordination complex, involving a pair of cysteine residues in the cytoplasmic domain of CD4 (184). This association is resistant to non-ionic detergents, which are used during immunoprecipitation procedures, but can be disrupted by ionic detergents and reagents reactive with free sulfhydryl groups (184). While CD4 is not phosphorylated itself, L-MAG is a formidable protein kinase substrate (Chapter 4).

Figure 5.2: CD4 cross-linking in HUT78 cells. Cell lysates from HUT78 cells were immunoprecipitated with a rabbit anti-mouse IgG specific antibody (lane 1), or polyclonal anti-CD4 antibodies (lanes 2-4). The samples were untreated (lanes 1 and 4), or incubated with anti-CD4 antibodies for 30 minutes on ice (lanes 2 and 3). Cross-linking of CD4 on the cell surface was performed with goat anti-rabbit IgG specific antibodies for two minutes at 37°C (lanes 3 and 4). The immunoprecipitates were subjected to in vitro kinase assays and subsequently resolved on SDS-PAGE (10% polyacrylamide). The gels were fixed, treated with alkali and subjected to autoradiography. Molecular weight standards are indicated as well as the position of $p56^{lck}$.

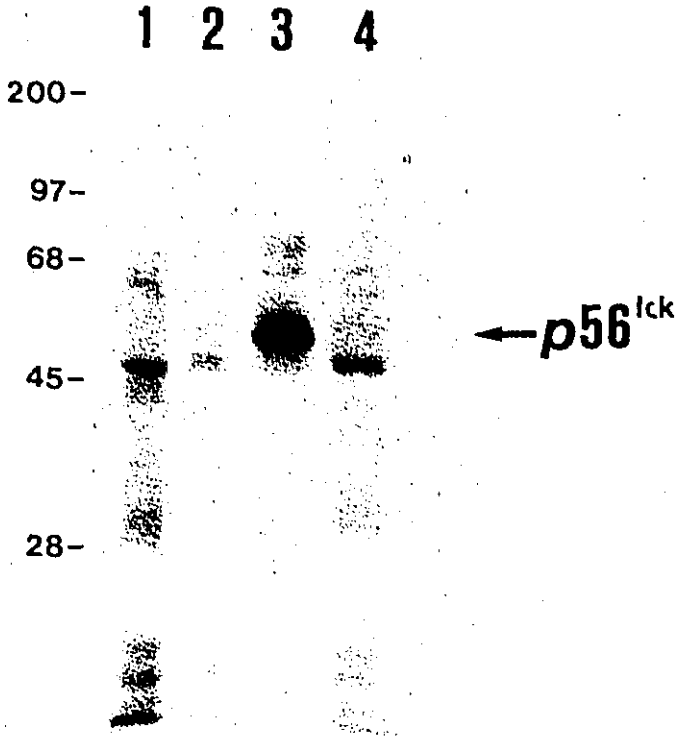
1 2 3 4
200-
97-
68-
45-
28-
←p56lck

To investigate whether the phosphorylation pattern of L-MAG is altered during cross-linking, L-MAG expressing fibroblasts and oligodendrocytes were labeled with ^{32}P-orthophosphate and cross-linked with antibody 513. Phosphorylated MAG was immunoprecipitated and analyzed by tryptic digest mapping. The results, obtained in L cell fibroblasts, are summarized in Figure 5.3. No effect of cross-linking was detected on the phosphorylation pattern of L-MAG. Identical observations were made with oligodendrocytes (data not shown), suggesting that the interaction of MAG with signal transduction molecules differs from the association of CD4 with Lck. It may be that activation of other signalling pathways occur via MAG, as has been determined for other CAMs (31,152), but these remain to be investigated for MAG.

5.2.3 Association of tyrosine phosphorylated L-MAG with the SH2 domain of PLC

Activation of growth factor receptor tyrosine kinases (GFRs) leads to phosphorylation of a number of cellular proteins, resulting in cellular proliferation and/or differentiation (182). Many of the effects of GFRs have been attributed to a multi-component protein complex that forms with the GFR upon GFR activation. These include phospholipase C-gamma (PLC), the cytoplasmic PTKs Src, Fyn and Yes, the Raf-1 serine/threonine kinase, the phosphatidyl inositol (PI)-3 kinase, and the GTPase activating protein (GAP) involved in controlling ras activity (6,28,86,95,110,187). All of these molecules, with the exception of Raf-1, exhibit non-catalytic functional domains termed src-homology regions 2 and 3 (SH2 and SH3 respectively) due to sequence homologies with a stretch of about 100 amino acids residing in the c-src encoded PTK.

Figure 5.3: Effect of cross-linking L-MAG on its phosphorylation in C5 cells. C5 cells were labeled with ^{32}P-orthophosphate and were left untreated on ice (panels a and e), or were incubated with 513 anti-MAG antibodies on ice (panels b, c and d). The samples were then harvested for immunoprecipitation (panels a and b), or were treated with no antibodies (panel c) or with rabbit-anti mouse IgG specific antibodies (panels d and e) at 37°C. Phosphorylated L-MAG was immunoprecipitated and digested with trypsin. The digests were resolved on thin-layer chromatography (TLC) and subsequent thin-layer electrophoresis (TLE). The thin-layer plates were then visualized by autoradiography.

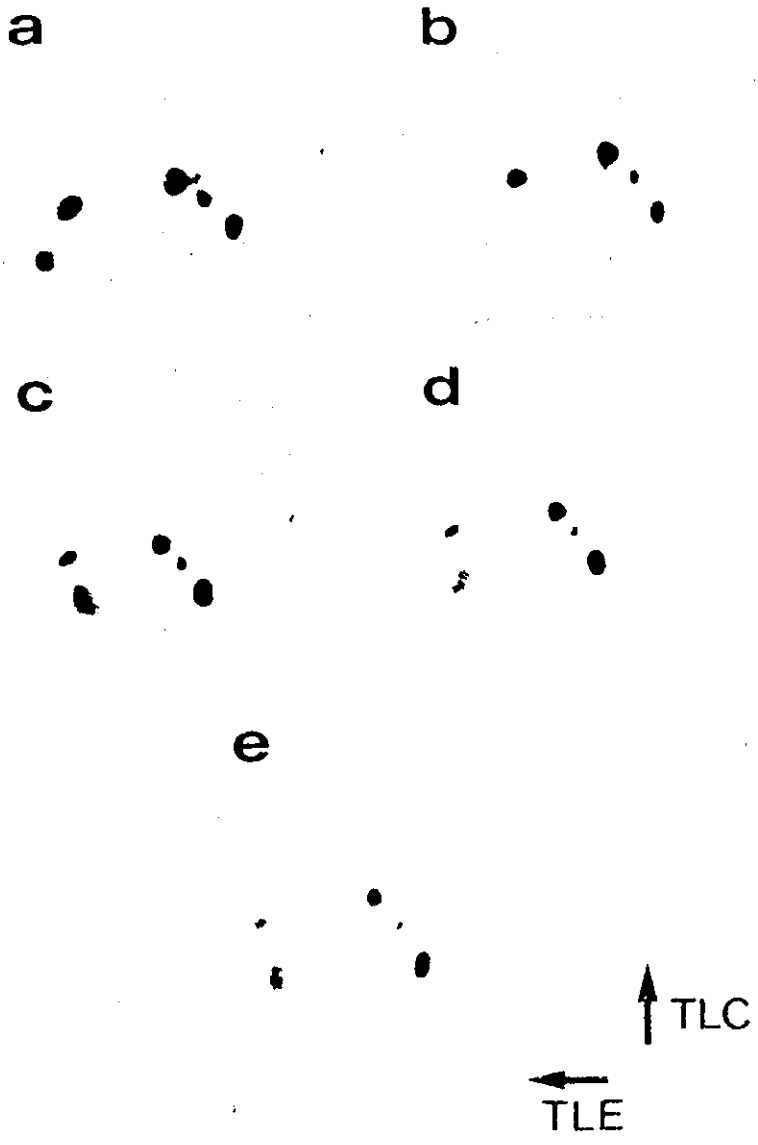
a
b
c
d
e
TLC
TLE

It is via their SH2 domains that many of these signalling molecules bind to specific phosphorylated tyrosine residues in GFRs and, thus, participate in a growth factor-mediated signal (6,91).

There are certain analogies that can be drawn between GFRs and MAG. They are both transmembrane proteins, with some GFRs also belonging to the Ig supergene family (189). L-MAG is also phosphorylated on tyrosine similar to activated GFRs. MAG is one of the earliest markers of oligodendrocyte differentiation and seems to be responsible for the initiation of myelin synthesis (9,122,124). In this context the function of MAG may not be restricted to cell adhesion. It is possible that upon ligand binding MAG also participates in transducing signals to initiate the myelin program.

To test the prospect of an interaction of MAG with different signal transduction molecules, an in vitro binding assay, in principle similar to immunoblotting, was utilized. The SH2 domains of PLC, Src, Crk and GAP were introduced into a bacterial expression vector and expressed as TrpE-SH2 fusion proteins in Escherichia coli (E. coli) (6). Bacterial extracts were then incubated with anti-MAG immunoprecipitates, that were resolved by SDS-PAGE and immobilized on nitrocellulose filters. The immunoprecipitates were obtained from L-MAG and S-MAG expressing cells that were either left untreated or treated with vanadate. TrpE-SH2 fusion proteins binding to MAG were visualized using a secondary screening with an anti-TrpE specific antibody and a final probing of the filters with a radioiodinated anti-IgG antibody. TrpE fusion proteins containing the SH2 domain of PLC specifically bound tyrosine phosphorylated L-MAG (Figure 5.4, panel c), whereas TrpE fusions with the other SH2 domains failed to

recognize MAG (data not shown). As shown previously (Chapter 4) vanadate treatment does not significantly alter the expression of MAG isoforms in fibroblasts (Figure 5.4, panel a). It, however, significantly increases the tyrosine phosphorylation of L-MAG, but not of S-MAG (Figure 5.4, panel b). Figure 5.4, panel c, clearly shows that TrpE-PLC-SH2 fusion proteins interact only with tyrosine phosphorylated L-MAG. This interaction was inhibited with phenyl phosphate (Figure 5.4, panel d), an analogue of phosphotyrosine, clearly demonstrating the specificity for this interaction. TrpE protein alone did not bind any proteins specifically (Figure 5.4, panel e).

These findings demonstrate the ability of MAG to bind the SH2 domain of PLC. This interaction is regulated by tyrosine phosphorylation of MAG and was specific to the SH2 domain of PLC. This is in agreement with studies on activated GFRs, where the specificity of binding is determined by the SH2 domain, as well as the context in which the phosphorylated tyrosine residue is presented (6,87). In effect, the surrounding amino acids play a determining role in the binding phenomena. The significance of MAG binding the SH2 domain of PLC is uncertain, since an interaction with the enzyme itself was not demonstrated. However, this finding raises some interesting possibilities, where L-MAG may function in an analogous fashion to a GFR. A signalling event may result in the tyrosine phosphorylation of L-MAG and its subsequent association with SH2 domain containing proteins (either PLC or as yet unidentified molecules). These proteins may then serve as PTK substrates, where L-MAG operates as a common docking site for these signalling molecules to interact.

Figure 5.4: Association of the PLC-SH2 domain with tyrosine phosphorylated L-MAG. L-MAG (lanes 1 and 2) and S-MAG (lanes 4 and 5) were immunoprecipitated from C5 cells and $3TV_29$ cells respectively, that were either left untreated (lanes 1 and 4) or pre-treated with 500 μM vanadate (lanes 2 and 5). An aliquot of each cell extract was pooled and immunoprecipitated secondary antibodies only (i.e. without anti-MAG specific antibodies) (lane 3). The samples were resolved on SDS-PAGE (7.5% polyacrylamide), transferred to nitrocellulose and then probed with (a) anti-MAG specific antibodies Gen S1 and Gen S3, (b) anti-phosphotyrosine antibodies (UBI), (c) TrpE-PLC-SH2 fusion protein, (d) TrpE-PLC-SH2 fusion protein in the presence of 10 mM phenyl phosphate, and (e) TrpE protein alone. The blots were then probed with anti-TrpE specific antibodies (panels c, d and e) and secondary ^{125}I-goat anti-mouse IgG specific antibodies. The signals were visualized by autoradiography.

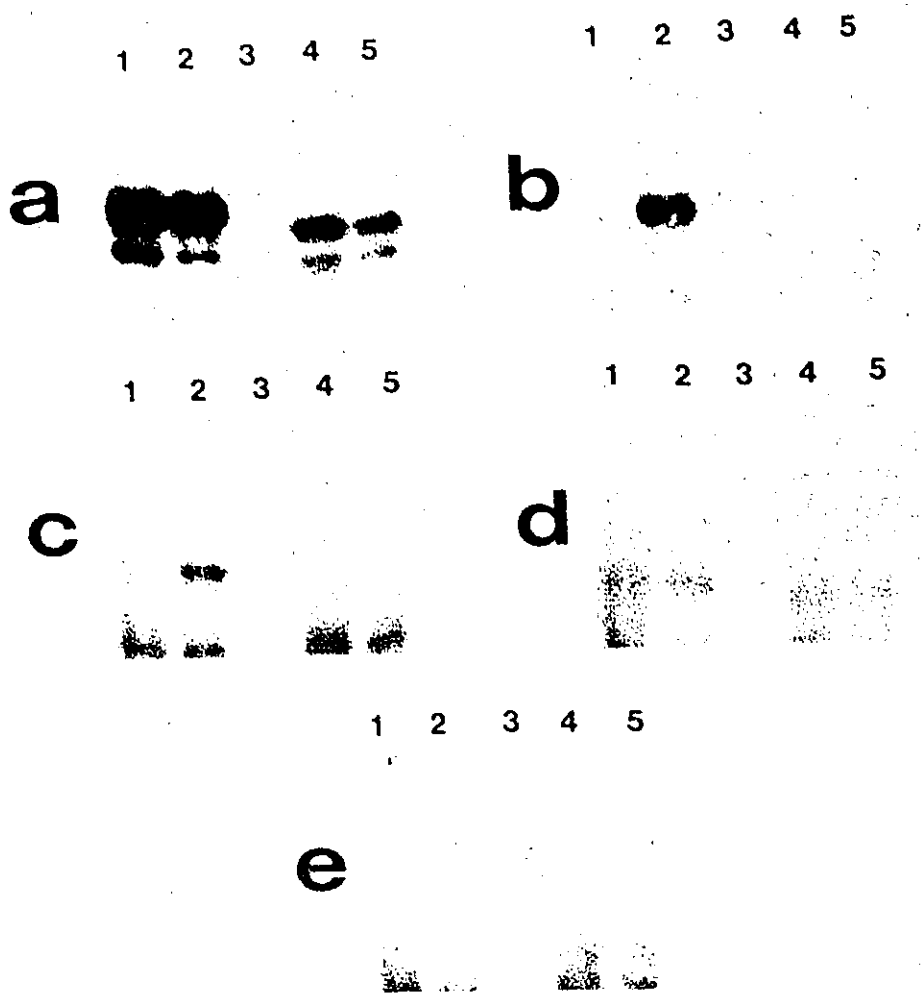
1 2 3 4 5
a
1 2 3 4 5
b
1 2 3 4 5
c
1 2 3 4 5
d
1 2 3 4 5
e

This scenario would lead to a cascade of events not unlike the ones demonstrated for GFRs. Since it appears that S-MAG would not participate in such interactions, this may be the basis of the alternative expression of the different isoforms during development.

CHAPTER 6

GENERAL DISCUSSION AND CONCLUSIONS

6.1 MAG in cell adhesion

The properties of the myelin-associated glycoproteins (MAG) as cell adhesion molecules and protein kinase substrates were examined in this thesis. Both MAG isoforms, L-MAG and S-MAG conferred cell adhesion properties to non-adherent L cell fibroblasts. This is the first evidence demonstrating the ability of the MAGs to function as CAMs when expressed in intact cells. MAG-mediated adhesion in L cells proceeded independently of calcium and temperature, confirming previously described experiments using purified MAG incorporated into liposomes (145). In addition, the adhesion was heterophyllic in nature, indicating the presence of a MAG receptor on the cell surface of L cells. Although it is unknown whether L cells express the neuronal receptor for MAG, it is intriguing to note that L cells express other neuronal markers (2). The experiments in this thesis, however, were unable to rule out homophyllic interactions between MAG molecules. Future investigations using SP10, HL60 or embryonic stem cells expressing MAG would resolve this question, since these cells do not express an endogenous MAG receptor.

The identity of the MAG receptor is unknown. However, its presence in L cell fibroblasts, fibroblast-like cells derived from brain (145) and neurons (133) suggests that it may belong to a family of related proteins that are expressed in a variety of cell types. Integrins occur in many different tissues and some are known to bind Ig related molecules in a heterotypic fashion (104,165). Although direct evidence implicating integrins in MAG-mediated binding is lacking, this large family of proteins may provide a versatile recognition system for MAG in different cell types. It should be noted that the

MAG receptor is absent in embryonic neurons but not in post-natal neurons destined to be myelinated (145). This illustrates that the receptor exhibits a distinct spacial and temporal expression pattern. In order to further explore the cell adhesion properties of MAG, extracellular deletion mutants can be generated and expressed in L cells. Defining the receptor binding sites in MAG may provide additional clues as to the identity of the receptor.

A major finding in this thesis is that L cells require a threshold level of MAG expression in order to aggregate. The significance of this result is that small changes in MAG expression may dramatically affect MAG-mediated intercellular interactions in vivo. This could be of major importance in the developing brain, where MAG levels change dramatically during post-natal development (128). Alterations in MAG protein levels may have major biological effects during myelination. For example, dysmyelinating mouse mutants exhibit major decreases in MAG protein levels, which may contribute to their phenotypes (138). In the brain of quaking mice there is also an apparent imbalance between the different MAG isoforms. L-MAG is almost completely absent from quaking mouse brain (46,47). In order to determine whether the phenotypic abnormalities in quaking mice may be partly caused by a reduction in MAG levels, future experiments should include the overexpression of L-MAG in transgenic quaking mice.

6.2 Cell adhesion and phosphorylation

The developmental differences in L-MAG and S-MAG expression led to the speculation that they perform distinct functions in vivo. The cell adhesion properties of

L-MAG and S-MAG when expressed in L cells were comparable to each other and no major differences were observed. Since the cell adhesion functions of other CAMs have been known to be regulated by the cytoplasmic domains (63,111,118), it was of interest to investigate this possibility for MAG. A striking feature of the intracellular regions of both MAG isoforms are the multiple potential phosphorylation sites, including possible tyrosine phosphorylation sites. In this thesis the phosphorylation of both MAGs was extensively characterized and the major tyrosine phosphorylation site was identified as tyrosine 558. This tyrosine is homologous to the major tyrosine phosphorylation site in the ß-chain of integrin (149,171). Phosphorylation of this tyrosine residue (tyrosine 788) abolishes the binding activity of integrin to fibronectin and talin in an in vitro assay (172). Increasing the tyrosine phosphorylation of MAG in L cells, however, had no major effect on cell adhesion. As discussed previously (Chapter 5), this result may reflect problems intrinsic to the L cell system. Another interpretation is that tyrosine phosphorylated MAG performs a different role in vivo.

A novel cell adhesion regulator protein (CAR) has recently been cloned and identified. It induces non-adherent cells to bind collagen in an integrin dependent manner (137). This activity was found to be dependent on a putative carboxyl terminal tyrosine phosphorylation site (137). While CAR itself is not a CAM, it may function as an intermolecular bridge linking cell surface molecules (integrins) to some unknown cytoplasmic components (possibly cytoskeletal proteins). MAG may function in an analogous fashion, regulating some intermolecular recognition event in a phosphotyrosine dependent manner.

6.3 Tyrosine phosphorylated MAG in signal transduction

Tyrosine phosphorylation controls many cellular regulatory processes. Recent findings demonstrate that the phosphotyrosine moiety can act as a docking site for various signal transduction molecules. These signalling proteins often exhibit an SH2 domain (91). Results presented in this thesis reveal that L-MAG, when phosphorylated on tyrosine, will bind specifically to the SH2 domain of phospholipase C (PLC). Thus, similar to tyrosine phosphorylated growth factor receptors, L-MAG may function as an anchor for the assembly of a signalling complex (Figure 6.1). Potentially, this complex may get activated during MAG-receptor interaction, leading to signals important for myelination. It is still unknown whether L-MAG-PLC interactions actually occur in vivo and whether this leads to changes in phosphatidyl inositol hydrolysis. It is clear, however, that the repertoire of proteins with homologies to the SH2 region is very large, encompassing a diverse group of molecules with distinct functions and activities (6,11,22,91,103,106,107). It is, therefore, conceivable that L-MAG has the capacity to interact with a variety of as yet unidentified proteins.

It is curious to note that tyrosine phosphorylation of L-MAG precludes serine/threonine phosphorylation of the same L-MAG molecules. As a consequence, at least two L-MAG populations exist, each possibly exhibiting an alternate function. While tyrosine phosphorylated L-MAG may serve as a docking site for signalling proteins, the role of serine/threonine phosphorylated L-MAG is unclear. Proteins with SH2 domains have been known to bind phosphorylated serine/threonine residues (130). Experiments in chapter 5, however, show that only tyrosine phosphorylation of L-MAG permits SH2

Figure 6.1: Schematic representation of a hypothetical signalling mechanism via L-MAG. A neuronal receptor binds to L-MAG on the oligodendrocyte membrane. This interaction induces the activation of protein tyrosine kinases (PTK). The PTK phosphorylates an adjacent L-MAG molecule, which subsequently associates with an SH2 domain containing protein (SH2). This protein possibly also bec omes a target for the PTK, resulting in the activation of a signalling pathway.

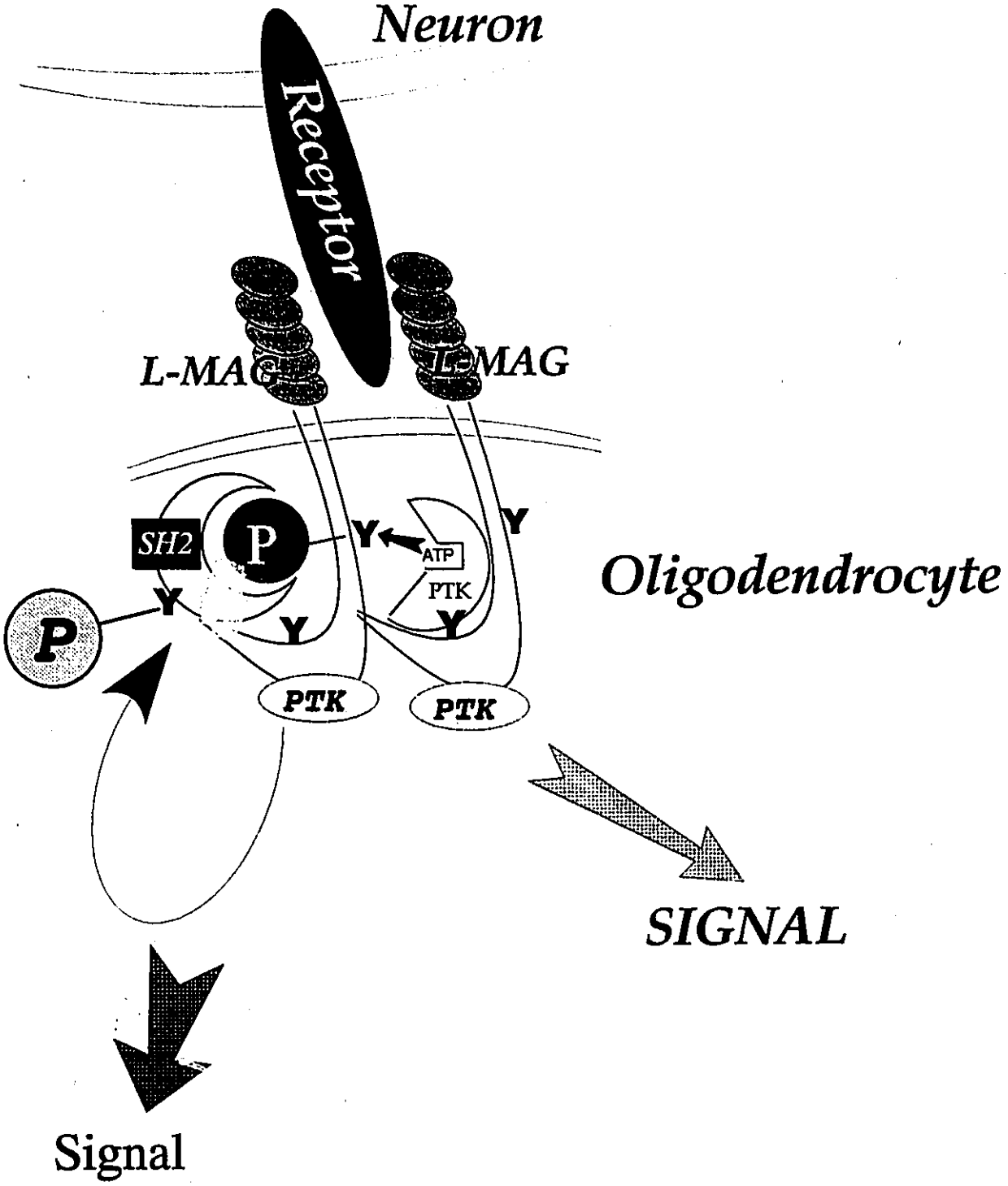
Neuron
Receptor
L-MAG
L-MAG
SH2
P
Y
ATP
PTK
Y
Y
Y
P
Y
PTK
PTK
Oligodendrocyte
SIGNAL
Signal

domain binding.

An intriguing possibility is that L-MAG may dimerize on the cell surface. While one L-MAG protein recruits a PTK, the other molecule serves as the kinase substrate (Figure 6.1). A manifestation of this dimerization theory is the generation of two pools of L-MAG with alternative phosphorylation patterns. This hypothetical dimer could then operate as a coupling complex where a number of signalling molecules interact with each other (Figure 6.1). The evidence presented in this thesis, however, allows for several interpretations, where the different pools of L-MAG may not interact with eachother. While tyrosine phosphorylation may serve to incorporate L-MAG into a signalling complex, the other L-MAG molecules may perform in cell adhesion related functions, in an anlogous fashion to S-MAG.

6.4 Differential phosphorylation of MAG isoforms

The differential phosphorylation of L-MAG and S-MAG is partly due to additional phosphorylation sites present in L-MAG. Tryptic digest mapping of the phosphorylation sites in L-MAG and S-MAG, however, demonstrated that some of the phosphorylation sites in L-MAG are actually shared by S-MAG, including tyrosine 558, the major tyrosine phosphorylated residue. The stoichiometry of phosphorylation was determined to be at least one order of magnitude higher in L-MAG. In fact, while L-MAG phosphorylation of tyrosine 558 is induced with vanadate treatment of the cells, phosphorylation of the same residue in S-MAG is not altered by vanadate treatment. As discussed in chapter 4, a possible explanation is that the unique carboxyl terminus of L-

MAG exhibits a phosphorylation activating sequence. This putative domain would serve as a kinase binding site. In the absence of this domain, as is the case in S-MAG, phosphorylation proceeds inefficiently, resulting in low stoichiometry of phosphorylation.

Analysis of the carboxyl tail of L-MAG reveals an interesting homology with other Ig related cell adhesion molecules. As described in figure 6.2, the carboxyl terminal 8 amino acids, EYAEIRVK, are identical to the terminal residues identified in the recently cloned Schwann cell myelin protein (SMP) (33), and highly homologous to carboxyl regions in CD22 (164,190), CD33 (160), CD31 (platelet-endothelial cell adhesion molecule-1 or PECAM-1) (113), and biliary glycoprotein (BGP) (8). Apart from MAG, only BGP has been shown to be phosphorylated on tyrosine residues (5). It is possible that this sequence represents a novel structural motif whose function is to regulate the interaction of transmembrane proteins with protein tyrosine kinases (PTKs). This intermolecular association can then be monitored, at least in the case of MAG and BGP, by tyrosine phosphorylation of the cytoplasmic domains. In order to test this hypothesis, cytoplasmic deletion mutants of MAG need to be constructed and expressed in mammalian cells. According to this model, deletion of the terminal 8 amino acids would abolish the increase in tyrosine phosphorylation of MAG, while deletion of internal sequences may have no effect.

Figure 6.2: Homologies of carboxyl terminal amino acids in several Ig related CAMs. Amino acid residues 619-626 in L-MAG were compared to residues: 614-621 in SMP; 520-527 in BGP; 821-828 in CD22; 357-364 in CD33; 685-692 in CD31.

Molecule	Carboxyl-terminal sequence
MAG	EYAE I RVK
SMP	EYAE I RVK
BGP	I YSEVKKQ
CD22	HYSEL I QF
CD33	EYSEVRTQ
CD31	VYSEVRKA

6.5 Conclusions

Based on the results in this thesis and previous work in the field a possible model of MAG function is presented:

The purpose of generating two MAG isoforms is to provide the cell with a CAM that exhibits a wide scope of signalling and cell recognition functions. In the CNS, L-MAG plays a role in the primary binding event of neurons destined to be myelinated (9). Adhesion to the neuronal receptor may activate signals via L-MAG that are important in the initiation of myelin synthesis. Prominently featured in this mechanism is the carboxyl terminus of L-MAG, which recruits PTKs and possibly other molecules. Intracellular messages are then generated by the interaction of PTKs with their targets (such as PLC) that associate with the cytoplasmic domain of L-MAG. As the brain matures, a different information input is required for the maintenance of the myelin structure. At this point L-MAG expression decreases, possibly serving as a mechanism for down-regulating a signalling pathway. S-MAG expression increases, accounting for most of the MAG-receptor interactions. The biological role for S-MAG is more restricted and possibly confined to cell adhesion. However, S-MAG is the predominant isoform expressed in the PNS, even during the initial stages of myelination (128), implying a more active role for S-MAG in the biology of myelin. Furthermore, S-MAG protein in the PNS co-localizes to the cytoplasmic channels in the myelin sheath (177). Therefore, the cytoplasmic domain of S-MAG may play an active role in the maintenance of the myelin architecture by interacting with cytoskeletal proteins via the integrin homology region. In contrast to L-MAG, however, the regulation of S-MAG-protein interactions may be less dynamic.

Future work on MAG must include the generation of transgenic mice, which overexpress the different MAG isoforms and mutant MAG proteins during the initial stages of myelin synthesis. The cell adhesion properties and phosphorylation of the mutant MAG proteins may be tested in the L cell system prior to generating transgenic mice. Phenotypic changes in myelin in vivo can then be correlated with differences in the biochemical properties of the MAG proteins.

APPENDIX 1

TYROSINE PHOSPHORYLATION OF BILIARY GLYCOPROTEIN, A CELL ADHESION MOLECULE RELATED TO CARCINOEMBRYONIC ANTIGEN

SUMMARY

Biliary-glycoprotein (BGP), a cell adhesion molecule related to carcinoembryonic antigen (CEA), has been shown to exist as several alternatively spliced isoforms. Here we show that BGPa and BGPb are phosphorylated in the chronic myelogenous leukaemia cell line KG-1, which constitutively expresses several BGP isoforms, and chinese hamster LR-73 cells transfected with the cDNAs encoding BGPa and BGPb. The phosphorylation can be augmented with the protein tyrosine phosphatase inhibitor ammonium vanadate and with TPA (an activator of protein kinase C). Phospho-amino acid analysis of phosphorylated BGPs demonstrated that phosphorylation occurs on serine, threonine and tyrosine residues. Phosphorylation reactions carried out in in vitro membrane preparations from KG-1 cells revealed a close association of BGP proteins with membrane associated protein tyrosine kinases. These observations suggest an association of BGP proteins with signal transduction molecules which is regulated by alternative splicing of the cytoplasmic domain.

A.1 Introduction

Carcinoembryonic antigen (CEA) was originally identified as a tumor specific antigen in colorectal cancer (50). Currently the CEA family of proteins encompasses a group of many cross-reactive cell-surface and secreted glycoproteins that are present in a variety of normal and cancerous tissue types (8,10,68,89,112,159,188). The sequence and structural features of these proteins include them in the immunoglobulin super gene family. This class of proteins is mainly involved in intercellular recognition and signalling processes, and embraces molecules such as growth factor receptors, T-cell receptors and a variety of cell adhesion molecules specific to nervous tissue (189). An interesting addition to the CEA family was identified with the cloning of biliary glycoprotein (BGP) (68) and its alternatively spliced isoforms (8). Unlike other members of the CEA family, these molecules exhibit transmembrane and cytoplasmic domains. Furthermore, the cytoplasmic coding region of two BGP isoforms, BGPa and BGPb, exhibit several potential phosphorylation sites. To examine the significance of the alternatively spliced cytoplasmic domains we determined the phosphorylation status of the BGP proteins in cell culture.

A.2 Materials and Methods

Phosphorylation of BGP proteins in cell culture

The human acute myelogenous leukaemia cell line KG-1 (generously provided by Dr. N. Beauchemin) was maintained in αMEM supplemented with 20% serum (fetal calf serum/newborn serum 1:1). LR-73 cells, derived from the chinese hamster ovary cell

line, were transfected with the cDNAs of BGPa and BGPb inserted in the animal cell expression vector P91023B, as described previously (142). Cell lines were labelled with 1mCi [^{32}P]-orthophosphate (NEN-Dupont) per ml of phosphate free DMEM, 10% fetal calf serum for four hours in the presence or absence of 500 μM Ammonium Vanadate (Fluka). To determine the effects of phorbol esters on BGP phosphorylation LR-73 cells expressing BGPs were treated with 100 nM 4α Phorbol (Sigma) or 100 nM 12-O-Tetradecanoylphorbol 13-acetate (TPA) (Sigma) for 10 minutes at 37°C at the end of ^{32}P-labeling of cells. Labeled cells were harvested in 250 μl of hot (100°C) 2% SDS. The cell lysates were diluted to one ml with immunoprecipitation buffer (10 mM Tris HCl pH7.4, 5 mM EDTA, 150 mM NaCl, 1% Triton, 0.5% SDS, 500 uM NH_4 VO_4, 2mM sodium fluoride, 2 mM sodium pyrophosphate, 2 μg/ml aprotinin, 5 μg/ml leupeptin, 0.4 μg/ml pepstatin, 200 μg/ml PMSF) and were incubated for one hour with 5 μl of an anti-CEA polyclonal antibody (DAKOPATTS), which cross- reacts with BGP. After an additional one hour incubation with protein A sepharose, the immunoprecipitate was washed 5 times with the immunoprecipation buffer and BGPs were eluted using SDS sample buffer. The samples were resolved by sodium dodecyl sulfate polyacrylamide gel electrophoresis (SDS-PAGE) (7.5% polyacrylamide) and ^{32}P- labeled proteins were detected by autoradiography.

Phosphorylation of BGPs <u>in vitro</u>

A membrane enriched fraction was prepared from KG-1 cells as described previously (4). Fifty μg of membrane proteins were resuspended in 50 μl of kinase buffer (20 mM

Hepes pH 7.4, 10 mM $MnCL_2$, 10 mM $MgCl_2$, 500 μM NH_4VO_4, 2 mM sodium fluoride, 2 mM sodium pyrophosphate, 2μg/ml aprotinin, 5 μg/ml leupeptin, 0.4μg/ml pepstatin, 200 μg/ml PMSF). In vitro phosphorylation was initiated with the addition of 5 μCi of [gamma-^{32}P]-ATP (NEN-Dupont), and was carried out for 20 minutes at 0°C. The reaction was stopped by the addition of immunoprecipitation buffer. Phosphorylated BGPs were immunoprecipitated as described above, resolved on SDS-PAGE and visualized by autoradiography.

Phospho-amino acid analysis and tryptic digest analysis

Phosphorylated BGP proteins were immunoprecipitated, resolved on SDS-PAGE, and transferred to Immobilon-P membranes (Millipore). For phospho- amino acid analysis: radioactive bands corresponding BGPs were excised from the membranes and hydrolyzed directly in 6N double-distilled HCl for 75 minutes at 110°C as described previously (84). The hydrolysate was lyophilized and resolved by two dimensional thin- layer electrophoresis as described by Cooper et al. (27). Phospho-amino acid standards were detected by ninhydrin staining of the thin-layer plates. Radioactive phospho-amino acids were detected by autoradiography. Two dimensional tryptic peptide mapping was essentially performed as described by Luo et al. (100). Membrane slices containing radioactive BGPs were soaked in 0.5% polyvinylpyrrolidone in 100 mM acetic acid for 30 minutes. After briefly washing in water, the membranes were incubated with 25 μg of trypsin in 50 mM ammonium bicarbonate (pH 8.5) at 37°C for two hours. After two hours an additional 25 μg of trypsin were added for two more hours. The samples were

then centrifuged and the liquid was lyophilized. After one wash with 100 μl of water and lyophilization, the samples were oxidized in 100 μl of performic acid for one hour at 0°C. One ml of water was then added and the samples were lyophilized. The dried phosphopeptides were resuspended in 10 μl of chromatography buffer (17), spotted onto CEL-300 thin-layer plates and were separated by ascending chromatography. The chromatogram was dried, rotated 90°, and thin-layer electrophoresis was performed at pH 1.9 for 30 minutes at 1000 V. Phospho-tryptic peptides were then visualized by autoradiography.

A.3 Results and Discussion

KG-1 cells, which express several of the BGP isoforms (8), were incubated with ^{32}P-orthophosphate and BGP proteins were immunoprecipitated from cell lysates using a polyclonal anti-CEA antibody. Figure A.1 (panel A) shows that two BGP isoforms are constitutively phosphorylated (lane A). Phospho-amino acid analysis demonstrated that these proteins are phosphorylated mainly on serine residues (Fig. A.1B). Incubation with 500 μM ammonium vanadate, a phosphotyrosine protein phosphatase inhibitor (90), during the labeling period causes a quantitative increase in BGP phosphorylation (Fig. A.1A). The increase in phosphorylation is mainly due to elevated phosphotyrosine levels as determined by phospho-amino acid analysis (Fig. A.1B). Similar results were obtained using the colonic adenocarcinoma cell line HT29 (data not shown). Incubation of live cells with [gamma-^{32}P]ATP did not result in ^{32}P-labeling of BGP proteins, indicating that all phosphorylation occurred on cytoplasmic domain residues (data not shown).

Figure A.1: Phosphorylation of BGPs in KG-1 cells. (A) Membrane extracts from ^{32}P labeled KG-1 cells were immunoprecipitated with polyclonal antibodies directed against CEA. KG-1 cells were either left untreated (lane A) or labeled in the presence of 500 μM ammonium vanadate (lane B). An aliquot of KG-1 membrane extract from labeled cells was immunoprecipitated with a non-immune serum (lane C). The samples were resolved on SDS-PAGE and detected by autoradiography. (B) Phospho-amino acid analysis. Phosphorylated BGP proteins were acid hydrolyzed as described in the text. Phospho-amino acids were analyzed by two-dimensional thin-layer electrophoresis. The numbers underneath each phospho-amino acid analysis in panel B corresponds to the numbered phosphorylated protein bands in panel A. The positions of phosphoserine (S), phosphothreonine (T) and phosphotyrosine (Y) are indicated for reference in panel B-3.

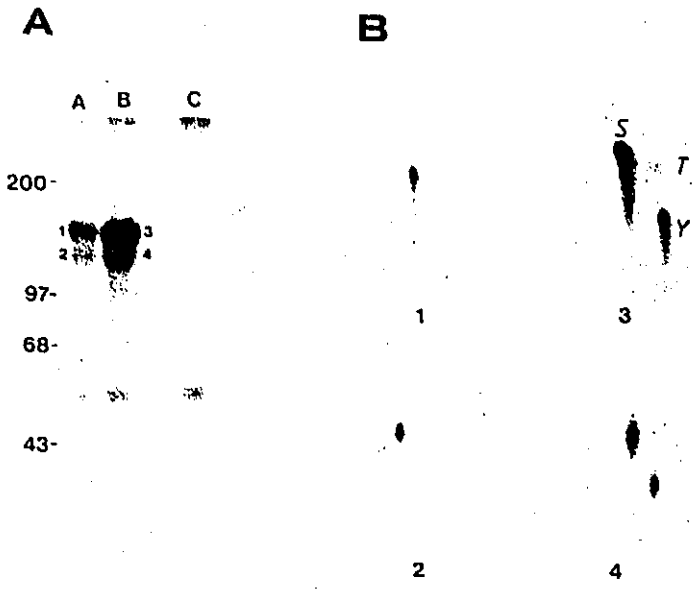
A
A B C
200-
1
2
3
4
97-
68-
43-
B
S
T
Y
1
3
2
4

While the cytoplasmic domains of BGPa and BGPb contain tyrosine residues, the isoforms with shorter carboxyl-termini (BGPc and BGPd) harbour only serine and threonine residues (8).This suggests that the proteins phosphorylated in KG-1 cells are BGPa and BGPb. To confirm the identity of the phosphorylated BGP proteins, the cDNAs encoding BGPa and BGPb were transfected into LR-73 cells. Clonal lines expressing relatively high amounts of each isoform were isolated (142). The transfectants were then labeled with ^{32}P-orthophosphate. SDS-PAGE analysis of immunoprecipitated BGPa and BGPb shows that both isoforms are constitutively phosphorylated (Fig. A.2A, lane A and lane C). Incubation with ammonium vanadate during the labeling period increased the phosphorylation of both isoforms (Fig. A.2A, lanes B and D). Similar to the phosphorylation pattern observed in KG-1 cells, constitutive phosphorylation occurs mainly on serine residues (Fig. A.2B, panels A and C), while vanadate treatment results in a significant stimulation of tyrosine phosphorylation (Fig. A.2B, panels B and D). These results support the identification of BGPa and BGPb as the phosphorylated proteins in KG-1 cells and indicate that the BGPc and BGPd isoforms are not phosphorylated.

Figure A.2: Phosphorylation of BGPa and BGPb in LR-73 cells. (A) Chinese hamster LR-73 cells were transfected with the cDNAs corresponding to either BGPa or BGPb. Expression of BGP proteins was verified by immunoblotting (data not shown). BGPa and BGPb expressing cells were labeled with ^{32}P-orthophosphate. Whole cell extracts were immunoprecipitated with an anti CEA polyclonal antibody, resolved on SDS-PAGE and visualized by autoradiography. Lanes (A) (untreated cells) and (B) (cells treated with 500 μM vanadate) represent immunoprecipitates from BGPb expressing cells; lanes (C) (untreated cells) and (D) (vanadate treated cells) represent immunoprecipitates from BGPa expressing cells. Lane (E) represents an immunoprecipitate form LR-73 cells transfected with the anti-sense orientation to BGPb. (B) Phospho-amino acid analysis was performed on phosphorylated BGPs immunoprecipitated from transfectant LR-73 cells. (A) corresponds to BGPb, untreated; (B) corresponds to BGPb, vanadate treated; (C) corresponds to BGPa, untreated; (D) corresponds to BGPa, vanadate treated. The relative positions of phosphoserine (S), phosphothreonine (T) and phosphotyrosine (Y) are indicated in (B).

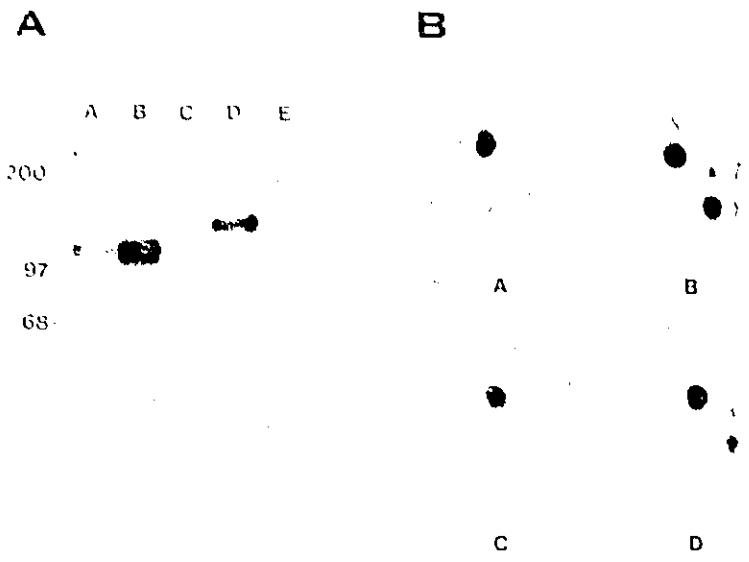
A
A B C D E
200
97
68
B
A
B
C
D

A membrane enriched fraction isolated from KG-1 cells was subjected to an in vitro kinase assay in order to determine whether any of the kinases that phosphorylate BGP proteins are membrane associated. SDS-PAGE analysis of total membranes subjected to in vitro kinase activity reveals the presence of multiple phospho-proteins (Fig. A.3a, lane 2). Phospho-amino acid analysis of total membrane phospho-proteins demonstrates the presence of serine\threonine as well as tyrosine kinases in the membrane preparation (Fig. A.3b, panel 3). Immunoprecipitation of BGP proteins from in vitro phosphorylated membranes reveals that both isoforms are phosphorylated by a membrane associated kinase(s) (Fig. A.3a, lane 1). Phospho-amino acid analysis shows that, under the conditions used in the assay, only tyrosine phosphorylation occurs (Fig. A.3b, panels 1 and 2), suggesting that the enzymes associated with the BGPs in isolated membranes are exclusively tyrosine kinases.

Analysis of the amino- acid sequence of the BGPa\b cytoplasmic domain revealed the presence of a serine residue (ser 461) residing in a sequence homologous to potential protein kinase C phosphorylation sites (GRASDQRD compared to XRXXSXRX) (88). We treated LR-73 cells expressing BGPa and BGPb with TPA or 4α Phorbol and determined the effect on phosphorylation. Fig. A.4 shows that TPA stimulated the phosphorylation of BGPa and BGPb significantly, suggesting that BGPa and BGPb are substrates for PKC. Phospho-amino acid analysis showed that TPA treatment increased phosphorylation on serine and possibly on threonine residues (data not shown).

Figure A.3: In vitro phosphorylation of BGP proteins. (a) Membranes were isolated from KG-1 cells and subjected to an in vitro phosphorylation reaction as described in the text. Total membrane phospho-proteins (lane 2) were compared to phosphorylated BGPs immunoprecipitated with an anti-CEA antibody (lane 1) as determined by SDS-PAGE with subsequent autoradiography. Lane 1 represents a film exposure of 16 hours, while lane 2 was exposed to film for 30 minutes at -70°C. (b) Phospho-amino acid analysis of BGPa (panel 1), BGPb (panel 2), and total membrane phospho-proteins from in vitro kinase reactions. The dotted circles in panels 1 and 2 represent the positions of non-radioactive standards for phosphoserine (S) and phosphothreonine (T). Phosphotyrosine is denoted as Y.

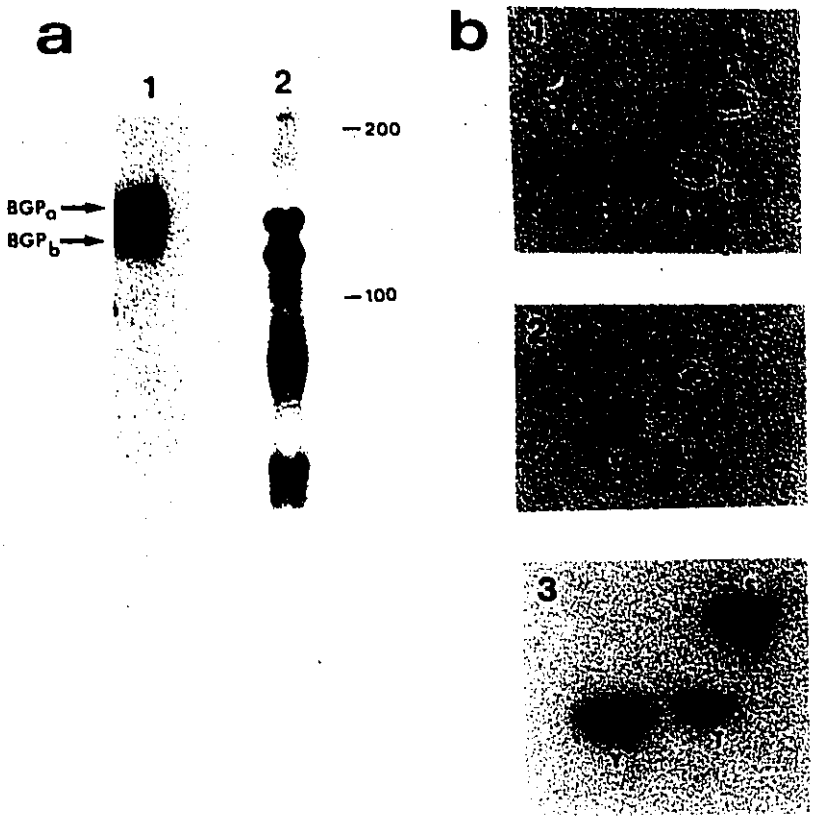
a
1
2
—200
—100
BGP$_a$
BGP$_b$
b
1
2
3

Figure A.4: Stimulation of BGP phosphorylation with TPA. LR-73 cells expressing BGPa and BGPb were labeled with ^{32}P. At the end of the labeling period the cells were stimulated for 10 minutes with either 4α Phorbol, an inactive phorbol ester, or TPA, a phorbol ester that stimulates protein kinase C (PKC) activity. Whole cell extracts were immunoprecipitated using an anti-CEA polyclonal antibody, resolved on SDS-PAGE and visualized by autoradiography. Lanes (A) (4α Phorbol treated) and (B) (TPA treated) represent immunoprecipitates from BGPa expressing cells; lanes (C) (4α Phorbol treated) and (D) (TPA treated) represent immunoprecipitates from BGPb expressing cells.

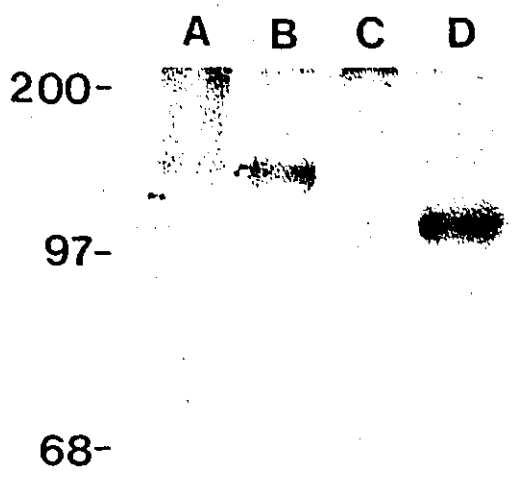
A
B
C
D
200-
97-
68-

To characterize the phosphorylation sites further, phospho-tryptic peptides obtained from phosphorylated BGP proteins were analyzed. The results in Fig. A.5 indicate that a total of four different phosphopeptides are obtained from trypsin treated BGPb. Identical results were obtained with phosphorylated BGPa proteins treated with the same method (data not shown). Unstimulated cells display a faint appearance of phospho-peptides 1 and 2 (Fig. A.5a). TPA augments the phosphorylation of phospho-peptide 2 and induces the appearance of phospho-peptide 3, indicating that these peptides contain phosphoserine and possibly phosphothreonine (Fig. A.5b). Vanadate treatment increases the phosphorylation mainly of phospho-peptides 1 and 4 (Fig. A.5c). Tryptic map analysis of in vitro phosphorylated BGPb from KG-1 cells reveals the presence of two phosphopeptides (Fig. A.5d). They were recognized as phospho-peptides 1 and 4 by mixing them with trypsinized BGPb purified from vanadate treated BGPb transfected LR-73 cells labeled in vivo (Fig. A.5e), demonstrating that BGP proteins are phosphorylated on the same tyrosine residue(s) in vivo and in vitro. The result in Fig. A.5e further confirms the identity of BGP proteins in KG-1 cells as BGPa and BGPb, since tryptic digests of phosphorylated BGPa/b proteins from transfected cells share phospho-tryptic fragments with immunopurified protein from KG-1 cells.

The BGP primary sequence reveals the presence of 2 tyrosine residues (amino acids 493 and 521) in the cytoplasmic tail, which reside on the same tryptic peptide. Therefore, our data indicates that one or both of these tyrosines are phosphorylated. The difference in mobility of the two peptides may reflect a charge difference due to differential phosphorylation (either on tyrosine or on serine residues).

Figure A.5: Tryptic digest mapping of phosphorylated BGP proteins. Phosphorylated BGPb was digested with trypsin, resolved by thin-layer chromatography (TLC) and thin-layer electrophoresis (TLE) and analyzed by autoradiography as described in the text. BGPb was isolated from LR-73 cells that were (a) untreated, (b) treated with 100 nM TPA, or (c) treated with 500 μM vanadate. Panel (d) represents BGPb immunoprecipitated from an in vitro kinase assay performed in KG-1 cell membranes, while panel (e) is a mixture of samples (c) and (d) resolved on the same thin-layer plate. The arrows point to phospho-peptides that were numbered and referred to in the text. The origin of sample application is marked by an O.

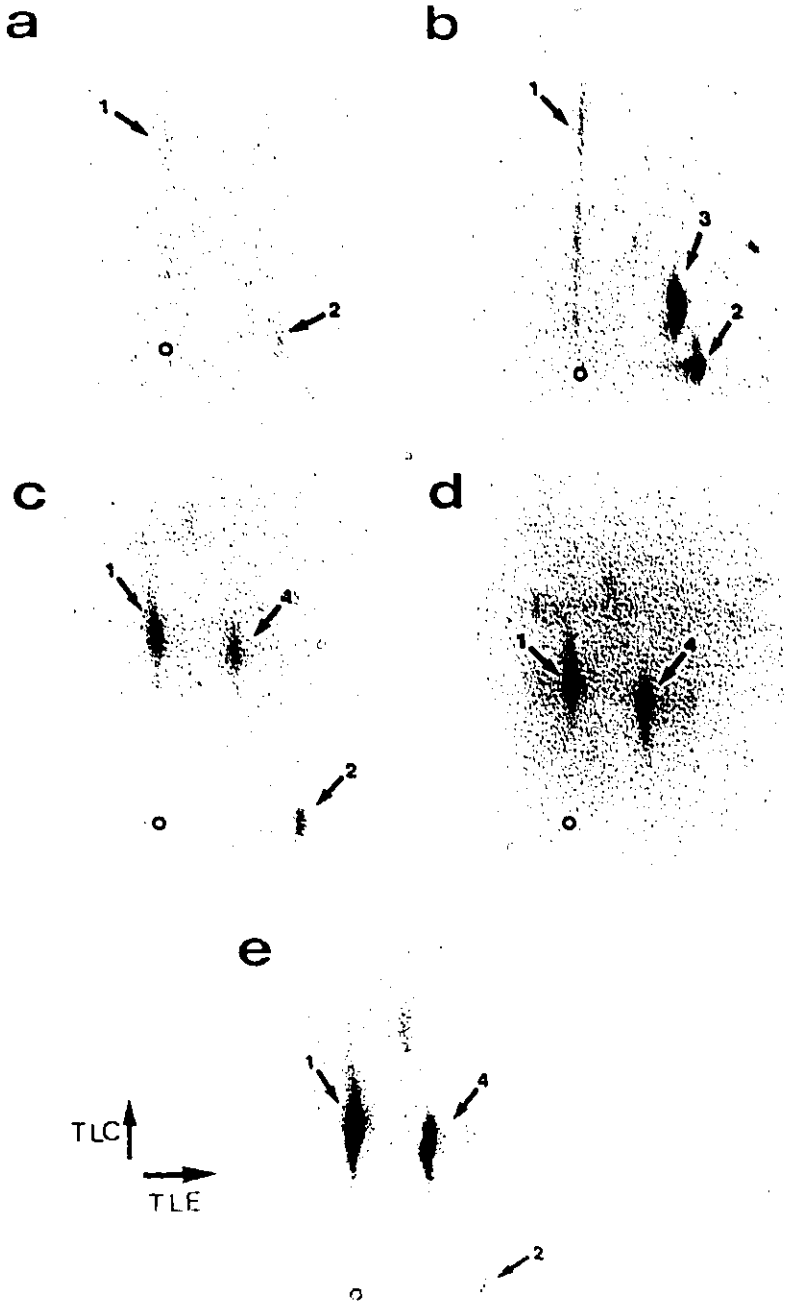
a
b
c
d
e
1
2
3
4
TLC
TLE

The close association of BGPs with tyrosine kinases in vivo and in vitro suggests that BGPs may be linked to signal transduction pathways as has been suggested for other cell adhesion molecules (41,51,150,152,185).

BGPs share structural homology with the immunoglobulin gene superfamily and have been recently shown to have the properties of cell adhesion molecules in in vitro assays (142). Another member of this family, myelin-associated glycoprotein, (MAG), bears significant homology to the BGPs in their respective cytoplasmic domains (8). It is intriguing that similar to BGP, MAG is alternatively spliced to generate isoforms with different cytoplasmic domains (7,43,96,149). In both cases the isoforms with the shorter cytoplasmic domains show low or undetectable in vivo phosphorylation, while the isoforms with the longer cytoplasmic domain are extensively phosphorylated on serine and tyrosine residues (this study and (4)). The homology between BGPa\b and the long MAG isoform is confined mainly to the area containing the BGP tyrosine phosphorylation sites identified in this study. The observation that there are conserved phosphorylation sites in two distinct cell adhesion molecules suggests that phosphorylation/dephosphorylation events may be important in regulating their biochemical and biological properties. Furthermore, two recently identified cell adhesion molecules, platelet-endothelial cell adhesion molecule (PECAM-1) (113) and B-cell antigen CD22 (164), contain in their cytoplasmic tails, peptide segments with significant homology to the amino acids surrounding the potential tyrosine phosphorylation sites in BGPa/b (Fig. A.6). We predict, that similar to BGP and MAG, these domains are sites of tyrosine phosphorylation in vivo. Since the cytoplasmic domains of other cell adhesion

molecules have been implicated in regulating binding activity (81,125,126,172) it may be that phosphorylation of tyrosine residues in the cytoplasmic domains of certain cell adhesion molecules is involved in modulating their adhesive properties. Of interest is the observation that morphological transformation of src- transformed cells is correlated with the tyrosine phosphorylation of certain as yet unidentified transmembrane glycoproteins (60,94). It is tempting to speculate that these tyrosine kinase substrates are cell adhesion molecules, whose uncontrolled phosphorylation leads to a transforming phenotype. Another possibility is that these proteins are involved in transmembrane signalling events which are triggered by ligand binding. Other cell adhesion molecules have been known to function in such a manner (152,185) and we are presently exploring these possibilities for BGP and MAG.

Figure A.6: Amino acid sequence similarities to the tyrosine phosphorylation sites in BGPa\b. Amino acids surrounding potential tyrosine phosphorylation sites in the cell adhesion molecules PECAM-1 and CD22 are shown to be homologous to short cytoplasmic peptides containing the tyrosine phosphorylation sites in BGPa\b. Conserved and similar residues are indicated by a solid line or a dot, respectively, extending between compared amino acids. Amino acids 516-526 in BGPa/b and amino acids 682-691 in PECAM-1 share seven identical and two similar residues, while amino acids 491-496 in BGPa/b have five identical and one similar residues in common with amino acids 608-613 in CD22.

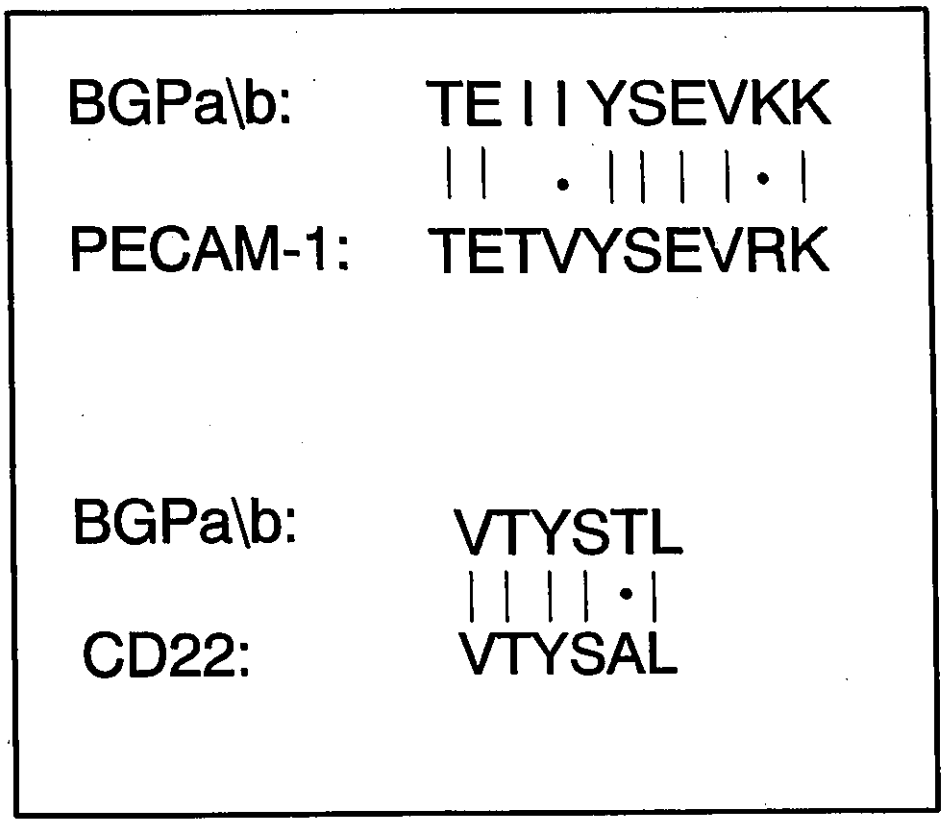
BGPa\b: TE I I YSEVKK
PECAM-1: TETVYSEVRK
BGPa\b: VTYSTL
CD22: VTYSAL

REFERENCES

1. Abraham, N. and Veillette, A. (1991) The lymphocyte specific tyrosine protein kinase p56lck. Cancer Investigation 9:455-463.

2. Acheson, A., Barker, P.A., Alderson, R.F., Miller, F.D. and Murphy, R.A. (1991) Detection of brain-derived neurotrophic factor-like activity in fibroblasts and Schwann cells: inhibition by antibodies to NGF. Neuron 7:265-275.

3. Afar, D.E.H., Marius, R.M., Salzer, J.L., Stanners, C.P., Braun, P.E. and Bell, J.C. (1991) Cell adhesion properties of myelin-associated glycoprotein in L cell fibroblasts. J.Neurosci.Res. 29:429-436.

4. Afar, D.E.H., Salzer, J.L., Roder, J., Braun, P.E. and Bell, J.C. (1990) Differential phosphorylation of myelin-associated glycoprotein isoforms in cell culture. J.Neurochem. 55:1418-1426.

5. Afar, D.E.H., Stanners, C.P. and Bell, J.C. (1992) Tyrosine phosphorylation of biliary glycoprotein, a cell adhesion molecule related to carcinoembryonic antigen. Biochim.Biophys.Acta 1134:46-52.

6. Anderson, D., Koch, C.A., Greg, L., Ellis, C., Moran, M.F. and Pawson, T. (1990) Binding of SH2 domainsof phospholipase C-gamma 1, GAP, and src to activated growth factor receptors. Science 250:979-982.

7. Arquint, M., Roder, J., Chia, L.-S., Down, J., Wilkinson, D., Bayley, H., Braun, P.E. and Dunn, R. (1987) Molecular cloning and primary structure of myelin-associated glycoprotein. Proc.Natl.Acad.Sci.(USA) 84:600-604.

8. Barnett, R.T., Kretschmer, A., Austen, D.A., Goebel, S.J., Hart, J.T., Elting, J.J. and Karmack, M.E. (1989) Carcinoembryonic antigens: alternative splicing accounts for the multiple mRNAs that code for novel members of the carcinoembryonic antigen family. J.Cell Biol. 108:267-276.

9. Bartsch, U., Kirchhoff, F. and Schachner, M. (1989) Immunohistological localization of the adhesion molecules L1, N-CAM, and MAG in the developing and adult optic nerve of mice. J.Comp.Neurol. 284:451-462.

10. Beauchemin, N., Benchimol, S., Cournoyer, D., Fuks, A. and Stanners, C.P.S. (1987) Isolation and characterization of full-length functional cDNA clones for human carcinoembryonic antigen. Mol.Cell.Biol. 7:3221-3230.

11. Bellacosa, A., Testa, J.R., Staal, S.P. and Tsichlis, P.N. (1991) A retroviral oncogene, akt, encoding a serine-threonine kinase containing an SH2-like region. Science 254:274-277.

12. Ben-David, Y., Letwin, K., Tannock, L., Bernstein, A. and Pawson, T. (1991) A mammalian protein kinase with potential for serine/threonine and tyrosine phosphorylation is related to cell cycle regulators. Embo J. 10:317-325.

13. Benchimol, S., Fuks, S., Jothy, S., Shirota, K. and Stanners, C.P. (1989) Carcinoembryonic antigen, a human tumor marker, functions as an intercellular adhesion molecule. Cell 57:327-334.

14. Bennett, J.S. and Vilaire, G. (1979) Exposure of platelet fibrinogen receptors by ADP and epinephrine. J.Clin.Invest. 64:1393-1401.

15. Bond, J.S. Commercially available proteases. In: Proteolytic enzymes- a practical approach, edited by Beynon, R.J. and Bond, J.S. Oxford, New York and Tokyo: IRL Press, 1989, p. 232-240.

16. Boucaut, J.-C., Darribere, T., Poole, T.J., Aoyama, H., Yamada, K.M. and Thiery, J.P. (1984) Biologically active synthetic peptides as probes of embryonic development: a competitive peptide inhibitor of fibronectin function inhibits gastrulation in amphibian embryos and neural crest cell migration in avian embryos. J.Cell Biol. 99:1822-1830.

17. Brown, E.G. and Prevec, L. (1978) Proteins of vesicular stomatitis virus IV. A comparison of tryptic peptides of the vesicular stomatitis group of rhabdoviruses. Virology 89:7-21.

18. Brown, M.S., Anderson, R.G.W. and Goldstein, J.B. (1983) Recycling receptors: the round-trip itinerary of migrant membrane proteins. Cell 32:663-667.

19. Brugge, J., Cotton, P., Lustig, A., Yonemoto, W., Lipsich, L., Coussens, P., Barrett, J.N., Nonner, D. and Keane, R.W. (1987) Characterization of the altered form of the c-src gene product in neuronal cells. Genes Dev. 1:287-296.

20. Bunge, M.B., Williams, A.K. and Wood, P.M. (1982) Neuron-Schwann cell interaction in basal lamina formation. Dev.Biol. 92:449-460.

21. Burridge, K., Fath, K., Kelly, T., Nuckolls, C. and Turner, C. (1987) Focal adhesions: transmembrane junctions between the extracellular matrix and the cytoskeleton. Annu.Rev.Cell Biol. 4:487-525.

22. Bustelo, X.R., Ledbetter, J.A. and Barbacid, M. (1992) Product of vav proto-oncogene defines a new class of tyrosine protein kinase substrates. Nature 356:68-71.

23. Carbonetto, S. (1984) The extracellular matrix of the nervous system. Trends in Neurosci. 7:382-387.

24. Caroni, P. and Schwab, M.E. (1988) Two membrane protein fractions from rat central myelin with inhibitory properties for neurite growth and fibroblast spreading. J.Cell Biol. 106:1281-1288.

25. Chattila, T.A., Geha, R.S. and Arnaut, A. (1989) Constitutive and stimulus induced phosphorylation of CD11/CD18 leukocyte adhesion molecules. J.Cell Biol. 109:3435-3444.

26. Clark, S.S., McLaughlin, J., Timmons, M., Pendergast, A.M., Ben-Neriah, Y., Dow, L.W., Crist, W., Rovera, G., Smith, S.D. and Witte, O.N. (1988) Expression of a distinctive BCR-ABL oncogene in Ph-positive acute lymphocytic leukemia (ALL). Science 239:775-777.

27. Cooper, J.A., Sefton, B.M. and Hunter, T. (1983) Detection and quantification of phosphotyrosine in proteins. Methods Enzymol. 99:387-405.

28. Coughlin, S.R., Escobedo, J.A. and Williams, L.T. (1989) Role of phosphatidyl inositol kinase in PDGF receptor signal transduction. Science 243:1191-1194.

29. D'Eustachio, P., Colman, D.R. and Salzer, J.L. (1988) Chromosomal location of the mouse gene that encodes the myelin-associated glycoproteins. J.Neurochem. 50:589-593.

30. Diamond, M.S., Staunton, D.E., Marlin, S.D. and Springer, T.A. (1991) Binding of the integrin Mac-1 (CD11b/CD18) to the third immunoglobulin-like domain of ICAM-1 (CD54) and its regulation by glycosylation. Cell 65:961-971.

31. Doherty, P., Ashton, S.V., Moore, S.E. and Walsh, F.S. (1991) Morphoregulatory activities of NCAM and N-cadherin can be accounted for by G protein-dependent activation of L- and N-type neuronal Ca2+ channels. Cell 67:21-33.

32. Doherty, P., Fruns, M., Seaton, P., Dickson, G., Barton, C.H., Sears, T.A. and Walsh, F.S. (1990) A threshold effect of the major isoform of NCAM on neurite outgrowth. Nature 343:464-466.

33. Dulac, C., Tropak, M.B., Cameron-Curry, P., Rossier, J., Marshak, D.R., Roder, J. and Le Douarin, N.M. (1992) Molecular characterization of the Schwann cell myelin protein, SMP: structural similarities within the immunoglobulin superfamily. Neuron 8:323-334.

34. Dustin, M.L. and Springer, T.A. (1989) T-cell receptor cross-linking transiently stimulates adhesiveness through LFA-1. Nature 341:619-624.

35. Dymecki, S.M., Niederhuber, J.E. and Desiderio, S.V. (1990) Specific expression of a tyrosine kinase gene, blk, in B lymphoid cells. Science 247:332-336.

36. Edwards, A.M., Arquint, M., Braun, P.E., Roder, J.C., Dunn, R.J., Pawson, T. and Bell, J.C. (1988) Myelin-associated glycoprotein, a cell adhesion molecule of oligodendrocytes, is phosphorylated in brain. Mol.Cell.Biol. 8:2655-2658.

37. Edwards, A.M., Braun, P.E. and Bell, J.C. (1989) Phosphorylation of myelin-associated glycoprotein in vivo and in vitro occurs only in the cytoplasmic domain of the large isoform. J.Neurochem. 52:317-320.

38. Elkins, T., Hortsch, M., Bieber, A.J., Snow, P.M. and Goodman, C.S. (1990) Drosophila fasciclin I is a novel homophillic adhesion molecule that along with fasciclin III can mediate cell sorting. J.Cell Biol. 110:1825-1832.

39. Elkins, T., Zinn, K., McAllister, L., Hoffmann, F.M. and Goodman, C.S. (1990) Genetic analysis of a Drosophila neural cell adhesion molecule: interaction of Fasciclin I and Abelson tyrosine kinase mutations. Cell 60:565-575.

40. Fahrig, T., Landa, C., Peshava, P., Kuehn, K. and Schachner, M. (1987) Characterization of binding properties of the myelin-associated glycoprotein to extracellular matrix constituents. Embo J. 6:2875-2883.

41. Ferrell, J.E. and Martin, G.S. (1989) Tyrosine specific protein phosphorylation is regulated by glycoprotein IIb-IIIa in platelets. Proc.Natl.Acad.Sci.(USA) 86:2234-2238.

42. Filbin, M.T., Walsh, F.S., Trapp, B.D., Pizzey, J.A. and Tennekoon, G.I. (1990) Role of myelin Po protein as a homophilic adhesion molecule. Nature 344:871-872.

43. Frail, D.E. and Braun, P.E. (1984) Two developmentally regulated messenger RNAs differing in their coding region may exist for myelin-associated glycoprotein. J.Biol.Chem. 259:14857-14862.

44. Franz, W.M., Berger, P. and Wang, J.Y.J. (1989) Deletion of an N-terminal regulatory domain of the c-abl tyrosine kinase activates its oncogenic potential. Embo J. 8:137-147.

45. Freed, E., Gailit, J., van der Geer, P., Ruoslahti, E. and Hunter, T. (1989) A novel integrin β subunit is associated with the vitronectin receptor α subunit (αv) in a human osteosarcoma cell line and is a substrate for protein kinase C. Embo J. 8:2955-2965.

46. Fujita, N., Sato, S., Ishiguro, H., Inuzuka, T., Baba, H., Kurihara, T., Takahashi, Y. and Miyatake, T. (1990) The large isoform of myelin-associated glycoprotein is scarcely expressed in the Quaking mouse brain. J.Neurochem. 55:1056-1059.

47. Fujita, N., Sato, S., Kurihara, T., Inuzuka, T., Takahashi, Y. and Miyatake, T. (1988) Developmentally regulated alternative splicing of brain myelin-associated glycoprotein mRNA is lacking in the quaking mouse. FEBS Lett. 232:323-327.

48. Gardner, P. (1989) Calcium and T lymphocyte activation. Cell 59:15-20.

49. Geissler, E.N., Ryan, M.A. and Housman, D.E. (1988) The dominant white spotting (W) locus of the mouse encodes the c-kit proto-oncogene. Cell 55:185-192.

50. Gold, P. and Freedman, S. (1965) Specific carcinoembryonic antigens of the human digestive system. J.Exp.Med. 122:467-481.

51. Golden, A. and Brugge, J.S. (1989) Thrombin treatment induces rapid changes in tyrosine phosphorylation in platelets. Proc.Natl.Acad.Sci.(USA) 86:901-905.

52. Golden, A., Brugge, J.S. and Shattil, S.J. (1990) Role of platelet membrane glycoprotein IIb-IIIa in agonist induced tyrosine phosphorylation of platelet proteins. J.Cell Biol. 111:3117-3127.

53. Golden, A., Nemeth, S.P. and Brugge, J.S. (1986) Blood platelets express high levels of the pp60c-src-specific tyrosine kinaseactivity. Proc.Natl.Acad.Sci.(USA) 83:852-856.

54. Gordon, J.A. (1991) Use of vanadate as protein-phosphotyrosine phosphatase inhibitor. Methods Enzymol. 201:477-482.

55. Gould, K.L. and Hunter, T. (1988) Platelet-derived growth factor induces multisite phosphorylation of pp60c-src and increases its protein-tyrosine kinase activity. Mol.Cell.Biol. 8:3345-3356.

56. Graham, F.L. and van der Eb, A.J. (1973) A new technique for the assay of infectivity of human adenovirus 5 DNA. Virology 52:456-467.

57. Greene, L.A. and Tischler, A.S. (1976) Establishment of a noradrenergic clonal line of rat adrenal pheochromocytoma cells which respond to nerve growth factor. Proc.Natl.Acad.Sci.(USA) 73:424-428.

58. Hafen, E., Basler, K., Edstroem, J.-E. and Rubin, G. (1987) Sevenless, a cell-specific homeotic gene of Drosophila, encodes a putative transmembrane receptor with a tyrosine kinase domain. Science 236:55-63.

59. Haller, J., Cote, S., Broenner, G. and Jaeckle, H. (1987) Dorsal and neural expression of a tyrosine kinase-related Drosophila gene during embryonic development. Genes Dev. 1:862-867.

60. Hamaguchi, M., Matsuda, M. and Hanafusa, H. (1990) A glycoprotein in the plasma membrane matrix as a major potential substrate of p60v-src. Mol.Cell.Biol. 10:830-836.

61. Hanks, S.K., Quinn, A.M. and Hunter, T. (1988) The protein kinase family: conserved features and deduced phylogeny of the catalytic domains. Science 241:42-52.

62. Hatakeyama, M., Kono, T., Kobayashi, N., Kawahara, A., Levin, S.D., Perlmutter, R.M. and Taniguchi, T. (1991) Interaction of the IL-2 receptor with the src-family kinase p56lck: identification of novel intermolecular association. Science 252:1523-1528.

63. Hayashi, Y., Haimovich, B., Reszka, A., Boettiger, D. and Horwitz, A. (1990) Expression and function of chicken integrin $\beta 1$ subunit and its cytoplasmic domain mutants in mouse NIH 3T3 cells. J.Cell Biol. 110:175-184.

64. Heasman, J., Hynes, R.O., Swan, A.P., Thomas, V. and Wylie, C.C. (1981) Primordial germ cells of Xenopus embryos: the role of fibronectin in their adhesion during migration. Cell 27:437-447.

65. Hess, J.F., Bourret, R.B. and Simon, M.I. (1988) Histidine phosphorylation and phosphoryl group transfer in bacterial chemotaxis. Nature 336:139-143.

66. Hibbs, M.L., Xu, H., Stacker, S.A. and Springer, T.A. (1991) Regulation of adhesion to ICAM-1 by the cytoplasmic domain of LFA-1 integrin β subunit. Science 251:1611-1613.

67. Higgins, G.A., Schmale, H., Bloom, F.E., Wilson, M.C. and Milner, R.J. (1989) Celuular localization of 1B236/myelin-associated glycoprotein mRNA during rat brain development. Proc.Natl.Acad.Sci.(USA) 86:2074-2078.

68. Hinoda, Y., Neumaier, M., Hefta, S.A., Drzeniek, Z., Wagener, C., Shively, L., Hefta, L.J.F., Shively, L.E. and Paxton, R.J. (1988) Molecular cloning of a cDNA coding biliary glycoprotein 1: primary structure of a glycoprotein immunologically crossreactive with carcinoembryonic antigen. Proc.Natl.Acad.Sci.(USA) 85:6959-6963.

69. Hirano, A.A., Greengard, P. and Huganir, R.L. (1988) Protein tyrosine kinase activity and its endogenous substrates in rat brain: a subcellular and regional survey. J.Neurochem. 50:1447-1455.

70. Hirst, R., Horwitz, A., Buck, C. and Rohrschneider, L. (1986) Phosphorylation of the fibronectin receptor complex in cells transformed by the oncogenes that encode tyrosine kinases. Proc.Natl.Acad.Sci.(USA) 83:6470-6474.

71. Hoffman, S. and Edelman, G.M. (1983) Kinetics of homophillic binding by embryonic and adult forms of the neural cell adhesion molecule. Proc.Natl.Acad.Sci.(USA) 80:5762-5766.

72. Horvath, A.R., Elmore, M.A. and Kellie, S. (1990) Differential tyrosine-specific phosphorylation of integrin in Rous sarcoma virus transformed cells with differing transformed phenotypes. Oncogene 5:1349-1357.

73. Howell, B.W., Afar, D.E.H., Lew, J., Douville, E.M.J., Icely, P.L.E., Gray, D.A. and Bell, J.C. (1991) Sty, a tyrosine-phosphorylating enzyme with sequence homology to serine/threonine kinases. Mol.Cell.Biol. 11:568-572.

74. Hunter, T. (1987) A tail of two src's: mutatis mutandis. Cell 49:1-4.

75. Hunter, T. (1987) A thousand and one protein kinases. Cell 50:823-829.

76. Hunter, T. and Sefton, B.M. (1980) Transforming gene product of Rous sarcoma virus phosphorylates tyrosine. Proc.Natl.Acad.Sci.(USA) 77:1311-1315.

77. Hyafil, F., Morello, D., Babinet, C. and Jacob, F. (1980) A cell surface glycoprotein involved in the compaction of embryonic carcinoma cells and cleavage stage embryos. Cell 21:927-934.

78. Hynes, R.O. (1987) Integrins: a family of cell surface receptors. Cell 48:549-554.

79. Jackson, P. and Baltimore, D. (1989) N-terminal mutations activate the leukemogenic potential of the myristoylated form of c-abl. Embo J. 8:449-456.

80. Jaconi, M.E.E., Theler, J.M., Schlegel, W., Appel, R.D., Wright, S.D. and Lew, P.D. (1991) Multiple elevations of cytosolic-free Ca2+ in human neutrophils: initiation by adherence receptors of the integrin family. J.Cell Biol. 112:1249-1257.

81. Jaffe, S.H., Friedlander, D.R., Matsuzaki, F., Crosssin, K.L., Cunningham, B.A. and Edelman, G.M. (1990) Differential effects of the cytoplasmic domains of cell adhesion molecules on cell aggregation and sorting-out. Proc.Natl.Acad.Sci.(USA) 87:3589-3593.

82. Jessel, T.M. (1988) Adhesion molecules and the hierarchy of neural development. Neuron 1:3-13.

83. Johnson, P.W., Abramow-Newerly, W., Seilheimer, B., Sadoul, R., Tropak, M.B., Arquint, M., Dunn, R.J., Schachner, M. and Roder, J.C. (1989) Recombinant myelin-associated glycoprotein confers neural adhesion and neurite outgrowth function. Neuron 3:377-385.

84. Kamps, M.P. and Sefton, B.M. (1989) Acid and base hydrolysis of phosphoproteins bound to immobilon facilitates analysis of phosphoamino acids in gel-fractionated proteins. Anal.Biochem. 176:22-27.

85. Kaplan, D.R., Martin-Zanca, D. and Parada, L.F. (1991) Tyrosine phosphorylation and tyrosine kinase activity of the trk proto-oncogene product induced by NGF. Nature 350:158-160.

86. Kaplan, D.R., Morrison, D.K., Wong, G., McCormick, F. and Williams, L.T. (1990) PDGF β-receptor stimulates tyrosine phosphorylation of GAP and association of GAP with a signalling complex. Cell 61:125-133.

87. Kazlauskas, A. and Cooper, J.A. (1989) Autophosphorylation of the PDGF receptor in the kinase insert region regulates interactions with cell proteins. Cell 58:1121-1133.

88. Kemp, B.E. and Pearson, R.B. (1990) Protein kinase recognition sequence motifs. Trends in Biochem.Sci. 15:342-346.

89. Khan, W.N., Osterman, A. and Hammerstrom, S. (1989) Molecular cloning and expression of cDNA for a carcinoembryonic antigen-related fetal liver glycoprotein. Proc.Natl.Acad.Sci.(USA) 86:3332-3336.

90. Klarlund, J.K. (1985) Transformation of cells by an inhibitor of phosphatases acting on phosphotyrosine proteins. Cell 41:707-717.

91. Koch, C.A., Anderson, D., Moran, M.F., Ellis, C. and Pawson, T. (1991) SH2 and SH3 domains:elements that control interactions of cytoplasmic signaling proteins. Science 252:668-674.

92. Konopka, J.B., Watanabe, S.M. and Witte, O.N. (1984) An alteration of the human c-abl protein in K562 leukemia cells unmasks associated tyrosine kinase activity. Cell 37:1035-1042.

93. Kornberg, L.J., Earp, S.H., Turner, C.E., Prockop, C. and Juliano, R.L. (1991) Signal transduction by integrins: increased protein tyrosine phosphorylation caused by clustering of β1 integrins. Proc.Natl.Acad.Sci.(USA) 88:8392-8396.

94. Kozma, L.M., Reynolds, A.B. and Weber, M.J. (1990) Glycoprotein tyrosine phosphorylation in rous sarcoma virus- transformed chicken embryo fibroblasts. Mol.Cell.Biol. 10:837-841.

95. Kypta, R.M., Goldberg, Y., Ulug, E.T. and Courtneidge, S.A. (1990) Association between the PDGF receptor and members of the src family of tyrosine kinases. Cell 62:481-492.

96. Lai, C., Brow, M.A., Nave, K.-A., Noronha, A.B., Quarles, R.A., Bloom, F.E., Milner, R.J. and Sutcliffe, J.G. (1987) Two forms of 1B236/myelin-associated glycoprotein, a cell adhesion molecule for postnatal neural development, are produced by alternative splicing. Proc.Natl.Acad.Sci.(USA) 84:4337-4341.

97. Lees, M.B. and Brostoff, S.W. Proteins of myelin. In: Myelin, edited by Morell, P. New York and London: Plenum Press, 1984, p. 197-224.Ed. 2nd

98. Lemke, G., Lamar, E. and Patterson, J. (1988) Isolation and analysis of the gene encoding peripheral myelin protein zero. Neuron 1:73-83.

99. Linnemann, D. and Bock, E. (1989) Cell adhesion in neural development. Dev.Neurosci. 11:149-173.

100. Luo, K., Hurley, T.R. and Sefton, B.M. (1990) Transfer of proteins to membranes facilitates both cyanogen bromide cleavage and two-dimensional proteolytic mapping. Oncogene 5:921-923.

101. Maher, P. (1988) Nerve growth factor induces protein-tyrosine phosphorylation. Proc.Natl.Acad.Sci.(USA) 85:6788-6791.

102. Maniatis, T., Fritsch, E.F. and Sambrook, J. Molecular cloning: a laboratory manual, Cold Spring Harbour:Cold Spring Harbour Laboratory, (1982)

103. Margolis, B., Hu, P., Katzav, S., Li, W., Oliver, J.M., Ullrich, A., Weiss, A. and Schlessinger, J. (1992) Tyrosine phosphorylation of vav proto-oncogene product containing SH2 domain and transcription factor motifs. Nature 356:71-74.

104. Marlin, S.D. and Springer, T.A. (1987) Purified intercellular adhesion molecule-1 (ICAM-1) is a ligand for lymphocyte function-associated antigen 1 (LFA-1). Cell 51:813-819.

105. Martini, R. and Schachner, M. (1986) Immunological microscopic localization of neural cell adhesion molecules and their shared carbohydrate epitope and myelin basic protein in developing sciatic nerve. J.Cell Biol. 103:2439-2448.

106. Mayer, B.J., Hamaguchi, M. and Hanafusa, H. (1988) A novel viral oncogene with structural similarity to phospholipase C. Nature 332:272-275.

107. Mayer, B.J., Jackson, P.K. and Baltimore, D. (1991) The noncatalytic src homology region 2 segment of abl tyrosine kinase binds to tyrosine-phosphorylated cellular proteins with high affinity. Proc.Natl.Acad.Sci.(USA) 88:627-631.

108. Mellstroem, K., Bjelfman, C., Hammerling, U. and Pahlman, S. (1987) Expression of c-src in cultured human neuroblastoma and small cell lung carcinoma cell lines correlates with neurocrine differentiation. Mol.Cell.Biol. 7:4178-4184.

109. Miyatani, S., Shimamura, K., Hatta, M., Nagafuchi, A., Nose, A., Matsunaga, M., Hatta, K. and Takeichi, M. (1989) Neural cadherin: role in selective cell-cell adhesion. Science 245:631-635.

110. Morrison, D.K., Kaplan, D.R., Escobedo, J.A., Rapp, U.R., Roberts, T.M. and Williams, L.T. (1989) Direct activation of the serine/threonine kinase activity of Raf-1 through tyrosine phosphorylation by the PDGF β-receptor. Cell 58:649-657.

111. Nagafuchi, A. and Takeichi, M. (1988) Cell binding function of E-cadherin is regulated by the cytoplasmic domain. Embo J. 7:3679-3684.

112. Neumeier, M., Zimmermann, W., Shively, L., Hinoda, Y., Riggs, A.D. and Shively, J.E. (1988) Characterization of a cDNA clone for the non-specific cross-reacting antigen (NCA) and a comparison of NCA and carcinoembryonic antigen. J.Biol.Chem. 263:3202-3207.

113. Newman, P.J., Berndt, M.C., Gorski, J., White II, G.C., Lyman, S., Paddock, C. and Muller, W.A. (1990) PECAM-1 (CD31) cloning and relation to adhesion molecules of the immunoglobulin gene superfamily. Science 247:1219-1222.

114. Nishibe, S., Wahl, M.I., Hernandez-Sotomayor, S.M.T., Tonks, N.K., Rhee, S.G. and Carpenter, G. (1990) Increase of the catalytic activity of phospholipase C-gamma 1 by tyrosine phosphorylation. Science 250:1253-1256.

115. Nishizuka, Y. (1984) The role of protein kinase C in cell surface signal transduction and tumor promotion. Nature 308:693-698.

116. Nose, A., Nagafuchi, A. and Takeichi, M. (1988) Expressed recombinant cadherins mediate cell sorting in model systems. Cell 54:993-1001.

117. Nose, A., Tsuji, K. and Takeichi, M. (1990) Localization of specificity determining sites in cadherin cell adhesion molecules. Cell 61:147-155.

118. O'Toole, T.E., Mandelmann, D., Forsyth, J., Shattil, S.J., Plow, E.F. and Ginsberg, M.H. (1991) Modulation of the affinity of integrin αIIb β3 (GPIIb-IIIa) by the cytoplasmic domain of αIIb. Science 254:845-847.

119. Omlin, F.X., Matthieu, J.-M., Phillipe, E., Roch, J.M. and Droz, B. (1985) Expression of myelin-associated glycoprotein by small neurons of the dorsal root ganglion of chickens. Science 227:1359-1360.

120. Owens, G.C. and Boyd, C.J. (1991) Expressing antisense Po RNA in Schwann cells perturbs myelination. Develop. 112:639-649.

121. Owens, G.C., Boyd, C.J., Bunge, R.P. and Salzer, J.L. (1990) Expression of recombinant myelin-associated glycoprotein in primary Schwann cells promotes the initial investment of axons by myelinating Schwann cells. J.Cell Biol. 111:1171-1182.

122. Owens, G.C. and Bunge, R.P. (1989) Evidence for an early role of myelin-associated glycoprotein in the process of myelination. Glia 2:119-128.

123. Owens, G.C. and Bunge, R.P. (1990) Schwann cells depleted of galactocerebroside express myelin-associated glycoprotein and initiate but do not continue the process of myelination. Glia 3:118-124.

124. Owens, G.C. and Bunge, R.P. (1991) Schwann cells infected with a recombinant retrovirus expressing myelin-associated glycoprotein antisense RNA do not form myelin. Neuron 7:565-575.

125. Ozawa, M., Baribault, H. and Kemler, R. (1989) The cytoplasmic domain of the cell adhesion molecule uvomorulin associates with three independent proteins structurally related in different species. Embo J. 8:1711-1717.

126. Ozawa, M., Ringwald, M. and Kemler, R. (1990) Uvomorulin-catenin complex formation is regulated by a specific domain in the cytoplasmic region of the cell adhesion molecule. Proc.Natl.Acad.Sci.(USA) 87:4246-4250.

127. Pardi, R., Inverardi, L., Rugarli, C. and Bender, J.R. (1992) Antigen-receptor complex stimulation triggers protein kinase C-dependent CD11a/CD18-ctoskeleton association in T lymphocytes. J.Cell Biol. 116:1211-1220.

128. Pedraza, L., Frey, A.B., Hempstead, B.L., Colman, D.R. and Salzer, J.L. (1991) Differential expression of MAG isoforms during development. J.Neurosci.Res. 29:141-148.

129. Pedraza, L., Owens, G.C., Green, L.A.D. and Salzer, J.L. (1990) The myelin-associated glycoproteins: membrane disposition, evidence for a novel disulphide linkage between immunoglobulin-like domains, and posttranslational palmitylation. J.Cell Biol. 111:2651-2661.

130. Pendergast, A.M., Muller, A.J., Havlik, M.H., Maru, Y. and Witte, O.N. (1991) BCR sequences essential for transformation by the BCR-ABL oncogene bind to the ABL SH2 regulatory domain in a non-phosphotyrosine-dependent manner. Cell 66:161-171.

131. Philippe, E., Omlin, F.X. and Droz, B. (1986) Myelin-associated glycoprotein immunoreactive material: an early neuronal marker of dorsal root ganglion cells during chick development. Dev.Brain Res. 27:275-277.

132. Pollerberg, G.E., Burridge, K., Krebs, K.E., Goodman, S.R. and Schachner, M. (1987) The 180-kd component of the neural cell adhesion molecule NCAM is involved in cell-cell contacts and cytoskeleton-membrane interactions. Cell Tissue Res. 250:227-236.

133. Poltorak, M., Sadoul, R., Keilhauer, G., Landa, C., Fahrig, T. and Schachner, M. (1987) Myelin-associated glycoprotein, a member of the L2/HNK-1 family of neural cell adhesion molecules, is involved in neuron-oligodendrocyte and oligodendrocyte-oligodendrocyte adhesion. J.Cell Biol. 105:1893-1899.

134. Popko, B., Puckett, C., Lai, E., Shine, H.D., Readhead, C., Takahashi, N., Hunt, S.W.III, Sidman, R.L. and Hood, L. (1987) Myelin deficient mice: expression of myelin basic protein and generation of mice with varying levels of myelin. Cell 48:713-721.

135. Privat, A., Jacque, C., Bourre, J.M., Depouey, P. and Baumann, N. (1979) Absence of major dense line in the myelin of the mutant mouse shiverer. Neurosci.Lett. 12:107-112.

136. Prywes, R., Foulkes, J.G. and Baltimore, D. (1985) The minimum transforming region of v-abl is the segment encoding protein-tyrosine kinase. J.Virol. 54:114-122.

137. Pullman, W.E. and Bodmer, W.F. (1992) Cloning and characterization of a gene that regulates cell adhesion. Nature 356:529-532.

138. Quarles, R.H. (1991) The biochemistry of myelin in X-linked mutants. Ann.New York Acad.Sci. 605:135-145.

139. Radziejewski, C., Miller, W.T., Mobashery, S., Goldberg, A.R. and Kaiser, E.T. (1989) Purification of recombinant pp60v-src protein tyrosine kinase and phosphorylation of peptides with different secondary structure preference. Biochemistry 28:9047-9052.

140. Raine, C.S. Morphology of myelin and myelination. In: Myelin, edited by Morell, P. New York and London: Plenum Press, 1984, p. 1-50.Ed. 2nd

141. Readhead, C., Popko, B., Takahashi, N., Shine, H.D., Saavedra, R.A., Sidman, R.L. and Hood, L. (1987) Expression of a myelin basic protein gene in transgenic shiverer mice: correction of the dysmyelinating phenotype. Cell 48:703-712.

142. Rojas, M., Fuks, A. and Stanners, C.P. (1990) Biliary glycoprotein, a member of the immunoglobulin supergene family, functions in vitro as a Ca^{2+}-dependent intercellular adhesion molecule. Cell Growth Different. 1:527-533.

143. Ruoslahti, E. and Pierschbacher, M.D. (1987) New perspectives in cell adhesion: RGD and integrins. Science 238:491-497.

144. Rutishauser, U., Hoffman, S. and Edelman, G.M. (1982) Binding properties of a cell adhesion molecule from neural tissue. Proc.Natl.Acad.Sci.(USA) 79:685-689.

145. Sadoul, R., Fahrig, T., Bartsch, U. and Schachner, M. (1990) Binding properties of liposomes containing the myelin-associated glycoprotein MAG to neural cell cultures. J.Neurosci.Res. 25:1-13.

146. Sadoul, R., Hirn, M., Deagostini-Bazin, H., Rougon, G. and Goridis, C. (1983) Adult and embryonic mouse neural cell adhesion molecules have different binding properties. Nature 304:349-352.

147. Sadoul, R., Kirchhoff, F. and Schachner, M. (1989) A protein kinase activity is associated with and specifically phosphorylates the neural cell adhesion molecule L1. J.Neurochem. 53:1471-1478.

148. Sadowski, I., Stone, J.C. and Pawson, T. (1986) A noncatalytic domain conserved among cytoplasmic protein-tyrosine kinases modifies the kinase function and transforming activity of Fujinami sarcoma virus P130gag-fps. Mol.Cell.Biol. 6:4396-4408.

149. Salzer, J., Holmes, P.W. and Colman, D.R. (1987) The amino acid sequence of the myelin-associated glycoproteins: homology to the immunoglobulin gene superfamily. J.Cell Biol. 104:957-965.

150. Samelson, L.E., Phillips, A.F., Luong, E.T. and Klausner, R.D. (1990) Association of the fyn protein-tyrosine kinase with the T-cell antigen receptor. Proc.Natl.Acad.Sci.(USA) 87:4358-4362.

151. Sanes, J.R. (1983) Roles of extracellular matrix in neural development. Annu.Rev.Physiol. 45:581-600.

152. Schuch, U., Lohse, M.J. and Schachner, M. (1989) Neural cell adhesion molecules influence second messenger systems. Neuron 3:13-20.

153. Schwab, M.E. and Caroni, P. (1988) Oligodendrocytes and CNS myelin are nonpermissive substrates for neurite growth and fibroblast spreading. J.Neurosci. 8:2381-2393.

154. Schwab, M.E. and Thoenen, H. (1985) Dissociated neurons regenerate into sciatic but not optic nerve explants in culture irrespective of neurotrophic factors. J.Neurosci. 5:2415-2423.

155. Sefton, B.M., Hunter, T., Beemon, K. and Eckhart, W. (1980) Evidence that the phosphorylation of tyrosine is essential for cellular transformation by Rous sarcoma virus. Cell 20:807-816.

156. Sefton, B.M., Hunter, T. and Raschke, W.C. (1981) Evidence that the Ableson virus protein functions in vivo as a protein kinase that phosphorylates tyrosine. Proc.Natl.Acad.Sci.(USA) 78:1552-1556.

157. Shattil, S.J., Hoxie, J.A., Cunningham, M. and Brass, L.F. (1985) Changes in the platelet membrane glycoprotein IIb-IIIa complex during platelet activation. J.Biol.Chem. 260:11107-11114.

158. Shaw, L.M., Messier, J.M. and Mercurio, A.M. (1990) The activation dependent adhesion of macrophages to laminin involves cytoskeletal anchoring and phosphorylation of the $\alpha 6\beta 1$ integrin. J.Cell Biol. 110:2167-2174.

159. Shively, J.E. and Beatty, J.D. (1985) CEA-related antigens: molecular biology and clinical significance. Crit.Rev.Oncol.Hematol. 2:355-399.

160. Simmons, D. and Seed, B. (1988) Isolation of a cDNA encoding CD33, a differentiation antigen of myeloid progenitor cells. J.Immunol. 141:2797-2800.

161. Soriano, P., Montgomery, C., Geske, R. and Bradley, A. (1991) Targeted disruption of the c-src proto-oncogene leads to osteopetrosis in mice. Cell 64:693-702.

162. Sorkin, B.C., Hoffman, S., Edelman, G.M. and Cunningham, B.A. (1984) Sulfation and phosphorylation of the neural cell adhesion molecule, N-CAM. Science 225:1476-1478.

163. Springer, T.A. (1990) Adhesion receptors of the immune system. Nature 346:425-434.

164. Stamenkovic, I. and Seed, B. (1990) The B-cell antigen CD22 mediates monocyte and erythrocyte adhesion. Nature 345:74-77.

165. Staunton, D.E., Dustin, M.L. and Springer, T.A. (1989) Functional cloning of ICAM-2, a cell adhesion ligand for LFA-1 homologous to ICAM-1. Nature 339:61-64.

166. Stehelin, D., Varmus, H.E., Bishop, J.M. and Vogt, P.K. (1976) DNA relating to the transforming gene(s) of avian sarcoma viruses is present in normal avian DNA. Nature 260:170-173.

167. Sternberger, N.H., Quarles, R.H., Itoyama, Y. and deF.Webster, H. (1979) Myelin-associated glycoprotein demonstrated immunocytochemically in myelin and myelin-forming cells of developing rat. Proc.Natl.Acad.Sci.(USA) 76:1510-1514.

168. Streuli, M., Krueger, N.X., Hall, L.R., Schlossman, S.F. and Saito, H. (1988) A new member of the immunoglobulin superfamily that has a cytoplasmic region homologous to the leukocyte common antigen. J.Exp.Med. 168:1523-1530.

169. Takeichi, M. (1988) The cadherins: cell-cell adhesion molecules controlling animal morphogenesis. Develop. 102:639-655.

170. Takeichi, M. (1991) Cadherin cell adhesion receptors as a morphogenetic regulator. Science 251:1451-1455.

171. Tamkun, J.W., DeSimone, D.W., Fonda, D., Patel, R.S., Buck, C., Horwitz, A.F. and Hynes, R.O. (1986) Structure of integrin, a glycoprotein involved in the transmembrane linkage between fibronectin and actin. Cell 46:271-282.

172. Tapley, P., Horwitz, A.F., Buck, C., Duggan, K. and Rohrschneider, L. (1989) Integrins isolated from rous sarcoma-transformed chicken embryo fibroblasts. Oncogene 4:325-333.

173. Thiery, J.-P., Delouvee, A., Gallin, W.J., Cunningham, B.A. and Edelman, G.M. (1984) Ontogenetic expression of cell adhesion molecules: L-CAM is found in epithelia derived from the three primary germ layers. Dev.Biol. 102:61-78.

174. Thiery, J.-P., Duband, J.-L., Rutishauser, U. and Edelman, G.M. (1982) Cell adhesion molecules in early chicken embryogenesis. Proc.Natl.Acad.Sci.(USA) 79:6737-6741.

175. Togari, A., Dickens, G., Kozuya, H. and Guroff, G. (1985) The effect of fibroblast growth factor on PC12 cells. J.Neurosci. 5:307-316.

176. Townes, P.L. and Holtfreter, J. (1955) Directed movements and selective adhesion of embryonic amphibian cells. J.Exp.Zool. 128:53-118.

177. Trapp, B.D. (1988) Distribution of the myelin-associated glycoprotein and P_0 protein during myelin compaction in quaking mouse peripheral nerve. J.Cell Biol. 107:675-685.

178. Trapp, B.D. (1990) Myelin-associated glycoprotein: location and potential functions. Ann.New York Acad.Sci. 605:29-43.

179. Trapp, B.D., Andrews, S.B., Wong, A., O'Connell, M. and Griffin, J.W. (1989) Colocalization of the myelin-associated glycoprotein and the microfilament components f-actin and spectrin in Schwann ce4lls of myelinated fibers. J.Neurocytol. 18:47-60.

180. Trapp, B.D. and Quarles, R.H. (1982) Presence of the myelin-associated glycoprotein correlates with alterations in the periodicity of peripheral myelin. J.Cell Biol. 92:877-882.

181. Tropak, M.B., Johnson, P.W., Dunn, R.J. and Roder, J.C. (1988) Differential splicing of MAG transcripts during CNS and PNS development. Mol.Brain Res. 4:143-155.

182. Ullrich, A. and Schlessinger, J. (1990) Signal transduction by receptors with tyrosine kinase activity. Cell 61:203-212.

183. Vartanian, T.S., Szuchet, S., Dawson, G. and Campagnoni, A.T. (1986) Oligodendrocyte adhesion activates protein kinase C-mediated phosphorylation of myelin basic protein. Science 234:1395-1398.

184. Veillette, A., Abraham, N., Caron, L. and Davidson, D. (1991) The lymphocyte-specific tyrosine protein kinase p56lck. Seminars in Immunology 3:143-152.

185. Veillette, A., Bookman, M.A., Horak, E.M. and Bolen, J.B. (1988) The CD4 and CD8 T-cell surface antigens are associated with the internal membrane tyrosine-protein kinase $p56^{lck}$. Cell 55:301-308.

186. Veillette, A., Bookman, M.A., Horak, E.M., Samelson, L.E. and Bolen, J.B. (1989) Signal transduction through the CD4 receptor involves the activation of the internal membrane tyrosine-protein kinase p56lck. Nature 338:257-259.

187. Wahl, M.I., Daniel, T.O. and Carpenter, G. (1988) Antiphosphotyrosine recovery of phospholipase C activity after EGF treatment of A-431 cells. Science 241:968-970.

188. Watanabe, S. and Chou, J.Y. (1988) Isolation and characterization of complementary DNAs encoding human pregnancy-specific β_1-glycoprotein. J.Biol.Chem. 263:2049-2054.

189. Williams, A.F. (1987) A year in the life of the immunoglobulin superfamily. Immunol.Today 8:298-303.

190. Wilson, G.L., Fox, C.H., Fauci, A.S. and Kehrl, J.H. (1991) cDNA cloning of the B cell membrane protein CD22: a mediator of B-B cell interaction. J.Exp.Med. 173:137-146.

191. Witte, O.N., Rosenberg, N. and Baltimore, D. (1979) A normal cell protein cross reactive to the major Abelson murine leukemia virus gene product. Nature 281:396-398.

192. Wood, P., Okada, E. and Bunge, R. (1982) The use of networks of dissociated rat dorsal root ganglion neurons to induce myelination by oligodendrocytes in culture. Brain Res. 196:247-252.

193. Wood, P.M., Schachner, M. and Bunge, R.P. (1990) Inhibition of Schwann cell myelination in vitro by antibody to the L1 adhesion molecule. J.Neurosci. 10:3635-3645.

194. Yamanashi, Y., Kakiuchi, T., Mizuguchi, J., Yamamoto, T. and Toyoshima, K. (1991) Association of B cell antigen receptor with protein tyrosine kinase Lyn. Science 251:192-194.

195. Yoshida, C. and Takeichi, M. (1982) Teratocarcinoma cell adhesion: identification of a cell surface protein involved in calcium-dependent cell aggregation. Cell 28:217-224.

196. Zhou, H., Fuks, A. and Stanners, C.P. (1990) Specificity of intercellular adhesion mediated by various members of the immunoglobulin supergene family. Cell Growth Different. 1:209-215.

ORIGINAL CONTRIBUTIONS TO KNOWLEDGE

The following findings presented in this thesis represent original contributions to knowledge:

(i) Expression of L-MAG and S-MAG in L cell fibroblasts confers cell adhesion properties to these cells, when grown in suspension.

(ii) MAG-mediated L cell aggregation was heterotypic in nature, revealing the presence of a MAG receptor in L cell fibroblasts.

(iii) MAG-mediated cell adhesion requires a threshold level of MAG expression.

(iv) The first evidence for phosphorylation of S-MAG in live cells was presented.

(v) L-MAG and S-MAG were shown to share major phosphorylation sites, yet the stoichiometry of L-MAG phosphorylation was one order of magnitude greater. This implies the presence of a carboxyl terminal protein kinase activator sequence unique to the L-MAG cytoplasmic domain.

(vi) Tyrosine 558 was identified as the major tyrosine phosphorylation site in MAG. Vanadate treatment enhanced the phosphorylation of this residue in L-MAG, but had no effect on the phosphorylation of this tyrosine in S-MAG.

(vii) Tyrosine phosphorylated L-MAG binds the SH2 domain of phospholipase C-gamma in an in vitro assay.

(viii) Tyrosine phosphorylation of L-MAG prevents serine/threonine phosphorylation of the same MAG molecule. This indicates the presence of at least two populations of L-MAG molecules, those that are phosphorylated on tyrosine residues, and those that are phosphorylated at specific serine residues.

(ix) Evidence for and characterization of BGPa and BGPb as substrates for protein tyrosine kinases and serine/threonine kinases was presented.